

# Two-Timescale Design for Reconfigurable Intelligent Surface-Aided Massive MIMO Systems with Imperfect CSI

Kangda Zhi, Cunhua Pan, Hong Ren, Kezhi Wang, Maged El Kashlan, Marco Di Renzo, *Fellow, IEEE*, Robert Schober, *Fellow, IEEE*, H. Vincent Poor, *Fellow, IEEE*, Jiangzhou Wang, *Fellow, IEEE* and Lajos Hanzo, *Fellow, IEEE*

## Abstract

This paper investigates the two-timescale transmission design for reconfigurable intelligent surface (RIS)-aided massive multiple-input multiple-output (MIMO) systems, where the beamforming at the base station (BS) is adapted to the rapidly-changing instantaneous channel state information (CSI), while the passive beamforming at the RIS is adapted to the slowly-changing statistical CSI. Specifically, we first propose a linear minimum mean square error (LMMSE) estimator to obtain the aggregated channel from the users to the BS in each channel coherence interval. Based on the estimated channel, we apply the low-complexity maximal ratio combining (MRC) beamforming at the BS, and then derive the ergodic

(Corresponding author: Cunhua Pan). Part of this work will be presented in the IEEE SPAWC, 2021 [1].

K. Zhi, C. Pan, M El Kashlan are with the School of Electronic Engineering and Computer Science at Queen Mary University of London, London E1 4NS, U.K. (e-mail: k.zhi, c.pan, maged.elkashlan@qmul.ac.uk). H. Ren is with the National Mobile Communications Research Laboratory, Southeast University, Nanjing 210096, China. (e-mail: hren@seu.edu.cn). K. Wang is with Department of Computer and Information Sciences, Northumbria University, UK. (e-mail: kezhi.wang@northumbria.ac.uk). M. Di Renzo is with Université Paris-Saclay, CNRS and CentraleSupélec, Laboratoire des Signaux et Systèmes, Gif-sur-Yvette, France. (e-mail: marco.direnzo@centralesupelec.fr). R. Schober is with the Institute for Digital Communications, Friedrich-Alexander-University Erlangen-Nürnberg (FAU), Germany (e-mail: robert.schober@fau.de). H. V. Poor is with the Department of Electrical and Computer Engineering, Princeton University, Princeton, NJ 08544 USA (e-mail: poor@princeton.edu). Jiangzhou Wang is with the School of Engineering and Digital Arts, University of Kent, UK. (e-mail: J.Z.Wang@kent.ac.uk). Lajos Hanzo is with the School of Electronics and Computer Science, University of Southampton, Southampton, SO17 1BJ, U.K. (e-mail: lh@ecs.soton.ac.uk.).

This work has been submitted to the IEEE for possible publication. Copyright may be transferred without notice, after which this version may no longer be accessible.

achievable rate in a closed form expression. To draw design insights, we perform a detailed theoretical analysis departing from the derived ergodic achievable rate. If the BS-RIS channel is Rician distributed, we prove that the transmit power can be scaled proportionally to  $1/M$ , as the number of BS antennas,  $M$ , grows to infinity while maintaining a non-zero rate. If the BS-RIS channel is Rayleigh distributed, the transmit power can be scaled either proportionally to  $1/\sqrt{M}$  as  $M$  grows large, or proportionally to  $1/N$  as the number of reflecting elements,  $N$ , grows large, while still maintaining a non-zero rate. By capitalizing on the derived expression of the data rate under the statistical knowledge of the CSI, we maximize the minimum user rate by designing the passive beamforming at the RIS, which turns out to be a complicated optimization problem. To effectively tackle it, we propose a genetic algorithm (GA)-based method. Numerical results confirm that, even in the presence of imperfect CSI, the integration of an RIS in massive MIMO systems results in promising performance gains. In addition, the obtained results reveal that it is favorable to place the RIS close to the users rather than close to the BS.

### Index Terms

Intelligent reflecting surface (IRS), reconfigurable intelligent surface (RIS), massive MIMO, two-timescale design, channel estimation, statistical CSI.

## I. INTRODUCTION

As an emerging candidate for next-generation communication systems, reconfigurable intelligent surfaces (RISs), also termed intelligent reflecting surfaces (IRSs), have attracted significant interest from both academia and industry [2], [3]. An RIS is a reconfigurable engineered surface that does not require active radio frequency (RF) chains, power amplifiers, and digital signal processing units, and is usually made of a large number of low cost and passive scattering elements that are coupled with simple low power electronic circuits. By intelligently tuning the phase shifts of the impinging wave with the aid of a controller, an RIS can constructively strengthen the desired signal power or destructively weaken the interference signal, which yields an appealing passive beamforming gain.

Compared with existing multi-antenna systems [4]–[9], it has been demonstrated that RIS-aided systems have the potential to achieve better performance in terms of cost and energy consumption [10]–[16]. Recently, RISs have been considered for integration into various communication scenarios, such as terahertz, sub-terahertz, and millimeter-wave systems [17], [18], simultaneous wireless information and power transfer (SWIPT) [19], unmanned aerial vehicle (UAV) communications [20], cell-free systems [21], physical-layer security [22]–[24], mobile

edge computing (MEC) [25]–[27], device-to-device (D2D) communications [28], [29] and so on. Furthermore, the effectiveness of RIS-aided systems in the presence of practical imperfections has been demonstrated in [30]–[34]. Specifically, relying on imperfect instantaneous channel state information (CSI), the robust transmission design of RISs was studied in [30]–[32]. The authors in [33] studied the RIS beamforming design by considering transceiver hardware impairments. With the consideration of RF impairments and phase noises, the authors in [34] successfully conducted theoretical analysis on the fundamental tradeoffs between spectral and energy efficiency of the RIS communication network. In addition, a valuable experimental investigation of the RIS-assisted channel was carried out in [35].

While several benefits of RISs have been demonstrated in the above-mentioned contributions, most of them considered the design of the passive beamforming at the RIS based on the knowledge of instantaneous CSI in each channel coherence interval. In practice, these instantaneous CSI-based schemes face two challenges. The first one is the overhead for the acquisition of the instantaneous CSI. Due to the passive nature of the reflecting elements that constitute the RIS, many authors proposed to estimate the cascaded user-RIS-BS channels instead of the separated user-RIS and RIS-BS channels [36], [37]. The pilot overhead of these channel estimation schemes is still proportional to the number of RIS elements. However, an RIS generally consists of a large number of reflecting elements to reap its potential [38], which incurs a prohibitively high pilot overhead. Secondly, in each channel coherence time interval, the BS needs to calculate the optimal beamforming coefficients for the RIS, and send them back to the RIS controller via dedicated feedback links. For instantaneous CSI-based scheme, therefore, the beamforming calculation and information feedback need to be executed frequently in each channel coherence interval, which results in a high computational complexity, feedback overhead, and energy consumption.

To address these two practical challenges, recently, Han *et al.* [39] firstly proposed a novel two-timescale based RIS design scheme, which facilitates the deployment and operation of RIS-aided systems. This promising two-timescale scheme was further analyzed in recent research works [40]–[52]. In the two-timescale scheme, the BS beamforming is designed based on the instantaneous aggregated CSI, which includes the direct and RIS-reflected links. The dimension of this aggregated channel is the same as for conventional RIS-free systems, which is not related to the number of RIS reflecting elements. Hence, in the two-timescale scheme, the length of the pilot sequences only needs to be larger than the number of users, which significantly reduces

the channel estimation overhead. More importantly, the two-timescale scheme aims to design the RISs only based on long-term statistical CSI, such as the locations and the angles of the users with respect to the BS and the RIS, which vary much slower than the instantaneous CSI. The phase shifts of the reflecting elements of the RIS need to be redesigned only when the large-scale channel information changes. Compared with instantaneous CSI-based designs that need to update the phase shifts of the reflecting elements in each channel coherence interval, therefore, RIS-aided designs based on statistical CSI can significantly reduce the computational complexity, feedback overhead and energy consumption.

In addition, massive MIMO technology has been identified as the cornerstone of the fifth generation (5G) and future communication systems [53], [54]. Massive MIMO exploits tens or hundreds of BS antennas to serve multiple users simultaneously. Due to the complexity of wireless propagation environments, e.g., the presence of large blocking objects, however, the signal power received at the end-users may be still too weak, and it may be insufficient to support emerging applications that entail high data rate requirements, such as virtual reality (VR) or augment reality (AR). Inspired by the capability of RISs to customize the wireless propagation environment, a natural idea is to integrate them into massive MIMO systems. By constructing alternative transmission paths, it is envisioned that RIS-aided massive MIMO systems can achieve significant performance gains, especially when the direct links between the BS and the users are blocked by obstacles. In RIS-aided massive MIMO systems, the transmission scheme needs to be carefully designed, and the channel estimation overhead needs to be taken into account considering the large channel dimension. The application of instantaneous CSI-assisted schemes, in particular, may lead to a prohibitive complexity and overhead. Instead, due to the reduced channel estimation and feedback overhead, the two-timescale scheme is deemed more suitable for RIS-aided massive MIMO systems.

To the best of our knowledge, only a few research works investigated RIS-aided massive MIMO systems based on the two-timescale design [50], [51]. The authors of [50] proposed to employ the RIS for serving users that are located in the out-of-coverage areas of massive MIMO systems. In the presence of direct links, the authors of [51] demonstrated the effectiveness of using an RIS for enhancing the system performance of conventional massive MIMO systems. These two contributions are, however, based on the ideal assumption that the aggregated CSI is perfectly obtained at the BS. In practice, the CSI can only be acquired through some channel estimation methods, which cause an estimation overhead and result in estimation errors. There-

fore, it is still unclear whether RIS-aided massive MIMO systems can achieve large performance gains when considering the channel estimation overhead and the channel estimation error. This open research issue motivates our work.

In this paper, we focus on the uplink (UL) two-timescale transmission of an RIS-aided massive MIMO system that is subject to imperfect aggregated CSI. In each channel coherence interval, we utilize the linear minimum mean square error (LMMSE) method to estimate the instantaneous aggregated channel matrix from the users to the BS. Based on the estimated aggregated channel, the conventional low-complexity maximal ratio combining (MRC) scheme is applied at the BS. In addition, we derive analytical expressions of the ergodic achievable rate, which depend only on the statistical CSI and, thus, enable us to configure the RIS only based on slowly-changing CSI. The specific contributions of this paper are summarized as follows.

- A low-complexity LMMSE estimator is proposed to estimate the aggregated channel from the users to the BS, which has the same amount of overhead as conventional massive MIMO systems. We compute the mean square error (MSE) and normalized MSE (NMSE) of the estimated channels. Based on the analysis, we unveil that the MSE converges to an upper bound but the NMSE converges to zero when the number of RIS elements tends to infinity.
- A low-complexity MRC receiver is applied at the BS by exploiting the estimated aggregated channel, and the corresponding uplink ergodic achievable rate is derived and formulated in a closed-form expression. The derived results hold for arbitrary numbers of BS antennas and RIS elements. Based on obtained analytical expressions, we analyze the asymptotic behavior of the rate and the power scaling laws. We also analyze the rate performance for the single-user case.
- Using the derived closed-form expressions, we design the optimal phase shifts of the RIS based on statistical CSI. To guarantee the desired fairness among different users, a genetic algorithm (GA) is applied for maximizing the minimum rate of all the users. In the special case of a single-user, the optimal solution for the RIS phase shifts is formulated in a closed-form expression.
- Extensive simulation results are presented to evaluate the performance gain offered by RIS-aided massive MIMO systems compared to conventional massive MIMO systems. The numerical results unveil that it is preferable to deploy the RIS in the vicinity of the users rather than in the vicinity of the BS.

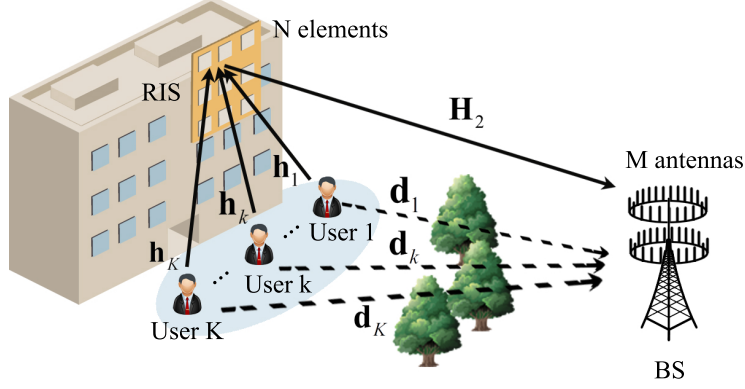


Fig. 1: An RIS-aided massive MIMO system.

The remainder of this paper is organized as follows. Section II describes the system model of the considered RIS-aided massive MIMO system. Section III derives the LMMSE channel estimator and evaluates the channel estimation quality. In Section IV, we derive closed-form expressions for the ergodic rate, and analyze the corresponding power scaling laws. In Section V, we introduce the statistical CSI-based design for RISs in the general multi-user scenario and in the special single-user scenario. Section VI provides extensive numerical results and Section VII concludes the paper.

*Notations:* Vectors and matrices are denoted by boldface lower case and upper case letters, respectively. The transpose, conjugate, conjugate transpose, and inverse of matrix  $\mathbf{X}$  are denoted by  $\mathbf{X}^T$ ,  $\mathbf{X}^*$ ,  $\mathbf{X}^H$  and  $\mathbf{X}^{-1}$ , respectively.  $[\mathbf{X}]_{m,n}$  denotes the  $(m,n)$ th entry of matrix  $\mathbf{X}$ . The real, trace, expectation, and covariance operators are denoted by  $\text{Re}\{\cdot\}$ ,  $\text{Tr}\{\cdot\}$ ,  $\mathbb{E}\{\cdot\}$ , and  $\text{Cov}\{\cdot\}$ , respectively. The  $l_2$  norm of a vector and the absolute value of a complex number are denoted by  $\|\cdot\|$  and  $|\cdot|$ , respectively.  $\mathbb{C}^{M \times N}$  denotes the space of  $M \times N$  complex matrices.  $\mathbf{I}_M$  and  $\mathbf{0}$  denote the  $M \times M$  identity matrix and all-zero matrix with appropriate dimension, respectively. The operator mod returns the remainder after division, and  $\lfloor x \rfloor$  denotes the nearest integer smaller than  $x$ .  $\mathbf{x} \sim \mathcal{CN}(\bar{\mathbf{x}}, \mathbf{C})$  is a complex Gaussian distributed vector with mean  $\bar{\mathbf{x}}$  and covariance matrix  $\mathbf{C}$ .  $\mathcal{O}$  denotes the standard big-O notation.

## II. SYSTEM MODEL

As illustrated in Fig. 1, we consider the UL transmission of an RIS-aided massive MIMO system, where an RIS is deployed in the proximity of  $K$  users to assist their UL transmissions to the BS. For convenience, we denote the set of users as  $\mathcal{K} = \{1, 2, \dots, K\}$ . The BS is equipped with  $M$  active antennas, the RIS comprises  $N$  passive reflecting elements, and the  $K$  users

are equipped with a single transmit antenna. The channels from user  $k$ ,  $k \in \mathcal{K}$  to the BS, from user  $k$ ,  $k \in \mathcal{K}$  to the RIS, and from the RIS to the BS are denoted by  $\mathbf{d}_k \in \mathbb{C}^{M \times 1}$ ,  $\mathbf{h}_k \in \mathbb{C}^{N \times 1}$ , and  $\mathbf{H}_2 \in \mathbb{C}^{M \times N}$ , respectively. Additionally, we define  $\mathbf{D} = [\mathbf{d}_1, \mathbf{d}_2, \dots, \mathbf{d}_K]$  and  $\mathbf{H}_1 = [\mathbf{h}_1, \mathbf{h}_2, \dots, \mathbf{h}_K]$ .

The RIS shapes the propagation environment by phase-shifting the impinging signals. Its phase shift matrix is denoted by  $\Phi = \text{diag}\{e^{j\theta_1}, e^{j\theta_2}, \dots, e^{j\theta_N}\}$ , where  $\theta_n \in [0, 2\pi)$  represents the phase shift of the  $n$ th reflecting element. Based on these definitions, the cascaded user  $k$ -RIS-BS channel can be written as  $\mathbf{g}_k = \mathbf{H}_2 \Phi \mathbf{h}_k$ , and the cascaded channels of the  $K$  users are collected in the matrix  $\mathbf{G} = [\mathbf{g}_1, \mathbf{g}_2, \dots, \mathbf{g}_K] = \mathbf{H}_2 \Phi \mathbf{H}_1 \in \mathbb{C}^{M \times K}$ .

The  $K$  users transmit their data in the same UL time-frequency resource. For ease of exposition, let  $\mathbf{Q} = \mathbf{G} + \mathbf{D} = [\mathbf{q}_1, \mathbf{q}_2, \dots, \mathbf{q}_K] \in \mathbb{C}^{M \times K}$  denote the aggregated instantaneous channel matrix from the users to the BS. Thereby, the signal vector received at the BS is given by

$$\mathbf{y} = \sqrt{p} \mathbf{Q} \mathbf{x} + \mathbf{n} = \sqrt{p} \sum_{k=1}^K \mathbf{q}_k x_k + \mathbf{n}, \quad (1)$$

where  $p$  is the average transmit power of each user,  $\mathbf{x} = [x_1, x_2, \dots, x_K]^T$  are the transmit symbols of the  $K$  users, and  $\mathbf{n} \sim \mathcal{CN}(\mathbf{0}, \sigma^2 \mathbf{I}_M)$  denotes the noise vector.

The BS applies a low-complexity MRC receiver to detect the transmitted symbols. Before designing the MRC matrix, the channel  $\mathbf{Q}$  has to be estimated at the BS. A standard LMMSE estimator is employed to obtain the estimated channel  $\hat{\mathbf{Q}}$ , as explained in the next section. Relying on the channel estimate, the BS performs MRC by multiplying the received signal  $\mathbf{y}$  with  $\hat{\mathbf{Q}}^H$ , as follows

$$\mathbf{r} = \hat{\mathbf{Q}}^H \mathbf{y} = \sqrt{p} \hat{\mathbf{Q}}^H \mathbf{Q} \mathbf{x} + \hat{\mathbf{Q}}^H \mathbf{n}. \quad (2)$$

Then, the  $k$ th element of the vector  $\mathbf{r}$  can be expressed as

$$r_k = \sqrt{p} \hat{\mathbf{q}}_k^H \mathbf{q}_k x_k + \sqrt{p} \sum_{i=1, i \neq k}^K \hat{\mathbf{q}}_k^H \mathbf{q}_i x_i + \hat{\mathbf{q}}_k^H \mathbf{n}, \quad k \in \mathcal{K}, \quad (3)$$

where  $\hat{\mathbf{q}}_k$  is the  $k$ th column of  $\hat{\mathbf{Q}}$ .

#### A. Channel Model

Since the users may be located far away from the BS and a large number of environmental blocking objects (i.e., blockages such as trees, vehicles, buildings) may exist in the area of interest, the line-of-sight (LoS) path between the users and the BS could be blocked. As in

[39], [47], [48], we adopt the Rayleigh fading model to describe the non-LoS (NLoS) channel between the user  $k$  and the BS, as follows

$$\mathbf{d}_k = \sqrt{\gamma_k} \tilde{\mathbf{d}}_k, \quad k \in \mathcal{K}, \quad (4)$$

where  $\gamma_k$  denotes the distance-dependent path-loss, and  $\tilde{\mathbf{d}}_k$  denotes the fast fading NLoS channel. The entries of  $\tilde{\mathbf{d}}_k$  are independent and identically distributed (i.i.d.) complex Gaussian random variables, i.e.,  $\tilde{\mathbf{d}}_k \sim \mathcal{CN}(\mathbf{0}, \mathbf{I}_M)$ .

Considering that the RIS is often installed on the facades of high-rise buildings and it could be placed near the users, the channels between the users and the RIS have a high LoS probability. In addition, the RIS and the BS are usually deployed at some heights above the ground, which implies that LoS paths are likely to exist between the RIS and the BS. Therefore, as in [39], [47]–[51], we adopt the Rician fading model for the user-RIS and RIS-BS channels, as follows

$$\mathbf{h}_k = \sqrt{\frac{\alpha_k}{\varepsilon_k + 1}} \left( \sqrt{\varepsilon_k} \bar{\mathbf{h}}_k + \tilde{\mathbf{h}}_k \right), \quad k \in \mathcal{K}, \quad (5)$$

$$\mathbf{H}_2 = \sqrt{\frac{\beta}{\delta + 1}} \left( \sqrt{\delta} \bar{\mathbf{H}}_2 + \tilde{\mathbf{H}}_2 \right), \quad (6)$$

where  $\alpha_k$  and  $\beta$  represent the path-loss coefficients,  $\varepsilon_k$  and  $\delta$  are the Rician factors that account for the ratio of the LoS power to the NLoS power of the corresponding propagation paths. Furthermore,  $\bar{\mathbf{h}}_k$  and  $\bar{\mathbf{H}}_2$  denote the LoS components, whereas  $\tilde{\mathbf{h}}_k$  and  $\tilde{\mathbf{H}}_2$  represent the NLoS components. For the NLoS paths, the components of  $\tilde{\mathbf{h}}_k$  and  $\tilde{\mathbf{H}}_2$  are i.i.d. complex Gaussian random variables with zero mean and unit variance. For the LoS paths, we utilize the uniform squared planar array (USPA) model. Hence,  $\bar{\mathbf{h}}_k$  and  $\bar{\mathbf{H}}_2$  are, respectively, modelled as follows

$$\bar{\mathbf{h}}_k = \mathbf{a}_N(\varphi_{kr}^a, \varphi_{kr}^e), \quad k \in \mathcal{K}, \quad (7)$$

$$\bar{\mathbf{H}}_2 = \mathbf{a}_M(\phi_r^a, \phi_r^e) \mathbf{a}_N^H(\varphi_t^a, \varphi_t^e), \quad (8)$$

where  $\varphi_{kr}^a$  ( $\varphi_{kr}^e$ ) is the azimuth (elevation) angle of arrival (AoA) of the incident signal at the RIS from the user  $k$ ,  $\varphi_t^a$  ( $\varphi_t^e$ ) is the azimuth (elevation) angle of departure (AoD) reflected by the RIS towards the BS, and  $\phi_r^a$  ( $\phi_r^e$ ) is the azimuth (elevation) AoA of the signal received at the BS from the RIS, respectively. Furthermore,  $\mathbf{a}_X(\vartheta^a, \vartheta^e) \in \mathbb{C}^{X \times 1}$  denotes the array response vector, whose  $x$ -th entry is

$$[\mathbf{a}_X(\vartheta^a, \vartheta^e)]_x = \exp \left\{ j 2\pi \frac{d}{\lambda} \left( \lfloor (x-1) / \sqrt{X} \rfloor \sin \vartheta^e \sin \vartheta^a + ((x-1) \bmod \sqrt{X}) \cos \vartheta^e \right) \right\}, \quad (9)$$



where  $d$  and  $\lambda$  denote the inter-element distance and the wavelength, respectively.

To simplify the notation, in the sequel, we denote  $\mathbf{a}_N(\varphi_{kr}^a, \varphi_{kr}^e)$ ,  $\mathbf{a}_M(\phi_r^a, \phi_r^e)$ , and  $\mathbf{a}_N(\varphi_t^a, \varphi_t^e)$  simply by  $\bar{\mathbf{h}}_k$ ,  $\mathbf{a}_M$ , and  $\mathbf{a}_N$ , respectively. Then, the aggregated channel from the user  $k$  to the BS can be expressed as

$$\begin{aligned} \mathbf{q}_k &= \mathbf{g}_k + \mathbf{d}_k = \mathbf{H}_2 \Phi \mathbf{h}_k + \mathbf{d}_k \\ &= \underbrace{\sqrt{c_k \delta \varepsilon_k} \bar{\mathbf{H}}_2 \Phi \bar{\mathbf{h}}_k}_{\mathbf{q}_k^1} + \underbrace{\sqrt{c_k \delta} \bar{\mathbf{H}}_2 \Phi \tilde{\mathbf{h}}_k}_{\mathbf{q}_k^2} + \underbrace{\sqrt{c_k \varepsilon_k} \tilde{\mathbf{H}}_2 \Phi \bar{\mathbf{h}}_k}_{\mathbf{q}_k^3} + \underbrace{\sqrt{c_k} \tilde{\mathbf{H}}_2 \Phi \tilde{\mathbf{h}}_k}_{\mathbf{q}_k^4} + \sqrt{\gamma_k} \tilde{\mathbf{d}}_k \\ &\triangleq \underline{\mathbf{q}}_k + \mathbf{d}_k, \end{aligned} \quad (10)$$

where  $c_k \triangleq \frac{\beta \alpha_k}{(\delta+1)(\varepsilon_k+1)}$ , and  $\underline{\mathbf{q}}_k = \sum_{\omega=1}^4 \mathbf{q}_k^\omega$ . Note that  $\underline{\mathbf{q}}_k$  and  $\mathbf{d}_k$  are mutually independent.

### III. CHANNEL ESTIMATION

In this section, we use the LMMSE method to obtain the estimated aggregated instantaneous channel  $\hat{\mathbf{Q}}$ . Specifically, the BS estimates the aggregated channel matrix  $\mathbf{Q}$  based on some predefined pilot signals. Let  $\tau_c$  and  $\tau$  denote the length of the channel coherence interval and the number of time slots used for channel estimation, respectively, where  $\tau$  is no smaller than  $K$ , i.e.,  $\tau \geq K$ . In each channel coherence interval, the  $K$  users simultaneously transmit mutually orthogonal pilot sequences to the BS. The pilot sequence of the user  $k$  is denoted by  $\mathbf{s}_k \in \mathbb{C}^{\tau \times 1}$ . By defining  $\mathbf{S} = [\mathbf{s}_1, \mathbf{s}_2, \dots, \mathbf{s}_K]$ , we have  $\mathbf{S}^H \mathbf{S} = \mathbf{I}_K$ . Then, the  $M \times \tau$  pilot signals received at the BS can be written as

$$\mathbf{Y}_p = \sqrt{\tau p} \mathbf{Q} \mathbf{S}^H + \mathbf{N}, \quad (11)$$

where  $\tau p$  is the transmit pilot power, and  $\mathbf{N}$  denotes the  $M \times \tau$  noise matrix whose entries are i.i.d. complex Gaussian random variables with zero mean and variance  $\sigma^2$ . Multiplying (11) by  $\frac{\mathbf{s}_k}{\sqrt{\tau p}}$  and exploiting the orthogonality of the pilot signals, the BS obtains the following observation vector for user  $k$

$$\mathbf{y}_p^k = \frac{1}{\sqrt{\tau p}} \mathbf{Y}_p \mathbf{s}_k = \mathbf{q}_k + \frac{1}{\sqrt{\tau p}} \mathbf{N} \mathbf{s}_k. \quad (12)$$

The optimal estimate of the  $k$ -th user's channel based on the observation vector  $\mathbf{y}_p^k$  can be determined based on the MMSE criterion, which has been widely utilized in conventional massive MIMO systems [55]–[57]. In RIS-aided massive MIMO systems where Rician fading is considered for all RIS-related channels, however, it is challenging to obtain the MMSE estimator.

This is because the cascaded user-RIS-BS channel  $\mathbf{G}$  in RIS-aided systems is not Gaussian distributed, but double Gaussian distributed instead [58]. To obtain closed-form channel estimates, as is needed for an insightful analysis, we adopt the sub-optimal but tractable LMMSE estimator. This is because the LMMSE estimator only requires the knowledge of first and second order statistics, and therefore does not need to know the exact channel distributions. In the following lemma, we present the required statistics for the channel vector  $\mathbf{q}_k$  and the observation vector  $\mathbf{y}_p^k$ .

**Lemma 1** *For  $k \in \mathcal{K}$ , the mean vectors and covariance matrices needed for the LMMSE estimator are given by*

$$\mathbb{E}\{\mathbf{q}_k\} = \mathbb{E}\{\mathbf{y}_p^k\} = \sqrt{c_k \delta \varepsilon_k} \bar{\mathbf{H}}_2 \Phi \bar{\mathbf{h}}_k, \quad (13)$$

$$\text{Cov}\{\mathbf{q}_k, \mathbf{y}_p^k\} = \text{Cov}\{\mathbf{y}_p^k, \mathbf{q}_k\} = \text{Cov}\{\mathbf{q}_k, \mathbf{q}_k\} = a_{k1} \mathbf{a}_M \mathbf{a}_M^H + a_{k2} \mathbf{I}_M, \quad (14)$$

$$\text{Cov}\{\mathbf{y}_p^k, \mathbf{y}_p^k\} = \text{Cov}\{\mathbf{q}_k, \mathbf{q}_k\} + \frac{\sigma^2}{\tau p} \mathbf{I}_M = a_{k1} \mathbf{a}_M \mathbf{a}_M^H + \left(a_{k2} + \frac{\sigma^2}{\tau p}\right) \mathbf{I}_M, \quad (15)$$

where  $a_{k1} = N c_k \delta$  and  $a_{k2} = N c_k (\varepsilon_k + 1) + \gamma_k$  are two auxiliary variables.

*Proof:* See Appendix B. ■

**Theorem 1** *Using the observation vector  $\mathbf{y}_p^k$ , the LMMSE estimate  $\hat{\mathbf{q}}_k$  of the channel vector  $\mathbf{q}_k$  is given by*

$$\hat{\mathbf{q}}_k = \mathbf{A}_k \mathbf{y}_p^k + \mathbf{B}_k \quad (16)$$

$$\begin{aligned} &= \underbrace{\sqrt{c_k \delta \varepsilon_k} \bar{\mathbf{H}}_2 \Phi \bar{\mathbf{h}}_k}_{\hat{\mathbf{q}}_k^1} + \underbrace{(M a_{k3} + a_{k4}) \sqrt{c_k \delta} \bar{\mathbf{H}}_2 \Phi \tilde{\mathbf{h}}_k}_{\hat{\mathbf{q}}_k^2} + \underbrace{\sqrt{c_k \varepsilon_k} \mathbf{A}_k \tilde{\mathbf{H}}_2 \Phi \bar{\mathbf{h}}_k}_{\hat{\mathbf{q}}_k^3} + \underbrace{\sqrt{c_k} \mathbf{A}_k \tilde{\mathbf{H}}_2 \Phi \tilde{\mathbf{h}}_k}_{\hat{\mathbf{q}}_k^4} \\ &\quad \underbrace{\hspace{10em}}_{\hat{\mathbf{q}}_k} \\ &+ \sqrt{\gamma_k} \mathbf{A}_k \tilde{\mathbf{d}}_k + \frac{1}{\sqrt{\tau p}} \mathbf{A}_k \mathbf{N} \mathbf{s}_k, \end{aligned} \quad (17)$$

where

$$\mathbf{A}_k = \mathbf{A}_k^H = a_{k3} \mathbf{a}_M \mathbf{a}_M^H + a_{k4} \mathbf{I}_M, \quad (18)$$

$$\mathbf{B}_k = (\mathbf{I}_M - \mathbf{A}_k) \sqrt{c_k \delta \varepsilon_k} \bar{\mathbf{H}}_2 \Phi \bar{\mathbf{h}}_k, \quad (19)$$

$$a_{k3} = \frac{a_{k1} \frac{\sigma^2}{\tau p}}{\left(a_{k2} + \frac{\sigma^2}{\tau p}\right) \left(a_{k2} + \frac{\sigma^2}{\tau p} + M a_{k1}\right)}, \quad (20)$$

$$a_{k4} = \frac{a_{k2}}{a_{k2} + \frac{\sigma^2}{\tau p}}, \quad (21)$$

and the NMSE of the estimate of  $\mathbf{q}_k$  is

$$\text{NMSE}_k = \frac{\text{Tr} \{ \text{Cov} \{ \mathbf{q}_k - \hat{\mathbf{q}}_k, \mathbf{q}_k - \hat{\mathbf{q}}_k \} \}}{\text{Tr} \{ \text{Cov} \{ \mathbf{q}_k, \mathbf{q}_k \} \}} = \frac{\frac{\sigma^2}{\tau p} \left( M a_{k1} a_{k2} + a_{k2}^2 + (a_{k1} + a_{k2}) \frac{\sigma^2}{\tau p} \right)}{\left( a_{k2} + \frac{\sigma^2}{\tau p} \right) \left( a_{k2} + \frac{\sigma^2}{\tau p} + M a_{k1} \right) (a_{k1} + a_{k2})}. \quad (22)$$

*Proof:* See Appendix C. ■

As is evident from Theorem 1, we only estimate the aggregated channel matrix  $\mathbf{Q} \in \mathbb{C}^{M \times K}$  including the reflected and direct channels, which has the same dimension as the user-BS channel matrix in conventional massive MIMO systems. Therefore, we only require that the length of the pilot sequences is no smaller than the number of users, i.e.,  $\tau \geq K$ . Compared to estimation methods that estimate the  $MN$  individual channels in RIS-aided communications [36], [37], the proposed method has lower overhead and computational complexity.

**Remark 1** When  $c_k = 0, \forall k$ , i.e., the RIS-assisted channels are absent, we have  $a_{k1} = 0$ ,  $a_{k2} = \gamma_k$ ,  $a_{k3} = 0$ ,  $a_{k4} = \frac{\gamma_k}{\gamma_k + \frac{\sigma^2}{\tau p}}$  and  $\mathbf{B}_k = \mathbf{0}$ . In this case, the estimate in (16) reduces to  $\hat{\mathbf{q}}_k = \frac{\gamma_k}{\gamma_k + \frac{\sigma^2}{\tau p}} \mathbf{y}_p^k$  and the MSE matrix in (107) reduces to  $\mathbf{MSE}_k = \frac{\gamma_k \frac{\sigma^2}{\tau p}}{\gamma_k + \frac{\sigma^2}{\tau p}} \mathbf{I}_M$ , which, as expected, is the same as the MSE in conventional massive MIMO systems [56]. If the RIS channels only have the LoS components, i.e.,  $\delta, \varepsilon_k \rightarrow \infty, \forall k$ , we can also obtain  $a_{k1} \rightarrow 0$  and  $a_{k2} \rightarrow \gamma_k$ . In this case, the MSE matrix in (107) is again the same as that in conventional massive MIMO systems. This is because the LoS channels are deterministic and known, and, thus, they do not bring additional estimation errors.

**Corollary 1** In the low pilot power-to-noise ratio regime, high pilot power-to-noise ratio regime, and large  $N$  regime, the asymptotic NMSE is, respectively, given by

$$\lim_{\frac{\sigma^2}{\tau p} \rightarrow \infty} \text{NMSE}_k \rightarrow 1, \quad (23)$$

$$\lim_{\frac{\sigma^2}{\tau p} \rightarrow 0} \text{NMSE}_k \rightarrow 0, \quad (24)$$

$$\lim_{N \rightarrow \infty} \text{NMSE}_k \rightarrow 0. \quad (25)$$

Besides, consider that the power  $p$  is scaled proportionally to  $p = E_u/N$ , where  $E_u$  denotes a constant. As  $N \rightarrow \infty$ , we have

$$\lim_{p = \frac{E_u}{N}, N \rightarrow \infty} \text{NMSE}_k < 1. \quad (26)$$

*Proof:* When  $\frac{\sigma^2}{\tau p} \rightarrow \infty$  or  $N \rightarrow \infty$ , by selecting the dominant terms in (22), which scale with  $(\frac{\sigma^2}{\tau p})^2$  or  $N^3$ , we arrive at (23) and (25), respectively. Substituting  $\frac{\sigma^2}{\tau p} = 0$  into (22), its numerator

reduces to zero, which leads to (24). Replacing the power  $p$  in (22) with  $p = E_u/N$ , as  $N \rightarrow \infty$ , we can readily find that all the dominant terms in the numerator are present in the denominator as well, which results in (26). We omit the specific limit of (26) since it is a complex expression but is simple to compute. ■

It is worth noting that NMSE values between 0 (i.e., perfect estimation) and 1 (i.e., using the mean value of the variable as the estimate) quantify the relative estimation error [54]. In conventional massive MIMO systems, a common method for reducing the NMSE is to increase the length of the pilot sequence  $\tau$ . In RIS-aided massive MIMO systems, Corollary 1 indicates that increasing the number of RIS elements  $N$  can play a similar role as increasing  $\tau$ . Therefore, increasing the number of RIS elements not only helps improve the system capacity, but also helps reduce the NMSE. Additionally, (26) reveals that an RIS equipped with a large number of reflecting elements  $N$  can help the NMSE converge to a limit lower than one, even for low pilot powers.

To better understand the impact of increasing  $N$  for channel estimation, we present the following asymptotic results.

**Corollary 2** *When  $\tau \rightarrow \infty$ , we have  $\hat{\mathbf{q}}_k \rightarrow \mathbf{q}_k$ , which implies that  $\mathbf{e}_k \rightarrow \mathbf{0}$  and therefore the channel estimation is perfect. When  $N \rightarrow \infty$ , by contrast, we have*

$$\hat{\mathbf{q}}_k \rightarrow \mathbf{q}_k + \frac{1}{\sqrt{\tau p}} \mathbf{N} \mathbf{s}_k, \quad (27)$$

$$\mathbf{e}_k = \mathbf{q}_k - \hat{\mathbf{q}}_k \rightarrow \frac{-1}{\sqrt{\tau p}} \mathbf{N} \mathbf{s}_k, \quad (28)$$

$$\text{MSE}_k = \mathbb{E} \{ \mathbf{e}_k \mathbf{e}_k^H \} \rightarrow \frac{\sigma^2}{\tau p} \mathbf{I}_M. \quad (29)$$

*Proof:* When  $\tau \rightarrow \infty$  or  $N \rightarrow \infty$ , based on Theorem 1, we have  $a_{k3} \rightarrow 0$ ,  $a_{k4} \rightarrow 1$ , and  $M a_{k3} + a_{k4} \rightarrow 1$ , which yields  $\mathbf{A}_k \rightarrow \mathbf{I}_M$ . If  $\tau \rightarrow \infty$ , we further get  $\frac{1}{\sqrt{\tau p}} \rightarrow 0$ , which completes the proof. ■

Although the NMSE converges to zero as  $N \rightarrow \infty$  (see (25)), Corollary 2 shows that, in contrast to increasing  $\tau$ , the MSE of the LMMSE estimator converges to a non-zero constant as  $N \rightarrow \infty$ . If we estimate the channel  $\mathbf{q}_k$  based on the least-squares (LS) estimator [54, (3.35)], it is interesting to note that we will obtain the same results as in (27) and (29). In general, the LS estimator, which does not exploit any prior channel statistics, has worse estimation performance (higher MSE) than the LMMSE estimator [37], [54], [59]. Therefore, Corollary 2 indicates that

the MSE performance of the LMMSE estimation converges towards an upper bound, which is the MSE performance of the LS estimation, as  $N \rightarrow \infty$ . This result will be validated in Section VI.

**Corollary 3** *When the RIS-BS channel reduces to the purely Rayleigh channel (i.e.,  $\delta = 0$ ), the estimated channel vector, MSE, and NMSE, respectively, reduce to*

$$\hat{\mathbf{q}}_k = a_{k4} \mathbf{I}_M \mathbf{y}_p^k = \frac{N\beta\alpha_k + \gamma_k}{N\beta\alpha_k + \gamma_k + \frac{\sigma^2}{\tau p}} \mathbf{y}_p^k, \quad (30)$$

$$\mathbf{MSE}_k = \frac{(N\beta\alpha_k + \gamma_k) \frac{\sigma^2}{\tau p}}{N\beta\alpha_k + \gamma_k + \frac{\sigma^2}{\tau p}} \mathbf{I}_M, \quad (31)$$

$$\text{NMSE}_k = \frac{\frac{\sigma^2}{\tau p}}{N\beta\alpha_k + \gamma_k + \frac{\sigma^2}{\tau p}}. \quad (32)$$

*Proof:* When  $\delta = 0$ , we have  $a_{k1} = 0$ ,  $a_{k2} = N\beta\alpha_k + \gamma_k$ ,  $a_{k3} = 0$ ,  $a_{k4} = \frac{N\beta\alpha_k + \gamma_k}{N\beta\alpha_k + \gamma_k + \frac{\sigma^2}{\tau p}}$  and  $\mathbf{B}_k = \mathbf{0}$ . The proof follows by inserting these results in Theorem 1 and (107). ■

Corollary 3 corresponds to a scenario where a large number of scatterers exist nearby the RIS and the BS, and the LoS path between the RIS and the BS is negligible. Therefore, the RIS-BS channel is dominated by the NLoS paths. In this case, both the MSE and NMSE have simple analytical expressions, which help us better understand the conclusions drawn in Corollary 1 and Corollary 2. It is apparent that the MSE (represented by the trace of  $\mathbf{MSE}_k$  in (31)) and the NMSE (represented by  $\text{NMSE}_k$  in (32)) are decreasing functions of the pilot power  $\tau p$ . As a function of  $N$ , on the other hand, the MSE is an increasing function, while the NMSE is a decreasing function. When  $N \rightarrow \infty$ , we have  $\mathbf{MSE}_k \rightarrow \frac{\sigma^2}{\tau p} \mathbf{I}_M$  but  $\text{NMSE}_k \rightarrow 0$ . Note that we can obtain the MSE and NMSE for conventional massive MIMO systems by setting  $N = 0$  in (31) and (32). Therefore, the obtained result implies that the MSE of RIS-aided massive MIMO systems is worse than the MSE of massive MIMO systems without RISs, while the NMSE of RIS-aided massive MIMO systems is better than the NMSE of massive MIMO systems without RISs. The reason is that an RIS introduces  $N$  additional paths to the system, but the pilot length  $\tau$  does not increase correspondingly, which increases the estimation error. However, the presence of an RIS results in better channel gains, which help decrease the normalized error.

Furthermore, if we reduce the power as  $p = E_u/N$ , as  $N \rightarrow \infty$ , the NMSE in (32) converges

to a limit less than one, as follows

$$\lim_{\delta=0, p=\frac{E_u}{N}, N \rightarrow \infty} \text{NMSE}_k \rightarrow \frac{\sigma^2}{\tau E_u \beta \alpha_k + \sigma^2} < 1. \quad (33)$$

#### IV. ANALYSIS OF THE ERGODIC UPLINK RATE

Based on the channel estimates provided in Theorem 1, closed-form expressions of the ergodic rate are derived and analyzed in this section. In the next section, the obtained analytical expressions are utilized for optimizing the phase shifts of the RIS based on statistical CSI.

##### A. Derivation of the Rate

As in [59]–[62], we utilize the so called use-and-then-forget bound, which is a tractable lower bound, to characterize the ergodic rate of RIS-aided massive MIMO systems. First, we rewrite  $r_k$  in (3) as

$$r_k = \underbrace{\sqrt{p} \mathbb{E} \{ \hat{\mathbf{q}}_k^H \mathbf{q}_k \}}_{\text{Desired signal}} x_k + \underbrace{\sqrt{p} (\hat{\mathbf{q}}_k^H \mathbf{q}_k - \mathbb{E} \{ \hat{\mathbf{q}}_k^H \mathbf{q}_k \})}_{\text{Signal leakage}} x_k + \underbrace{\sqrt{p} \sum_{i=1, i \neq k}^K \hat{\mathbf{q}}_k^H \mathbf{q}_i x_i}_{\text{Multi-user interference}} + \underbrace{\hat{\mathbf{q}}_k^H \mathbf{n}}_{\text{Noise}}. \quad (34)$$

Then, we formulate the lower bound of the  $k$ -th user's ergodic rate as  $\underline{R}_k = \frac{\tau_c - \tau}{\tau_c} \log_2 (1 + \text{SINR}_k)$ , where the pre-log factor  $\frac{\tau_c - \tau}{\tau_c}$  represents the rate loss that originates from the pilot overhead, and the SINR is expressed as

$$\text{SINR}_k = \frac{p |\mathbb{E} \{ \hat{\mathbf{q}}_k^H \mathbf{q}_k \}|^2}{p \left( \mathbb{E} \{ |\hat{\mathbf{q}}_k^H \mathbf{q}_k|^2 \} - |\mathbb{E} \{ \hat{\mathbf{q}}_k^H \mathbf{q}_k \}|^2 \right) + p \sum_{i=1, i \neq k}^K \mathbb{E} \{ |\hat{\mathbf{q}}_k^H \mathbf{q}_i|^2 \} + \sigma^2 \mathbb{E} \{ \|\hat{\mathbf{q}}_k\|^2 \}}. \quad (35)$$

To simplify the expression of  $\underline{R}_k$ , we define three auxiliary variables  $e_{k1}$ ,  $e_{k2}$ , and  $e_{k3}$ . These variables capture the performance degradation due to the imperfect knowledge of the CSI.

**Lemma 2** For  $k \in \mathcal{K}$ , we have  $\text{Tr} \{ \mathbf{A}_k \} = M e_{k1}$ ,  $\mathbf{A}_k \bar{\mathbf{H}}_2 = e_{k2} \bar{\mathbf{H}}_2$  and  $\text{Tr} \{ \mathbf{A}_k \mathbf{A}_k \} = M e_{k3}$ , where

$$e_{k1} \triangleq a_{k3} + a_{k4}, \quad (36)$$

$$e_{k2} \triangleq M a_{k3} + a_{k4}, \quad (37)$$

$$e_{k3} \triangleq M a_{k3}^2 + 2 a_{k3} a_{k4} + a_{k4}^2. \quad (38)$$

Furthermore,  $e_{k1}$ ,  $e_{k2}$  and  $e_{k3}$  are bounded in  $[0, 1]$ . When  $\tau p \rightarrow \infty$  or  $N \rightarrow \infty$ , we have  $e_{k1}, e_{k2}, e_{k3} \rightarrow 1$ . When  $\tau p \rightarrow 0$ , by contrast, we have  $e_{k1}, e_{k2}, e_{k3} \rightarrow 0$ .

*Proof:* See Appendix D. ■

In the following theorem, we derive a closed-form expression for the rate.

**Theorem 2** *A lower bound for the ergodic rate of the  $k$ -th user is given by*

$$\underline{R}_k = \frac{\tau_c - \tau}{\tau_c} \log_2 \left( 1 + \frac{pE_k^{(\text{signal})}(\Phi)}{pE_k^{(\text{leakage})}(\Phi) + p \sum_{i=1, i \neq k}^K I_{ki}(\Phi) + \sigma^2 E_k^{(\text{noise})}(\Phi)} \right), \quad (39)$$

where  $E_k^{(\text{signal})}(\Phi) = \left\{ E_k^{(\text{noise})}(\Phi) \right\}^2$ ,

$$E_k^{(\text{noise})}(\Phi) = M \left\{ |f_k(\Phi)|^2 c_k \delta \varepsilon_k + N c_k \delta e_{k2} + (N c_k (\varepsilon_k + 1) + \gamma_k) e_{k1} \right\}, \quad (40)$$

$$\begin{aligned} E_k^{(\text{leakage})}(\Phi) = & M |f_k(\Phi)|^2 c_k^2 \delta \varepsilon_k \left\{ N (M \delta + \varepsilon_k + 1) (e_{k2}^2 + 1) + 2 (M e_{k1} + e_{k2}) (e_{k2} + 1) \right\} \\ & + M |f_k(\Phi)|^2 c_k \delta \varepsilon_k \left\{ \gamma_k + \left( \gamma_k + \frac{\sigma^2}{\tau p} \right) e_{k2}^2 \right\} \\ & + M^2 N^2 c_k^2 \delta^2 e_{k2}^2 \\ & + M N^2 c_k^2 \left\{ 2 \delta (\varepsilon_k + 1) e_{k2}^2 + (\varepsilon_k + 1)^2 e_{k3} \right\} \\ & + M^2 N c_k^2 \left\{ (2 \varepsilon_k + 1) e_{k1}^2 + 2 \delta e_{k1} e_{k2} \right\} \\ & + M N c_k \left\{ c_k (2 \delta e_{k2}^2 + (2 \varepsilon_k + 1) e_{k3}) + \left( 2 \gamma_k + \frac{\sigma^2}{\tau p} \right) (\delta e_{k2}^2 + (\varepsilon_k + 1) e_{k3}) \right\} \\ & + M \gamma_k \left( \gamma_k + \frac{\sigma^2}{\tau p} \right) e_{k3}, \end{aligned} \quad (41)$$

and

$$\begin{aligned} I_{ki}(\Phi) = & M^2 |f_k(\Phi)|^2 |f_i(\Phi)|^2 c_k c_i \delta^2 \varepsilon_k \varepsilon_i \\ & + M |f_k(\Phi)|^2 c_k \delta \varepsilon_k \left\{ c_i (M N \delta + N \varepsilon_i + N + 2 M e_{k1}) + \gamma_i \right\} \\ & + M |f_i(\Phi)|^2 c_i \delta \varepsilon_i \left\{ c_k e_{k2} (M N \delta e_{k2} + N \varepsilon_k e_{k2} + N e_{k2} + 2 M e_{k1}) + \left( \gamma_k + \frac{\sigma^2}{\tau p} \right) e_{k2}^2 \right\} \\ & + M^2 N^2 c_k c_i \delta^2 e_{k2}^2 \\ & + M N^2 c_k c_i \left\{ \delta (\varepsilon_k + \varepsilon_i + 2) e_{k2}^2 + (\varepsilon_k + 1) (\varepsilon_i + 1) e_{k3} \right\} \\ & + M^2 N c_k c_i e_{k1} \left\{ (\varepsilon_k + \varepsilon_i + 1) e_{k1} + 2 \delta e_{k2} \right\} \\ & + M^2 c_k c_i \varepsilon_k \varepsilon_i e_{k1} \left( \left| \bar{\mathbf{h}}_k^H \bar{\mathbf{h}}_i \right|^2 e_{k1} + 2 \delta \text{Re} \left\{ f_k^H(\Phi) f_i(\Phi) \bar{\mathbf{h}}_i^H \bar{\mathbf{h}}_k \right\} \right) \\ & + M N \left\{ \left( \gamma_k + \frac{\sigma^2}{\tau p} \right) c_i (\delta e_{k2}^2 + (\varepsilon_i + 1) e_{k3}) + \gamma_i c_k (\delta e_{k2}^2 + (\varepsilon_k + 1) e_{k3}) \right\} \\ & + M \gamma_i \left( \gamma_k + \frac{\sigma^2}{\tau p} \right) e_{k3}, \end{aligned} \quad (42)$$

with

$$f_k(\Phi) \triangleq \mathbf{a}_N^H \Phi \bar{\mathbf{h}}_k = \sum_{n=1}^N e^{j(\zeta_n^k + \theta_n)}, \quad (43)$$

$$\begin{aligned} \zeta_n^k = & 2\pi \frac{d}{\lambda} \left( \lfloor (n-1)/\sqrt{N} \rfloor (\sin \varphi_{kr}^e \sin \varphi_{kr}^a - \sin \varphi_t^e \sin \varphi_t^a) \right. \\ & \left. + ((n-1) \bmod \sqrt{N}) (\cos \varphi_{kr}^e - \cos \varphi_t^e) \right). \end{aligned} \quad (44)$$

*Proof:* See Appendix E. ■

The closed-form expression in Theorem 2 does not involve the calculation of inverse matrices and the numerical computation of integrals. In contrast to time-consuming Monte Carlo simulations, the evaluation of the rate based on Theorem 2 has a low computational complexity even if  $M$  and  $N$  are large numbers, as usually is in RIS-aided massive MIMO systems. More importantly, Theorem 2 only relies on slowly-varying statistical CSI, i.e., the distance-based path loss factors, the AoA and AoD, and the environment-related Rician factors. By using the analytical expression of the rate in (39) as an objective function for system design, we are able to optimize the phase shifts of the RIS only based on long-term statistical CSI.

By comparing the formulation in Theorem 2 with that given in [50, Lemma 1], we can see that the impact of imperfect CSI is completely characterized by the parameters  $e_{k1}, e_{k2}, e_{k3}$  and  $\frac{\sigma^2}{\tau p}$ . In the perfect CSI scenario, we can assume  $\tau = \infty$ , which leads to  $e_{k1} = e_{k2} = e_{k3} = 1$  and  $\frac{\sigma^2}{\tau p} = 0$ . Based on Theorem 2, we can analyze the rate performance of RIS-aided massive MIMO systems for arbitrary system parameters. Thus, in the following, we will respectively investigate the asymptotic behavior of the rate for large values of  $M$  and  $N$ , study the power scaling laws, and quantify the impact of the Rician factors. To this end, we begin with a useful lemma.

**Lemma 3** • If  $N = 1$ , for arbitrary  $\Phi$ , we have  $|f_k(\Phi)| = 1$  in (43).

- If  $N > 1$ , by optimizing  $\Phi$ , the range of values  $0 \leq |f_k(\Phi)| \leq N$  is achievable in (43).
- If we configure the phase shifts of the RIS to achieve  $|f_k(\Phi)| = N$ , unless the user  $i, i \neq k$ , has the same azimuth and elevation AoA as the user  $k$ , the function  $|f_i(\Phi)|$  in (43) is bounded when  $N \rightarrow \infty$ .
- Unless the user  $i, i \neq k$ , has the same azimuth and elevation AoA as the user  $k$ , the term  $\left| \bar{\mathbf{h}}_k^H \bar{\mathbf{h}}_i \right|^2$  is bounded when  $N \rightarrow \infty$ .

*Proof:* See Appendix F. ■



### B. Multi-user Case

In this section, we consider the general multi-user scenario, i.e.,  $K > 1$ . Since any two users are unlikely to be in the same location, we assume that the azimuth and elevation AoA of any two users are different, i.e.,  $(\varphi_{kr}^a, \varphi_{kr}^e) \neq (\varphi_{ir}^a, \varphi_{ir}^e)$ . To begin with, we investigate the asymptotic behavior of the rate in (39) for large values of  $M$  and  $N$ .

**Remark 2** From Theorem 2, we observe that, as a function of  $M$ ,  $E_k^{(\text{signal})}(\Phi)$ ,  $E_k^{(\text{leakage})}(\Phi)$  and  $I_{ki}(\Phi)$  behave asymptotically as  $\mathcal{O}(M^2)$ . Therefore, the rate  $\underline{R}_k$  converges to a finite limit when  $M \rightarrow \infty$ . If, on the other hand, we align the phase shifts of the RIS for maximizing the intended signal for the user  $k$ , i.e., we set  $|f_k(\Phi)| = N$ , then we have  $\underline{R}_k \rightarrow \infty$  for user  $k$ , and  $\underline{R}_i \rightarrow 0$  for the other users  $i \neq k$  as  $N \rightarrow \infty$ , based on Lemma 3. In a multi-user scenario, this implies that it is necessary to enforce some fairness among the users when designing the phase shifts of the RIS.

Next, we study the power scaling laws of RIS-aided massive MIMO systems with different Rician factors. Note that the Rician factor characterizes the fading severity of the environment and the richness of scatterers in the environment. The smaller the Rician factor is, the larger the number of scatterers in the environment is. If the Rician factor is zero, we retrieve the Rayleigh fading channel as a special case in which only the NLoS components exist. If the Rician factor tends to infinity, the channel is deterministic and it is characterized only by the LoS component. It is worth mentioning that, under the assumption of imperfect CSI, decreasing the transmit power  $p$  results in a reduction of the power used for both the data and pilot signals.

We will analyze several scenarios for the RIS-BS and user-RIS channels. For ease of exposition, we summarize the obtained power scaling laws as a function of  $M$  and  $N$  in Table I. Specifically, the following notations are used. “Imperfect CSI” and “Perfect CSI” are referred

TABLE I: Power scaling laws in the multi-user case.

		(RIS-BS channel, user-RIS channels)			
		(Rician, Rician)	(Rician, Rayleigh)	(Rayleigh, Rician)	(Rayleigh, Rayleigh)
Imperfect CSI	$M$	$1/M$	$1/M$	$1/\sqrt{M}$	$1/\sqrt{M}$
	$N$	$\backslash$	$1/N$		
Perfect CSI	$M$	$1/M$			
	$N$	$\backslash$	$1/N$		

to the power scaling laws obtained for imperfect and perfect CSI, respectively. By setting  $e_{k1} = e_{k2} = e_{k3} = 1$  and  $\frac{\sigma^2}{\tau p} = 0$ , which are obtained from  $\tau \rightarrow \infty$ , the imperfect CSI setup reduces to the perfect CSI setup. The notation “(Rician, Rician)” means that the RIS-BS channel and all the user-RIS channels are Rician distributed, i.e.,  $\delta > 0$  and  $\varepsilon_k > 0, \forall k$ . Similarly, the notation “(Rician, Rayleigh)” means that the RIS-BS channel is Rician distributed and all the user-RIS channels are Rayleigh distributed, i.e.,  $\delta > 0$  and  $\varepsilon_k = 0, \forall k$ . The notations “ $1/M$ ”, “ $1/\sqrt{M}$ ” and “ $1/N$ ” imply that the rate tends to a non-zero value if the transmit power scales down proportionally to  $1/M$ ,  $1/\sqrt{M}$  and  $1/N$ , respectively. We mention, for completeness, that the readers interested in the power scaling laws as a function of  $M$  in conventional massive MIMO systems without RISs may refer to [55] and [56]. Besides, we stress that the rate does not depend on the RIS phase shift matrix  $\Phi$  if  $\delta = 0$  or  $\varepsilon_k = 0, \forall k$ , which will be proved in Corollary 5. In the following, we mainly focus on the proof for the imperfect CSI case, since the perfect CSI setup can be obtained in a similar manner, by setting  $e_{k1} = e_{k2} = e_{k3} = 1$  and  $\frac{\sigma^2}{\tau p} = 0$ .

**Corollary 4** (“ $1/M$ ” for “(Rician, Rician)” and “(Rician, Rayleigh)”) Assume that the transmit power  $p$  is scaled as  $p = E_u/M$ . For  $M \rightarrow \infty$ , the rate of the user  $k$ ,  $k \in \mathcal{K}$ , is lower bounded by

$$\underline{R}_k \rightarrow \frac{\tau_c - \tau}{\tau_c} \log_2 \left( 1 + \frac{E_u c_k^2 \delta^2 (|f_k(\Phi)|^2 \varepsilon_k + N e_{k2})^2}{E_u E_k^{(leakage)}(\Phi) + E_u \sum_{i=1, i \neq k}^K I_{ki}(\Phi) + \sigma^2 c_k \delta (|f_k(\Phi)|^2 \varepsilon_k + N e_{k2})} \right), \quad (45)$$

where

$$\begin{aligned} E_k^{(leakage)}(\Phi) &= N |f_k(\Phi)|^2 c_k^2 \delta^2 \varepsilon_k (e_{k2}^2 + 1) + \frac{\sigma^2}{\tau E_u} |f_k(\Phi)|^2 c_k \delta \varepsilon_k e_{k2}^2 \\ &\quad + N^2 c_k^2 \delta^2 e_{k2}^2 + \frac{\sigma^2}{\tau E_u} N c_k \delta e_{k2}^2, \end{aligned} \quad (46)$$

$$\begin{aligned} I_{ki}(\Phi) &= |f_k(\Phi)|^2 |f_i(\Phi)|^2 c_k c_i \delta^2 \varepsilon_k \varepsilon_i + N |f_k(\Phi)|^2 c_k c_i \delta^2 \varepsilon_k \\ &\quad + |f_i(\Phi)|^2 c_i \delta \varepsilon_i e_{k2}^2 \left( N c_k \delta + \frac{\sigma^2}{\tau E_u} \right) + N^2 c_k c_i \delta^2 e_{k2}^2 + N \frac{\sigma^2}{\tau E_u} c_i \delta e_{k2}^2, \end{aligned} \quad (47)$$

$$e_{k2} = \frac{N c_k \delta}{\frac{\sigma^2}{\tau E_u} + N c_k \delta}. \quad (48)$$

*Proof:* If  $p = E_u/M$  and  $M \rightarrow \infty$ , we have  $e_{k1} \rightarrow 0$ ,  $e_{k3} \rightarrow 0$ , and  $e_{k2}$  tends to (48). The proof is completed by substituting  $p = E_u/M$  into Theorem 2 and retaining the non-zero terms whose asymptotic behavior is  $\mathcal{O}(M)$ . ■

For a massive number of antennas, Corollary 4 shows that the rate of all the users tends to a non-zero value when the transmit power scales as  $p = E_u/M$ . From (45), we evince that the rate  $\underline{R}_k$  is still non-zero if  $\varepsilon_k = 0, \forall k$ , i.e., all the user-RIS channels are Rayleigh distributed. This proves the power scaling law “ $1/M$ ” for the “(Rician, Rayleigh)” setup in Table I. However, the rate  $\underline{R}_k$  in (45) reduces to zero if  $c_k = 0$  or  $\delta = 0$ , i.e., the RIS-aided channels are absent or the RIS-BS channel is Rayleigh distributed. This indicates that the power scaling law “ $1/M$ ” does not hold for these two case studies. Specifically, the considered system degenerates to an RIS-free massive MIMO system with Rayleigh fading if  $c_k = 0, \forall k$ . In this case, it has been proven that the rate can maintain a non-zero value when the power scales as  $p = E_u/\sqrt{M}$  [56, (37)]. As for the power scaling law for  $\delta = 0$ , we first provide the rate expression when  $\delta = 0$ .

**Corollary 5** *If the RIS-BS channel is Rayleigh distributed ( $\delta = 0$ ), the rate of user  $k$ ,  $k \in \mathcal{K}$ , is lower bounded by*

$$\underline{R}_k^{(\text{NL1})} = \frac{\tau_c - \tau}{\tau_c} \log_2 \left( 1 + \frac{pE_k^{(\text{signal})}}{pE_k^{(\text{leakage})} + p \sum_{i=1, i \neq k}^K I_{ki} + \sigma^2 E_k^{(\text{noise})}} \right), \quad (49)$$

where

$$E_k^{(\text{signal})} = M (Nc_k (\varepsilon_k + 1) + \gamma_k)^2 e_{k1}, \quad (50)$$

$$E_k^{(\text{noise})} = Nc_k (\varepsilon_k + 1) + \gamma_k, \quad (51)$$

$$\begin{aligned} E_k^{(\text{leakage})} = & N^2 c_k^2 (\varepsilon_k + 1)^2 e_{k1} + MNc_k^2 (2\varepsilon_k + 1) e_{k1} \\ & + Nc_k \left\{ c_k (2\varepsilon_k + 1) + \left( 2\gamma_k + \frac{\sigma^2}{\tau p} \right) (\varepsilon_k + 1) \right\} e_{k1} + \gamma_k \left( \gamma_k + \frac{\sigma^2}{\tau p} \right) e_{k1}, \end{aligned} \quad (52)$$

$$\begin{aligned} I_{ki} = & N^2 c_k c_i (\varepsilon_k + 1) (\varepsilon_i + 1) e_{k1} + MNc_k c_i (\varepsilon_k + \varepsilon_i + 1) e_{k1} + Mc_k c_i \varepsilon_k \varepsilon_i \left| \overline{\mathbf{h}}_k^H \overline{\mathbf{h}}_i \right|^2 e_{k1} \\ & + N \left\{ \left( \gamma_k + \frac{\sigma^2}{\tau p} \right) c_i (\varepsilon_i + 1) + \gamma_i c_k (\varepsilon_k + 1) \right\} e_{k1} + \gamma_i \left( \gamma_k + \frac{\sigma^2}{\tau p} \right) e_{k1}, \end{aligned} \quad (53)$$

and

$$e_{k1} = \frac{N\beta\alpha_k + \gamma_k}{N\beta\alpha_k + \gamma_k + \frac{\sigma^2}{\tau p}}. \quad (54)$$

*Proof:* When  $\delta = 0$ , we have  $a_{k1} = 0$ ,  $a_{k2} = N\beta\alpha_k + \gamma_k$ , and  $a_{k3} = 0$ . Then, we obtain  $e_{k3} = e_{k1}^2$ , where  $e_{k1} = a_{k4}$  is given in (54). Substituting  $\delta = 0$  into Theorem 2 and using  $e_{k3} = e_{k1}^2$ , the proof follows with the aid of some algebraic simplifications. ■

It is observed that the rate expression in Corollary 5 does not depend on  $\Phi$ . Therefore, with a purely NLoS RIS-BS channel, any RIS phase shift matrix will result in the same ergodic rate. This is because the RIS phase shift matrix  $\Phi$  is a unitary matrix and the entries of the NLoS channel  $\tilde{\mathbf{H}}_2$  are Gaussian distributed. Therefore,  $\tilde{\mathbf{H}}_2\Phi$  has the same statistical properties as  $\tilde{\mathbf{H}}_2$ . Likewise, there is no need to design the RIS phase shifts if all the user-RIS links are purely NLoS. This conclusion is apparent from (39) by setting  $\varepsilon_k = 0, \forall k$ .

By analyzing the dominant terms of (49) when  $M, N \rightarrow \infty$ , we evince that the rate increases without bound for all the users. This implies that fairness among the users is guaranteed in this special case. As  $N \rightarrow \infty$ , specifically, the dominant terms in (49) scale asymptotically as  $\mathcal{O}(N^2)$ , and the rate converges to

$$\underline{R}_k^{(\text{NL}_1)} \rightarrow \frac{\tau_c - \tau}{\tau_c} \log_2 \left( 1 + \frac{M\alpha_k}{\sum_{i=1}^K \alpha_i} \right), \text{ as } N \rightarrow \infty, \quad (55)$$

$$= \frac{\tau_c - \tau}{\tau_c} \log_2 (1 + M/K), \text{ if } \alpha_1 = \dots = \alpha_K. \quad (56)$$

From (55), we evince that the SINR,  $\frac{M\alpha_k}{\sum_{i=1}^K \alpha_i}$ , does not depend on the pilot power  $\tau p$  and it increases linearly with  $M$ . Therefore, promising rate performance can be achieved if  $\delta = 0$  and  $N \rightarrow \infty$ .

With the aid of Corollary 5, we investigate, in the following corollaries, the power scaling laws as a function of  $M$  and  $N$  when  $\delta = 0$ .

**Corollary 6** (“ $1/\sqrt{M}$ ” for “(Rayleigh, Rician)” and “(Rayleigh, Rayleigh)”) *If the RIS-BS channel is Rayleigh distributed ( $\delta = 0$ ), and the power is scaled as  $p = E_u/\sqrt{M}$  with  $M \rightarrow \infty$ , the rate of user  $k$ ,  $k \in \mathcal{K}$  tends to  $\underline{R}_k^{(\text{NL}_1)} \rightarrow \frac{\tau_c - \tau}{\tau_c} \log_2 (1 + \text{SINR}_k)$ , where the effective SINR is given by*

$$\text{SINR}_k = \frac{\tau E_u^2 (N c_k (\varepsilon_k + 1) + \gamma_k)^2}{\tau E_u^2 N c_k^2 (2\varepsilon_k + 1) + \sum_{i=1, i \neq k}^K \tau E_u^2 c_k c_i \left\{ N (\varepsilon_k + \varepsilon_i + 1) + \varepsilon_k \varepsilon_i \left| \bar{\mathbf{h}}_k^H \bar{\mathbf{h}}_i \right|^2 \right\} + \sigma^4}. \quad (57)$$

*Proof:* First, we substitute  $p = E_u/\sqrt{M}$  into Corollary 5 and ignore the terms that tend to zero as  $M \rightarrow \infty$ . Then, we divide the numerator and denominator of the SINR by  $\frac{N\beta\alpha_k + \gamma_k}{\sigma^2}$ . This yields (57) and the proof is completed. ■

From (57), we evince that the numerator of the SINR scales with  $\mathcal{O}(N^2)$ , but the denominator of the SINR only scales with  $\mathcal{O}(N)$ . Therefore, Corollary 6 indicates that the rate scales logarithmically with  $N$  if  $p = E_u/\sqrt{M}$  and  $M \rightarrow \infty$ , which is a promising result for RIS-aided massive MIMO systems. Besides, it is worth noting that (57) will reduce to the same expression as in [56, Eq. (37)] when  $c_k = 0, \forall k$ .

**Corollary 7** (“ $1/N$ ” for “(Rayleigh, Rician)” and “(Rayleigh, Rayleigh)”) *If the RIS-BS channel is Rayleigh distributed ( $\delta = 0$ ) and the power is scaled as  $p = E_u/N$  with  $N \rightarrow \infty$ , the rate of user  $k$ ,  $k \in \mathcal{K}$ , is lower bounded by*

$$\underline{R}_k^{(\text{NL}_1)} \rightarrow \frac{\tau_c - \tau}{\tau_c} \log_2 \left( 1 + \frac{E_u M \beta \alpha_k}{\sum_{i=1}^K \left( E_u \beta \alpha_i + \frac{\alpha_i}{\alpha_k} \frac{\sigma^2}{\tau} \right) + \sigma^2 \left( 1 + \frac{\sigma^2}{\tau E_u \beta \alpha_k} \right)} \right). \quad (58)$$

*Proof:* First, we substitute  $p = E_u/N$  into Corollary 5. When  $N \rightarrow \infty$ , we have  $e_{k1} \rightarrow \frac{\beta\alpha_k}{\beta\alpha_k + \frac{\sigma^2}{\tau E_u}}$ . Then, we remove the non-dominant terms that do not scale as  $\mathcal{O}(N)$ . By noting that  $c_k(\varepsilon_k + 1) = \beta\alpha_k, \forall k$ , and dividing the numerator and denominator of the SINR by  $\beta\alpha_k$ , we obtain (58). This completes the proof. ■

Corollary 7 sheds some interesting insights. Firstly, we note that Corollary 6 has unveiled that the transmit power  $p$  can only be reduced proportionally to  $1/\sqrt{M}$ , while maintaining a non-zero rate, when  $\delta = 0$ . Corollary 7, on the other hand, proves that the transmit power can be reduced proportionally to  $1/N$ , while maintaining a non-zero rate, when  $\delta = 0$ . This reveals the positive role of deploying RISs in massive MIMO systems. Secondly, the obtained power scaling law does not depend on the Rician factors of user-RIS links, i.e.,  $\varepsilon_k, \forall k$ . This implies that the rate in (58) is the same for LoS-only and NLoS-only user-RIS channels. Thirdly, in (58), the desired signal term in (58) scales as  $\mathcal{O}(M)$  and the interference term scales as  $\mathcal{O}(1)$ . As a result, the rate scales logarithmically with the number of BS antennas. When the number of antennas is large, the power of interference will be relatively small compared with the power of desired signal, and then a promising rate can be achieved with the setup in Corollary 7. Therefore, the rich-scattering environment between the RIS and the BS ( $\delta = 0$ ) is beneficial in RIS-aided massive MIMO systems, since it can provide sufficient spatial multiplexing gains and help mitigate the multi-user interference. Finally, (58) unveils that, if the users are all located at

the same distance from the RIS, i.e.,  $\alpha_1 = \dots = \alpha_K$ , they all achieve the same rate. Therefore, fairness can be guaranteed in this special case.

Corollary 7 sheds light on the achievable rate when the RIS-BS channel is Rayleigh distributed ( $\delta = 0$ ). In the next corollary, we analyze the opposite scenario in which the user-RIS channels are Rayleigh distributed ( $\varepsilon_k = 0, \forall k$ ).

**Corollary 8** (“ $1/N$ ” for “(Rician, Rayleigh)”) Assume  $\delta > 0$ . If the user-RIS channels are Rayleigh distributed ( $\varepsilon_k = 0, \forall k$ ) and the power is scaled as  $p = E_u/N$  with  $N \rightarrow \infty$ , the rate of user  $k$ ,  $k \in \mathcal{K}$ , is lower bounded by

$$\underline{R}_k^{(\text{NL}_2)} \rightarrow \frac{\tau_c - \tau}{\tau_c} \log_2 \left( 1 + \frac{E_u M c_k^2 (\delta e_{k2} + e_{k1})^2}{E_u \left( E_k^{(\text{leakage})} + \sum_{i=1, i \neq k}^K I_{ki} \right) + \sigma^2 c_k (\delta e_{k2} + e_{k1})} \right), \quad (59)$$

with

$$E_k^{(\text{leakage})} + \sum_{i=1, i \neq k}^K I_{ki} = \sum_{i=1}^K c_i \left\{ M c_k \delta^2 e_{k2}^2 + c_k (2\delta e_{k2}^2 + e_{k3}) + \frac{\sigma^2}{\tau E_u} (\delta e_{k2}^2 + e_{k3}) \right\}, \quad (60)$$

$$a_{k3} = \frac{c_k \delta \frac{\sigma^2}{\tau E_u}}{\left( c_k + \frac{\sigma^2}{\tau E_u} \right) \left( c_k + \frac{\sigma^2}{\tau E_u} + M c_k \delta \right)}, \quad (61)$$

$$a_{k4} = \frac{c_k}{c_k + \frac{\sigma^2}{\tau E_u}}. \quad (62)$$

*Proof:* It follows from Theorem 2 by setting  $\varepsilon_k = 0, \forall k$  and  $p = E_u/N$ , and by keeping only the dominant terms for  $N \rightarrow \infty$ . ■

Corollary 8 characterizes the achievable rate when the user-RIS channels are rich scattering. The obtained performance trends are very different from those unveiled in Corollary 7 (i.e., the RIS-BS channel is rich scattering). In contrast to Corollary 7, in particular, both the desired signal and the interference in (59) scale as  $\mathcal{O}(M)$ . As a result, if the user-RIS channels are Rayleigh distributed, the rate in (59) is still bounded from above even if the number of BS antennas is very large. Besides, it is not hard to prove that the rate (59) will reduce to the same expression as (58) if we further set  $\delta = 0$ . This result confirms our conclusion in Corollary 7 that the scaling law is not related with the Rician factor  $\varepsilon_k$  if  $\delta = 0$ .

The findings obtained from Corollary 7 and Corollary 8 allow us to draw important conclusions on the best deployment of RISs for maximizing the rate. Previous works, e.g., [63], have concluded that the rate of RIS-aided systems increases if the RISs are deployed either close to the BS or close to the users. It is often shown that RIS-aided systems offer similar rates in

both deployment scenarios. However, Corollary 7 and Corollary 8 show that it is preferable to deploy the RISs close to the users. In fact, the Rician factor is usually a decreasing function of the transmission distance [64]. If, therefore, we deploy the RIS close to the BS and far from the users, the scenario of Corollary 8 is likely to hold. If, on the other hand, we deploy the RIS close to the users and far from the BS, the scenario of Corollary 7 is likely to hold. As a result, a much higher rate is expected to be obtained in the latter case as the number of BS antennas increases.

### C. Single-user Case

In this subsection, we analyze the power scaling laws in the special case with only one user, i.e.,  $K = 1$ . Without loss of generality, the user is referred to as user  $k$ . Since no other user exists, the rate can be obtained from Theorem 2 by ignoring the multi-user interference term, i.e., by setting  $I_{ki}(\Phi) = 0$ . For analytical tractability, we further assume that the number of RIS elements is large. In this scenario (single-user and large  $N$ ), it can be proved that the optimal phase shift design that maximizes the rate corresponds to the condition  $|f_k(\Phi)| = N$ . This statement is formally proved in the next section (Theorem 3).

Therefore, by setting  $I_{ki} = 0$  and  $|f_k(\Phi)| = N$  in Theorem 2, we obtain that the power of the desired signal scales as  $\mathcal{O}(M^2N^4)$ , the power of the signal leakage scales as  $\mathcal{O}(M^2N^3)$ , and the power of the noise term scales as  $\mathcal{O}(MN^2)$ . Therefore, the rate is bounded for  $M \rightarrow \infty$ , but it can grow without bound for  $N \rightarrow \infty$ . For ease of exposition, similar to the multi-user case, we summarize the obtained power scaling laws in Table II. In the following, we report the proofs only for some (those that lead to insightful design guidelines) system setups that are summarized in Table II. The proof of each case study can, in fact, be obtained by using analytical steps similar to the multi-user case. Finally, we mention that the power scaling laws in the single-user case with perfect CSI can be derived readily based on [39, Eq. (17)].

**Corollary 9** *Consider a single-user system with  $|f_k(\Phi)| = N$ . If the transmit power is scaled as  $p = E_u/(MN^2)$  with  $M, N \rightarrow \infty$ , the rate is lower bounded by*

$$\underline{R}_k \rightarrow \frac{\tau_c - \tau}{\tau_c} \log_2 \left( 1 + \frac{E_u}{\sigma^2} \frac{\beta \alpha_k \delta \varepsilon_k}{(\delta + 1)(\varepsilon_k + 1)} \right). \quad (63)$$

*If the transmit power is scaled as  $p = E_u/N^2$  with  $N \rightarrow \infty$ , the rate is lower bounded by*

$$\underline{R}_k \rightarrow \frac{\tau_c - \tau}{\tau_c} \log_2 \left( 1 + \frac{E_u}{\sigma^2} M c_k \delta \varepsilon_k \right). \quad (64)$$

TABLE II: Power scaling laws in the single-user case.

		(RIS-BS channel, user-RIS channel)			
		(Rician, Rician)	(Rician, Rayleigh)	(Rayleigh, Rician)	(Rayleigh, Rayleigh)
Imperfect CSI	$M$	$1/M$	$1/M$	$1/\sqrt{M}$	$1/\sqrt{M}$
	$N$	$1/N^2$	$1/N$		
Perfect CSI	$M$	$1/M$			
	$N$	$1/N^2$	$1/N$		

*Proof:* Let us set  $p = E_u/(MN^2)$ ,  $|f_k(\Phi)| = N$  and  $I_{ki} = 0$  in Theorem 2. The rate in (63) follows by using the fact  $e_{k1}, e_{k2}, e_{k3} \rightarrow 0$  and by retaining the dominant terms that scale as  $\mathcal{O}(MN^2)$  for  $M, N \rightarrow \infty$ . Next, let us set  $p = E_u/N^2$ ,  $|f_k(\Phi)| = N$  and  $I_{ki} = 0$  in Theorem 2. The rate in (64) follows by retaining the dominant terms that scale as  $\mathcal{O}(N^2)$  for  $N \rightarrow \infty$ . ■

The SNRs in (63) and (64) do not depend on  $\tau$ , and except for a pre-log scaling factor, the same SNR as for perfect CSI-based systems can be derived readily from [39, Eq. (17)]. We evince, therefore, that  $\tau = K = 1$  is the optimal pilot length based on (63) and (64). Therefore, the overhead for channel estimation is relatively low. Furthermore, the rates in (63) and (64) are increasing functions of the Rician factors  $\delta$  and  $\varepsilon_k$ , which unveils that LoS-dominated environments are favorable for RIS-aided single-user systems. If both  $\delta \rightarrow \infty$  and  $\varepsilon_k \rightarrow \infty$ , (63) and (64) are maximized. On the contrary, if  $\delta = 0$  or  $\varepsilon_k = 0$ , we observe that (63) and (64) tend to zero. This implies that the power scaling law  $1/N^2$  does not hold anymore. In these two cases, the transmit power can be scaled only proportionally to  $1/N$  for maintaining a non-zero rate when  $N \rightarrow \infty$ . Mathematically, the corresponding power scaling laws can be proved from Corollary 7 and Corollary 8 by setting the multi-user interference to zero. As an example, the case study for  $\delta = 0$  is analyzed in the following corollary.

**Corollary 10** *Consider a single-user system with  $\delta = 0$ . If the transmit power is scaled as  $p = E_u/N$  with  $N \rightarrow \infty$ , the rate is lower bounded by*

$$\underline{R}_k^{(\text{NL}_1)} \rightarrow \frac{\tau_c - \tau}{\tau_c} \log_2 \left( 1 + \frac{E_u M \beta \alpha_k}{E_u \beta \alpha_k + \frac{\sigma^2}{\tau} + \sigma^2 \left( 1 + \frac{\sigma^2}{\tau E_u \beta \alpha_k} \right)} \right). \quad (65)$$

As  $\tau$  increases, the denominator of the SNR of (65) decreases. Therefore, the SNR of (65) is an increasing function of  $\tau$ . Therefore,  $\tau = 1$  is not guaranteed to be optimal in a rich-scattering



environment ( $\delta = 0$ ), and a relatively large number of pilots signals may be needed. Thus, Corollary 10 again emphasizes that LoS environments are favorable for RIS-aided single-user systems.

## V. DESIGN OF THE RIS PHASE SHIFTS

In this section, we optimize the phase shifts of the RIS that maximize the ergodic rate derived in Theorem 2. Since the ergodic rate in Theorem 2 depends only on statistical CSI, we do not need to update the phase shifts design of the RIS until the long-term CSI varies, which results in a much lower update frequency compared with conventional designs based on instantaneous CSI. Therefore, the proposed optimization criterion has a reduced computational complexity.

In this section, in particular, we only consider scenarios that correspond to the setups  $N > 1$ ,  $\delta > 0$  and  $\varepsilon_k > 0, \forall k$ . This is because, based on Lemma 3 and Corollary 5, the rate in Theorem 2 is independent of the RIS phase shifts, if  $N = 1$ ,  $\delta = 0$  or  $\varepsilon_k = 0, \forall k$ . In the following, we first consider the single-user case and then consider the general multi-user case.

### A. Single-user Case

In the single-user case, only the user  $k$  is present. We aim to find the phase shifts matrix  $\Phi$  that maximizes the ergodic rate  $\underline{R}_k$ , which is obtained by setting  $I_{ki}(\Phi) = 0$  in Theorem 2. We can then find that the rate depends on the phase shifts matrix  $\Phi$  only through the term  $|f_k(\Phi)|^2$ . By defining  $x \triangleq |f_k(\Phi)|^2$ , we can rewrite the rate  $\underline{R}_k$  in Theorem 2 as follows

$$\begin{aligned} \underline{R}_k &= \frac{\tau_c - \tau}{\tau_c} \log_2 (1 + \text{SNR}_k(x)) \\ &= \frac{\tau_c - \tau}{\tau_c} \log_2 \left( 1 + \frac{E_k^{(\text{signal})}(x)}{E_k^{(\text{leakage})}(x) + \frac{\sigma^2}{p} E_k^{(\text{noise})}(x)} \right) \\ &\triangleq \frac{\tau_c - \tau}{\tau_c} \log_2 \left( 1 + \frac{(s_1 x + s_2)^2}{t_1 x + t_2} \right), \end{aligned} \quad (66)$$

where  $\text{SNR}_k(x) \triangleq \frac{(s_1 x + s_2)^2}{t_1 x + t_2}$ ,  $E_k^{(\text{signal})}(x) \triangleq (s_1 x + s_2)^2$  and  $E_k^{(\text{leakage})}(x) + \frac{\sigma^2}{p} E_k^{(\text{noise})}(x) \triangleq t_1 x + t_2$ . The exact expressions of  $s_1$ ,  $s_2$ ,  $t_1$ , and  $t_2$  are omitted due to their cumbersome formulation and because they are irrelevant for solving the optimization problem of interest. They can be retrieved by direct inspection of Theorem 2. The only important property to highlight is that  $s_1, s_2, t_1, t_2 > 0$ .

Note that we have assumed that  $N > 1$  in this section. From Lemma 3, we know that the domain of the variable  $x$  is  $0 \leq x \leq N^2$ . Based on (66), therefore, the optimization problem can be formulated as follows

$$\max_x \text{SNR}_k(x) = \frac{(s_1x + s_2)^2}{t_1x + t_2}, \quad (67a)$$

$$\text{s.t.} \quad 0 \leq x \leq N^2. \quad (67b)$$

To solve the problem in (67), we compute the first-order derivative of  $\text{SNR}_k(x)$  with respect to  $x$ , as follows

$$\frac{\partial \text{SNR}_k(x)}{\partial x} = \frac{(s_1x + s_2)(s_1t_1x + 2s_1t_2 - s_2t_1)}{(t_1x + t_2)^2}. \quad (68)$$

The first-order derivative of  $\text{SNR}_k(x)$  is positive or negative depending on the numerator in (68), which is a quadratic function of  $x$ , i.e., a parabola opening upward, with two roots. The two roots can be obtained by setting (68) equal to zero, which yields

$$x_0^L = \frac{-s_2}{s_1}, \quad x_0^R = \frac{s_2t_1 - 2s_1t_2}{s_1t_1}, \quad (69)$$

where  $x_0^L < 0$  while  $x_0^R$  can be positive.

We can design the optimal configuration of  $\Phi$  by analyzing the derivative  $\frac{\partial \text{SNR}_k(x)}{\partial x}$  in the domain of  $x$ , i.e., (67b), which can be identified by discussing the value of  $x_0^R$ . For example, if  $x_0^R \leq 0$ , for a parabola opening upward, we obtain  $\frac{\partial \text{SNR}_k(x)}{\partial x} \geq 0$  in the domain  $0 \leq x \leq N^2$ . The design framework is summarized in the following theorem.

**Theorem 3** *The optimal phase shift matrix  $\Phi$  of an RIS-aided single-user system subject to imperfect CSI is as follows*

- *Case 1: If  $x_0^R \leq 0$ , the optimal design for  $\Phi$  corresponds to setting  $|f_k(\Phi)| = N$ .*
- *Case 2: If  $x_0^R \geq N^2$ , the optimal design for  $\Phi$  corresponds to setting  $|f_k(\Phi)| = 0$ .*
- *Case 3: If  $0 < x_0^R < N^2$ , the optimal design for  $\Phi$  corresponds to setting  $|f_k(\Phi)| = 0$  when  $\text{SNR}_k(0) > \text{SNR}_k(N^2)$  and  $|f_k(\Phi)| = N$  when  $\text{SNR}_k(0) \leq \text{SNR}_k(N^2)$ .*
- *Case 4: If  $N \rightarrow \infty$ , the optimal design for  $\Phi$  corresponds to setting  $|f_k(\Phi)| = N$ .*

*Proof:* In Case 1, we obtain  $\frac{\partial \text{SNR}_k(x)}{\partial x} \geq 0$  in the domain  $0 \leq x \leq N^2$ . Thus, the SNR is an increasing function of  $x$  in its domain, which implies that the maximum SNR is reached at the endpoint  $x = N^2$ . Therefore, it is optimal to set  $|f_k(\Phi)| = N$ . In Case 2, we obtain  $\frac{\partial \text{SNR}_k(x)}{\partial x} \leq 0$  in the domain of  $x$ . Thus, the SNR is a decreasing function of  $x$ , which implies that the maximum

SNR is reached at the endpoint  $x = 0$ . Therefore, it is optimal to set  $|f_k(\Phi)| = 0$ . In Case 3, the SNR first decreases for  $x < x_0^R$ , and then increases for  $x > x_0^R$ . Therefore, the maximum SNR is obtained either at  $x = 0$  or at  $x = N^2$ . By comparing  $\text{SNR}_k(0)$  with  $\text{SNR}_k(N^2)$ , we can identify the optimal design. In Case 4, from Theorem 2, we have the following: (1) if  $|f_k(\Phi)| = 0$ , the SNR is bounded if  $N \rightarrow \infty$ ; and (2) if  $|f_k(\Phi)| = N$ , the SNR increases without bound if  $N \rightarrow \infty$ . Therefore, the optimum SNR is attained for  $|f_k(\Phi)| = N$  if  $N \rightarrow \infty$ . ■

Finally, we note that the optimal design obtained in Case 4 substantiates the analysis reported in Section IV-C for large  $N$ .

### B. Multi-user Case

In this subsection, we turn our attention to the design of the RIS phase shifts in the general multi-user scenario for  $K > 1$ . In the multi-user case, as mentioned in Remark 2, it is necessary to guarantee some fairness among the different users at the design stage. To this end, we aim to maximize the minimum rate of the users. As a result, the optimization problem can be formulated as follows

$$\max_{\Phi} \min_{k \in \mathcal{K}} \underline{R}_k(\Phi), \quad (70a)$$

$$\text{s.t.} \quad 0 \leq \theta_n < 2\pi, \forall n, \quad (70b)$$

where  $\underline{R}_k(\Phi)$  is given by (39) in Theorem 2.

Due to the complex analytical expression of  $\underline{R}_k$  and the fairness requirement among the users, it is difficult to solve the problem in (70) by using conventional optimization methods, such as semi-definite programming (SDP), the majorization-minimization (MM) algorithm and the projected gradient ascent method. In this paper, we tackle the problem in (70) by leveraging GA-based methods, whose suitability and effectiveness to optimize RIS-aided systems has been recently validated in [49]. The main idea of a GA-based method applied to RIS-aided systems is to view the RIS phase shifts as the gene of a population. The approach consists of evolving the population by updating its gene, and finally setting the RIS phase shifts equal to the best gene in the last generation [65], [66]. The detailed process of the proposed GA-based method is stated as follows.

**1) Population initialization:** First, we generate an initial population having  $S = S_e + S_c + S_m$  individuals, where each individual has a chromosome with  $N$  genes. The chromosome of the

individual  $1 \leq t \leq S$  is denoted by  $\Phi^t = \text{diag} \{e^{j\theta_1^t}, \dots, e^{j\theta_N^t}\}$ , whose  $n$ th gene is  $\theta_n^t$  that is randomly generated in  $[0, 2\pi)$ . The three sets of individuals  $S_e$ ,  $S_c$ , and  $S_m$  are detailed next.

**2) Fitness evaluation and scaling:** Then, we define the raw fitness of the individual  $t$  with chromosome  $\Phi^t$  in the current population as  $f_t = \min_k R_k(\Phi^t)$ . The individuals having a better raw fitness in the current population have a higher probability to reproduce. To avoid premature convergence, we utilize the rank scaling method to map raw fitness values to expected values. Let  $\text{Rank}(t)$  denote the rank, in descending order, of the raw fitness of the individual  $t$ . Then, the expected fitness of the individual  $t$  is calculated as

$$\hat{f}_t = \frac{\text{Rank}(t)^{-0.5}}{\sum_{i=1}^S \text{Rank}(i)^{-0.5}}, 1 \leq t \leq S. \quad (71)$$

**3) Selection:** The  $S_e$  individuals with the highest expected fitness in the current population are selected as elite individuals. These elite individuals are directly passed to the next generation. Then, we apply the stochastic universal sampling method to select  $2S_c$  crossover parents and  $S_m$  mutation parents. The process is sketched in Algorithm 1.

---

**Algorithm 1** Stochastic universal sampling.

---

- 1: Input the population's expected fitness  $[\hat{f}_1, \dots, \hat{f}_S]$ , set  $\hat{F}_{sum} = 0$ ;
  - 2: Randomly initialize a pointer  $0 \leq ptr \leq \frac{1}{(2S_c + S_m)}$ ;
  - 3: **for**  $i = 1 : 2S_c + S_m$  **do**
  - 4:   **for**  $t = 1 : S$  **do**
  - 5:      $\hat{F}_{sum} = \hat{F}_{sum} + \hat{f}_t$ ;
  - 6:     **if**  $\hat{F}_{sum} \geq ptr$  **then**
  - 7:       Select the individual  $t$  as a parent and then break;
  - 8:     **end if**
  - 9:   **end for**
  - 10:    $\hat{F}_{sum} = 0$ ,  $ptr = ptr + \frac{1}{(2S_c + S_m)}$ ;
  - 11: **end for**
- 

**4) Crossover and mutation:** Based on the selected parents,  $S_c$  crossover offspring and  $S_m$  mutation offspring are reproduced according to Algorithm 2. Then, the current population can evolve to the next generation, which is composed of  $S_e$  elite individuals,  $S_c$  crossover offspring and  $S_m$  mutation offspring.

---

**Algorithm 2** Crossover and Mutation.

---

- 1: Input  $2S_c + S_m$  selected parents and disturb their order;
  - 2: **for**  $i = 1 : S_c$  **do**
  - 3:   Select the  $(2i - 1)$ -th and the  $2i$ -th parents. Assume that their chromosome is  $\Phi^{2i-1}$  and  $\Phi^{2i}$ , respectively;
  - 4:   Generate an integer crossover point  $s$  randomly from  $[1, N - 1]$ ;
  - 5:   Crossover the chromosome of two parents at point  $s$  to generate the  $i$ -th offspring. The offspring has the chromosome  $\text{diag} \left\{ e^{j\theta_1^{2i-1}}, \dots, e^{j\theta_s^{2i-1}}, e^{j\theta_{s+1}^{2i}}, \dots, e^{j\theta_N^{2i}} \right\}$ ;
  - 6: **end for**
  - 7: **for**  $i = 2S_c + 1 : S_m$  **do**
  - 8:   Select the  $i$ -th parent;
  - 9:   Reproduce the  $i$ -th offspring by mutating each gene of the  $i$ -th parent with a probability  $p_m$ . The mutated gene is generated randomly from  $[0, 2\pi)$ ;
  - 10: **end for**
- 

**5) Stopping criterion:** If the number of generations is higher than  $100N$  or the average change of the raw fitness is lower than  $10^{-4}$ , the GA is stopped. The output of the GA algorithm is the chromosome of the individual having the highest raw fitness in the current population. The obtained chromosome is the set of optimal phase shifts of the RIS. Otherwise, the GA is repeated from Step 2.

## VI. NUMERICAL RESULTS

In this section, we illustrate some numerical simulations in order to verify the analytical findings, and to characterize the impact of key design parameters on the performance of RIS-aided massive MIMO systems. The analytical results are obtained by using Theorem 2 and related corollaries, and the RIS phase shifts are optimized by using the GA to solve the problem in (70). The Monte Carlo simulation results are obtained from (35) by computing the sample average over  $10^5$  random channel realizations. We assume that  $K = 8$  users are evenly distributed on a semicircle centered at the RIS and of a radius  $d_{UI} = 20$  m. The distance between the RIS and the BS is  $d_{IB} = 700$  m. The distance between the user  $k$  and the BS are obtained from geometric relationship, i.e.,  $(d_k^{\text{UB}})^2 = (d_{IB} - d_{UI} \cos(\frac{\pi}{9}k))^2 + (d_{UI} \sin(\frac{\pi}{9}k))^2$ . The path-loss exponent of the direct links is larger than the path-loss exponent of the RIS-assisted links in

TABLE III: Simulation parameters.

$(\varphi_t^a, \varphi_t^e)$	(4.17, 0.09)	$(\phi_r^a, \phi_r^e)$	(6.28, 4.21)
$(\varphi_{1r}^a, \varphi_{1r}^e)$	(5.20, 4.32)	$(\varphi_{2r}^a, \varphi_{2r}^e)$	(0.41, 2.52)
$(\varphi_{3r}^a, \varphi_{3r}^e)$	(3.84, 1.78)	$(\varphi_{4r}^a, \varphi_{4r}^e)$	(1.35, 4.15)
$(\varphi_{5r}^a, \varphi_{5r}^e)$	(5.08, 5.76)	$(\varphi_{6r}^a, \varphi_{6r}^e)$	(4.75, 1.56)
$(\varphi_{7r}^a, \varphi_{7r}^e)$	(4.74, 5.36)	$(\varphi_{8r}^a, \varphi_{8r}^e)$	(0.09, 1.40)
BS antennas	$M = 64$	RIS elements	$N = 64$
Transmit power	$p = 30$ dBm	Noise power	$\sigma^2 = -104$ dBm
Rician factors	$\delta = 1, \varepsilon_k = 10, \forall k$		
GA parameters	$S = 200, S_e = 10, S_c = 152, S_m = 38, p_m = 0.1$		

order to characterize the more severe signal attenuation due to the presence of blockages on the ground. Accordingly, we set the distance-dependent path-loss factors equal to  $\alpha_k = 10^{-3}d_{\text{UI}}^{-2}$ ,  $\beta = 10^{-3}d_{\text{IB}}^{-2.5}$  and  $\gamma_k = 10^{-3}(d_k^{\text{UB}})^{-4}, \forall k$ . The number of symbols in each channel coherence time interval is  $\tau_c = 196$  [55], [56], and  $\tau = K = 8$  symbols are utilized for channel estimation. The other simulation parameters (unless stated otherwise) are listed in Table III.

#### A. Quality of LMMSE Channel Estimation

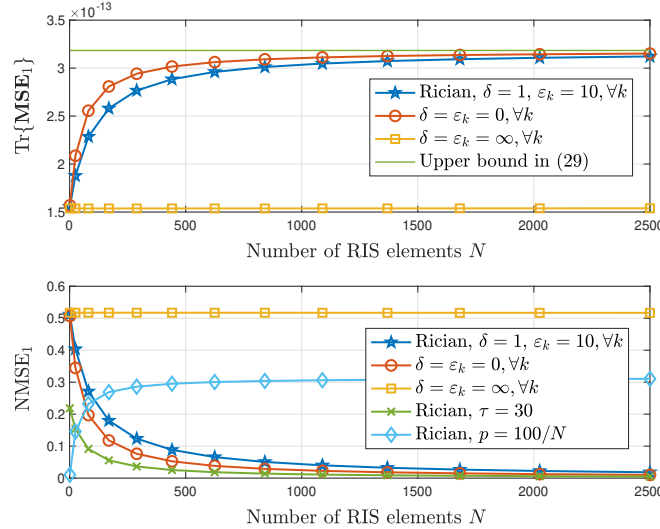


Fig. 2: MSE and NMSE of user 1 versus the number of RIS elements.

To begin with, we investigate the MSE and NMSE performance of the proposed channel estimation scheme. The MSE and NMSE of the channel estimation algorithm of the  $k$ -th user

are characterized through the functions  $\text{Tr}\{\mathbf{MSE}_k\}$  and  $\text{NMSE}_k$ , respectively. Without loss of generality, Fig. 2 illustrates the MSE and NMSE of user 1 versus the number of RIS elements  $N$ . In general Rician channels, we observe that the MSE is an increasing function of  $N$  while the NMSE is a decreasing function of  $N$ , which is consistent with Corollaries 1, 2 and 3. This is because the number of communication paths increases with  $N$ , but the pilot length  $\tau$  does not increase correspondingly, which increases the estimation error. However, the intensity of the channel gains increases with  $N$ , which, in turn, decreases the normalized errors. In purely LoS RIS-assisted channels ( $\delta = \varepsilon_k \rightarrow \infty$ ), the MSE and NMSE are, on the other hand, independent of  $N$ . This is because LoS channels are deterministic, and therefore do not introduce additional estimation errors. Also, we see that the MSE tends to an upper bound but the NMSE tends to zero when  $N \rightarrow \infty$ , which validates Corollary 1 and 2. Besides, by increasing the length of the pilot signals from 8 to 30, we see that the NMSE decreases. However, the NMSE that is obtained for  $\tau = 30$  can also be obtained for  $\tau = 8$  but by using a larger value for  $N$ . This validates that the increase of the RIS elements can play a similarly role as increasing  $\tau$ . Finally, we see that the NMSE tends to a limit less than 1 when the transmit power is scaled proportionally to  $p = 100/N$ , as  $N \rightarrow \infty$ . This validates the correctness of (26).

### B. Single-user Case

Next, we evaluate the ergodic achievable rate in the single-user scenario, where only user 1 is present.

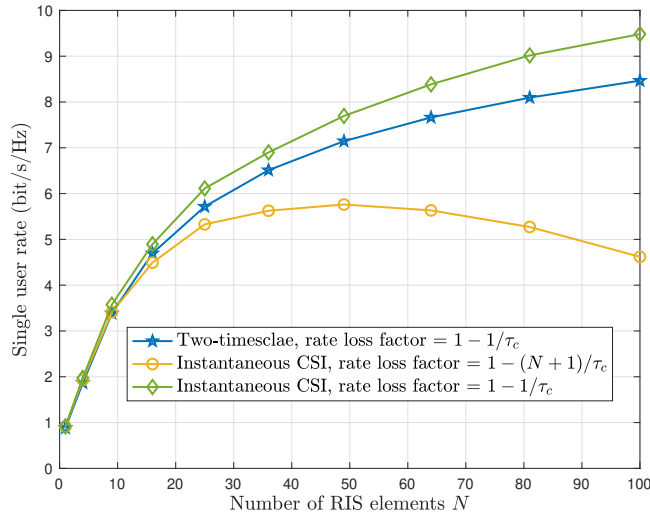


Fig. 3: Comparison of the two-timescale design and instantaneous CSI-based design.

In Fig. 3, we compare the proposed two-timescale scheme with the conventional instantaneous CSI-based scheme. The implementation of the instantaneous CSI-based scheme is detailed in Appendix G, where  $T_{ci} = 100$  is set in (201) and (202). By assuming the same rate loss factor (ideal but not achievable), it is seen that the instantaneous CSI-based scheme outperforms the proposed two-timescale scheme, especially when  $N$  is large. This is because the LoS and NLoS channel components are both exploited in the instantaneous CSI-based RIS design. By contrast, the fast-fading NLoS channel information is not used in the proposed statistical CSI-based RIS design. When considering the practical channel estimation overhead, however, the proposed scheme outperforms the instantaneous CSI-based scheme. This is because the instantaneous CSI-based scheme requires a longer pilot length, which is proportional to  $N$ , even though it can achieve a higher SNR. When  $N$  is large, the instantaneous CSI-based scheme needs a large number of time slots to transmit the pilot sequence, and then only a few symbols are left for data transmission. As a result of the high estimation overhead, the instantaneous CSI-based scheme incurs in a rate loss, which leads to a severe decrease of the rate in the large  $N$  regime. Therefore, Fig. 3 validates the effectiveness of the proposed two-timescale scheme.

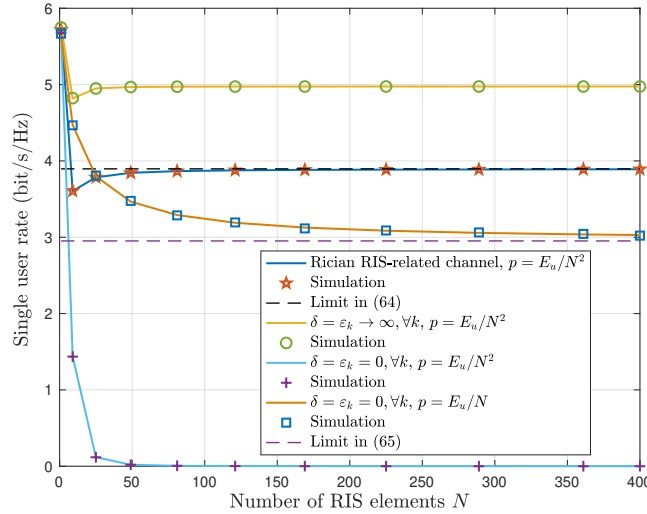


Fig. 4: Rate versus  $N$  in a single-user system. The transmit power is scaled as  $p = E_u/N^2$  or  $p = E_u/N$ , where  $E_u = 20$  dB.

In Fig. 4, we illustrate the power scaling law as a function of  $N$  in a single-user system. In agreement with Corollary 9, the rate converges to a limit if we reduce the power proportionally to  $1/N^2$  in Rician fading channels. Also, the limit is maximized in LoS-only RIS-assisted channels ( $\delta = \varepsilon_k \rightarrow \infty$ ). In NLoS-only RIS-assisted channels ( $\delta = \varepsilon_k = 0$ ), scaling the power



proportionally to  $1/N^2$  reduces the rate to zero. As proved in Corollary 10, in NLoS-only RIS-assisted channels, the power can only be scaled proportionally to  $1/N$  for maintaining a non-zero rate. These observations highlight that LoS environments are preferable for the deployment of RIS-aided single-user systems.

### C. Multi-user Case

In the following, we evaluate the performance of RIS-aided systems in the general multi-user scenario.

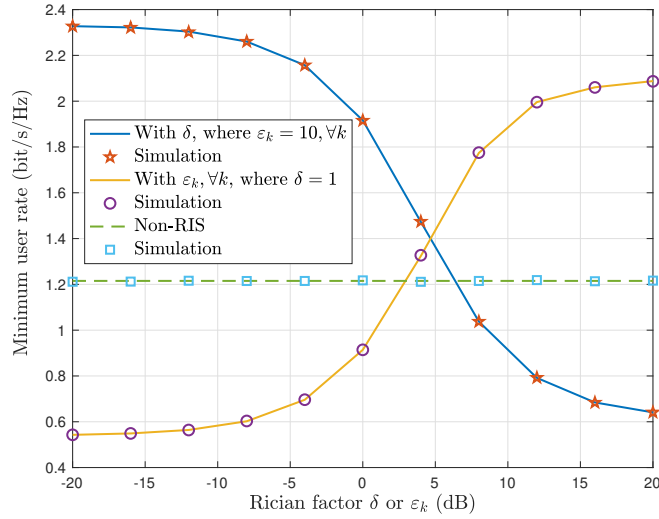


Fig. 5: Minimum user rate versus the Rician factor  $\delta$  or  $\epsilon_k, \forall k$ .

Fig. 5 shows the impact of the Rician factors. It can be observed that the achievable rate is a decreasing function of  $\delta$  but an increasing function of  $\epsilon_k, \forall k$ . This is because the rank of the LoS channel  $\bar{\mathbf{H}}_2$  between the RIS and the BS is 1, while the rank of the LoS channel  $\bar{\mathbf{H}}_1$  between the users and the RIS is not. When  $\delta \rightarrow \infty$ , the rank of the RIS-BS channel tends to 1, which leads to a rank-1 cascaded user-RIS-BS channel. As a result, the RIS-assisted channel becomes rank-deficient, which cannot effectively sustain the transmission of multiple users simultaneously. By contrast, for small values of  $\delta$ , the RIS-BS channel could have a high rank, which increases the achievable spatial multiplexing gains. To sum up, Fig. 5 indicates that a rich-scattering environment between the RIS and the BS and the absence of rich scattering between the users and the RIS are beneficial for RIS-aided massive MIMO systems. According to 3GPP channel models [64], the Rician factor is usually a decreasing function of the transmission distance. Therefore, it is preferable to deploy an RIS in the close proximity of the users rather

than in the close proximity of the BS, since this placement strategy leads to both a small  $\delta$  and a large  $\varepsilon_k$ .

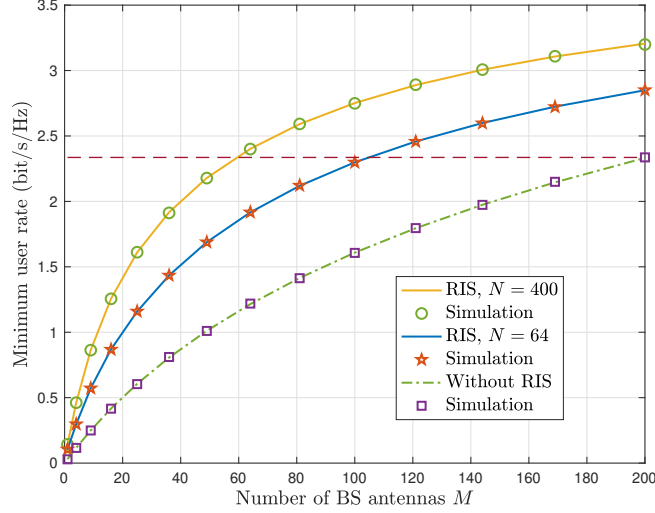


Fig. 6: Minimum user rate versus  $M$ .

In Fig. 6, we evaluate the rate as a function of the number of BS antennas. This figure illustrates the impact of deploying an RIS in conventional massive MIMO systems. It is observed that the deployment of an RIS effectively improves the rate, and the improvement increases with the number of RIS elements. It is worth nothing that this performance gain is obtained by using a simple MRC receiver at the BS, and that the LMMSE channel estimator requires the same amount of overhead as conventional massive MIMO systems. With the help of an RIS, we can achieve the same rate as conventional massive MIMO systems, but with a much smaller number of BS antennas. In particular, the rate obtained by a 200-antenna BS in conventional massive MIMO systems can be obtained by a 100-antenna BS in RIS-aided massive MIMO systems with  $N = 64$  RIS elements. The number of BS antennas can be further decreased to  $M = 64$  if the number of RIS elements is increased to  $N = 400$ . Since the cost and energy consumption of one RIS element is much lower than that of one BS antenna, we conclude that the integration of RISs in conventional massive MIMO systems is a promising and cost-effective solution for future wireless communication systems.

Fig. 7 illustrates the rate as a function of the number of RIS elements  $N$  for three channel models: general Rician channels, the NLoS-only channels ( $\delta = 0$  or  $\varepsilon_k = 0, \forall k$ ), and the LoS-only channels ( $\delta \rightarrow \infty$  or  $\varepsilon_k \rightarrow \infty, \forall k$ ). Over the general Rician channels, RIS-aided massive MIMO systems significantly enhance the minimum user rate compared with conventional massive

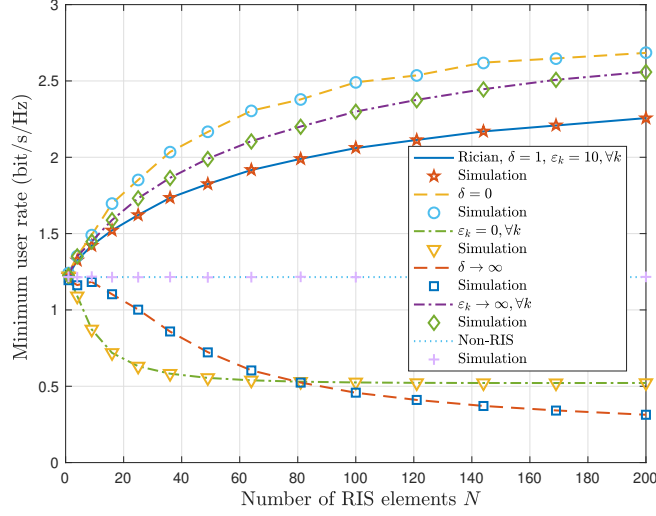


Fig. 7: Minimum user rate versus  $N$ .

MIMO systems. Fig. 7 also shows that the deployment location of the RIS needs to be carefully chosen. In particular, for small values of  $\delta$  and large values of  $\varepsilon_k$ , increasing  $N$  enhances the minimum rate. On the contrary, for large values of  $\delta$  and small values of  $\varepsilon_k$ , the increase of  $N$  results in a decrease of the minimum user rate.

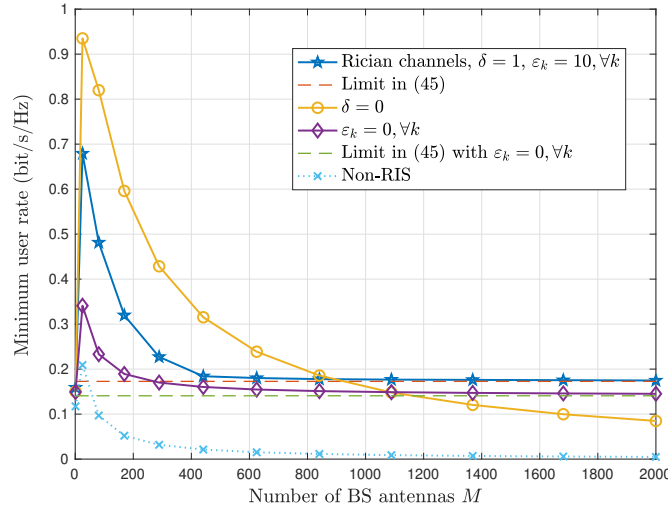


Fig. 8: Minimum user rate versus  $M$ , when the transmit power is scaled as  $p = E_u/M$ ,  $E_u = 10$  dB.

Fig. 8 illustrates the power scaling law when the transmit power  $p$  is scaled proportionally to  $1/M$ . In Rician channels and Rayleigh user-RIS channels ( $\varepsilon_k = 0, \forall k$ ), the rate can maintain a non-zero value as  $M \rightarrow \infty$ . In Rayleigh RIS-BS channel ( $\delta = 0$ ) and in non-RIS-aided systems, on the other hand, the rate reduces to zero as  $M \rightarrow \infty$ . These observations are consistent with

Corollary 4.

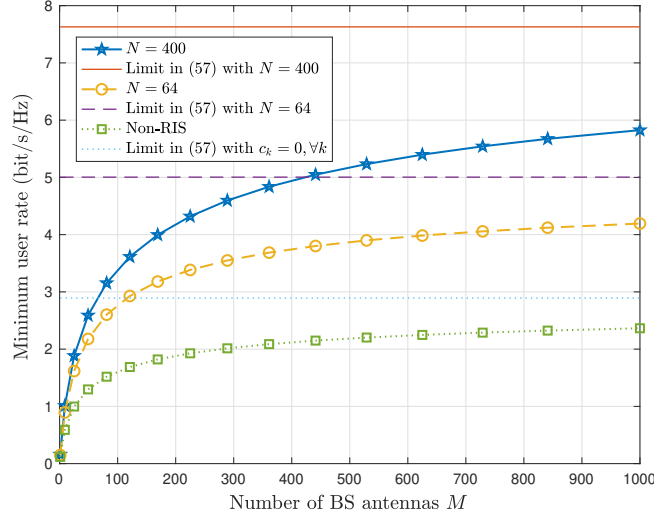


Fig. 9: Minimum user rate versus  $M$  when  $\delta = 0$ . The transmit power is scaled as  $p = E_u/\sqrt{M}$ , where  $E_u = 10$  dB.

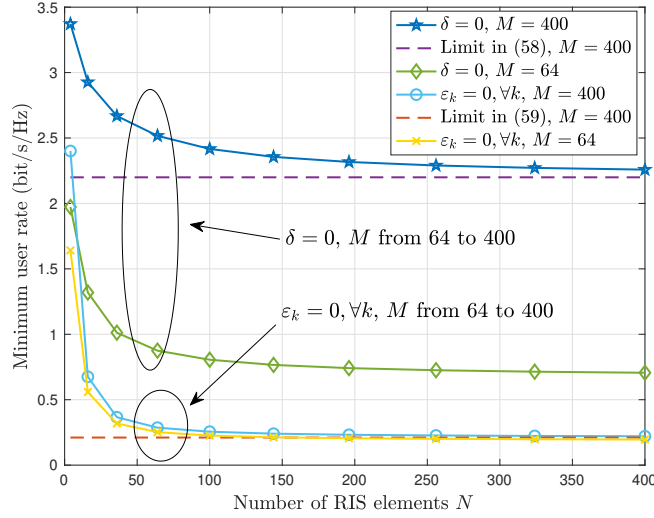


Fig. 10: Minimum user rate versus  $N$  when  $\delta = 0$  or  $\varepsilon_k = 0$ . The transmit power is scaled as  $p = E_u/N$ , where  $E_u = 10$  dB.

In Fig. 9 and Fig. 10, finally, we investigate the power scaling law over the purely NLoS RIS-BS channel ( $\delta = 0$ ) and the purely NLoS user-RIS channels ( $\varepsilon_k = 0, \forall k$ ). In Fig. 9, the transmit power is scaled proportionally to  $1/\sqrt{M}$  for the NLoS RIS-BS channel ( $\delta = 0$ ). In agreement with Corollary 6, if  $\delta = 0$ , the rate can be maintained to a non-zero value when the power is scaled proportionally to  $1/\sqrt{M}$  as  $M \rightarrow \infty$ . Compared with conventional massive MIMO

systems, the deployment of an RIS effectively improves the asymptotic limit when  $M \rightarrow \infty$ , and the rate gain could be further improved by increasing  $N$ .

In Fig. 10, the transmit power is scaled proportionally to  $1/N$  over the purely NLoS RIS-BS channel ( $\delta = 0$ ) or purely NLoS user-RIS channels ( $\varepsilon_k = 0, \forall k$ ). For  $N \rightarrow \infty$ , the rate maintains a non-zero value, which is consistent with Corollaries 7 and 8. Besides, in agreement with Corollary 7, the asymptotic limit for  $\delta = 0$  when  $N \rightarrow \infty$  can be significantly improved by increasing the number of BS antennas from  $M = 64$  to  $M = 400$ . This is because the RIS-BS channel has a high rank if  $\delta = 0$ , which decreases the spatial correlation among the users and mitigates the multi-user interference. Furthermore, in agreement with Corollary 8, the asymptotic limit for  $\varepsilon_k = 0, \forall k$  when  $N \rightarrow \infty$  only marginally increases when increasing  $M$  from 64 to 400. This observation confirms once again that it is preferable to deploy an RIS near the users, rather than near the BS.

## VII. CONCLUSION

This paper has investigated a two-timescale design for RIS-aided massive MIMO systems by taking into account the channel estimation errors. An LMMSE estimator has been proposed for obtaining the instantaneous CSI of the  $M \times K$  RIS-assisted aggregated channel, whose channel estimates are used by the BS for MRC. We have derived a closed-form expression for the ergodic achievable rate, and have studied the power scaling laws. Based on the derived analytical expressions, we have designed the RIS phase shifts by relying only on statistical CSI, which significantly reduces the signaling overhead and the computational complexity. For the single-user case, we have obtained a closed-form optimal solution. For the general multi-user case, we have adopted a GA for solving the minimum user rate maximization problem. The obtained numerical results show that the transmit power can be reduced proportionally to  $1/M$ , while maintaining a non-zero rate, as  $M \rightarrow \infty$  over RIS-BS Rician channels. If the RIS-BS channel is Rayleigh distributed, on the other hand, a non-zero rate can be maintained when the power is scaled proportionally to  $1/\sqrt{M}$  as  $M \rightarrow \infty$  or proportionally to  $1/N$  as  $N \rightarrow \infty$ . Finally, we have proved that it is preferable to deploy the RIS close to the users rather than close to the BS.

APPENDIX A  
SOME USEFUL RESULTS

**Lemma 4** Consider a matrix  $\mathbf{X} \in \mathbb{C}^{m \times n}$ ,  $m, n \geq 1$ , whose entries are i.i.d. random variables with zero mean and  $v_x$  variance. Consider a deterministic matrix  $\mathbf{W} \in \mathbb{C}^{n \times n}$ . Then, we have

$$\mathbb{E} \{ \mathbf{X} \mathbf{W} \mathbf{X}^H \} = v_x \text{Tr}\{\mathbf{W}\} \mathbf{I}_m. \quad (72)$$

*Proof:* Consider the matrix  $\mathbf{X} \mathbf{W} \mathbf{X}^H$ . The expectation of its  $(i, j)$ -th entry, where  $i \neq j$ , is given by

$$[\mathbb{E} \{ \mathbf{X} \mathbf{W} \mathbf{X}^H \}]_{ij} = \mathbb{E} \left\{ \sum_{l=1}^n \sum_{k=1}^n \mathbf{X}_{ik} \mathbf{W}_{kl} [\mathbf{X}^H]_{lj} \right\} = \sum_{l=1}^n \sum_{k=1}^n \mathbb{E} \{ \mathbf{X}_{ik} \mathbf{X}_{jl}^* \} \mathbf{W}_{kl} = 0. \quad (73)$$

Similarly, the expectation of its  $(i, i)$ -th entry is

$$[\mathbb{E} \{ \mathbf{X} \mathbf{W} \mathbf{X}^H \}]_{ii} = \sum_{l=1}^n \sum_{k=1}^n \mathbb{E} \{ \mathbf{X}_{ik} \mathbf{X}_{il}^* \} \mathbf{W}_{kl} = \sum_{k=1}^n \mathbb{E} \{ |\mathbf{X}_{ik}|^2 \} \mathbf{W}_{kk} = v_x \text{Tr}\{\mathbf{W}\}. \quad (74)$$

Therefore, the expectation of  $\mathbf{X} \mathbf{W} \mathbf{X}^H$  is a diagonal matrix and its diagonal entries are all equal to  $v_x \text{Tr}\{\mathbf{W}\}$ . This completes the proof.  $\blacksquare$

By letting  $m = 1$  or  $n = 1$ , corresponding results for random vectors can be obtained.

**Lemma 5** Consider the deterministic matrices  $\mathbf{W} \in \mathbb{C}^{N \times N}$  and vectors  $\mathbf{w}_1, \mathbf{w}_2 \in \mathbb{C}^{N \times 1}$ , and  $\mathbf{w}_3, \mathbf{w}_4 \in \mathbb{C}^{M \times 1}$ . Then, we have

$$\mathbb{E} \{ \tilde{\mathbf{H}}_2 \mathbf{W} \tilde{\mathbf{H}}_2 \} = \mathbb{E} \left\{ \text{Re} \left\{ \tilde{\mathbf{H}}_2 \mathbf{W} \tilde{\mathbf{H}}_2 \right\} \right\} = \mathbf{0}, \quad (75)$$

$$\mathbb{E} \left\{ \tilde{\mathbf{h}}_k^H \mathbf{w}_1 \tilde{\mathbf{h}}_k^H \mathbf{w}_2 \right\} = \mathbb{E} \left\{ \text{Re} \left\{ \tilde{\mathbf{h}}_k^H \mathbf{w}_1 \tilde{\mathbf{h}}_k^H \mathbf{w}_2 \right\} \right\} = 0, \quad (76)$$

$$\mathbb{E} \left\{ \mathbf{w}_3^H \tilde{\mathbf{d}}_k \mathbf{w}_4^H \tilde{\mathbf{d}}_k \right\} = \mathbb{E} \left\{ \text{Re} \left\{ \mathbf{w}_3^H \tilde{\mathbf{d}}_k \mathbf{w}_4^H \tilde{\mathbf{d}}_k \right\} \right\} = 0. \quad (77)$$

*Proof:* Let us consider a complex random variable  $v = v_r + jv_i$  with  $v_r, v_i \sim \mathcal{N}(0, 1/2)$ . Noting that for complex random variables, different from the result that  $\mathbb{E} \{ |v|^2 \} = \mathbb{E} \{ v_r^2 \} + \mathbb{E} \{ v_i^2 \} = 1$ , we have

$$\mathbb{E} \{ v^2 \} = \mathbb{E} \{ v_r^2 - v_i^2 + 2jv_r v_i \} = \mathbb{E} \{ v_r^2 \} - \mathbb{E} \{ v_i^2 \} + 2j\mathbb{E} \{ v_r \} \mathbb{E} \{ v_i \} = 0, \quad (78)$$

$$\mathbb{E} \{ \text{Re} \{ v^2 \} \} = \mathbb{E} \{ v_r^2 \} - \mathbb{E} \{ v_i^2 \} = 0. \quad (79)$$

The entries of  $\tilde{\mathbf{H}}_2$  are i.i.d., each having the same distribution as  $v$ . Then, we have

$$\mathbb{E} \left\{ \left[ \tilde{\mathbf{H}}_2 \mathbf{W} \tilde{\mathbf{H}}_2 \right]_{n1, n2} \right\} = \mathbb{E} \left\{ \sum_{i=1}^N \sum_{m=1}^N \left[ \tilde{\mathbf{H}}_2 \right]_{n1, m} \mathbf{W}_{m, i} \left[ \tilde{\mathbf{H}}_2 \right]_{i, n2} \right\}. \quad (80)$$

For  $(n1, m) \neq (i, n2)$  in (80), the expectation is zero, since the entries are independent and zero-mean. For  $(n1, m) = (i, n2)$  in (80), the expectation is zero by using (78). Therefore, (75) is proved. Equations (76) and (77) can be proved *mutatis mutandis*.

**Lemma 6** Consider a deterministic matrix  $\mathbf{W} \in \mathbb{C}^{N \times N}$ . Then, we have

$$\mathbb{E} \left\{ \tilde{\mathbf{H}}_2^H \mathbf{A}_k \tilde{\mathbf{H}}_2 \mathbf{W} \tilde{\mathbf{H}}_2^H \mathbf{A}_k \tilde{\mathbf{H}}_2 \right\} = e_{k1}^2 M^2 \mathbf{W} + e_{k3} M \text{Tr}\{\mathbf{W}\} \mathbf{I}_N, \quad (81)$$

where  $\tilde{\mathbf{H}}_2$  and  $\mathbf{A}_k$  are defined in (6) and (18), respectively, and  $e_{k1}$  and  $e_{k3}$  are defined in Lemma 2.

*Proof:* Before the derivation, we first introduce some useful results. Define  $\tilde{\mathbf{H}}_2 = [\mathbf{J}_1, \dots, \mathbf{J}_N]$ , where  $\mathbf{J}_n \in \mathbb{C}^{M \times 1}$  with  $1 \leq n \leq N$  are independent of each other, and  $\mathbf{J}_n \sim \mathcal{CN}(\mathbf{0}, \mathbf{I}_M)$ . Then, we have  $\tilde{\mathbf{H}}_2^H \mathbf{a}_M = [\mathbf{J}_1^H \mathbf{a}_M; \dots; \mathbf{J}_N^H \mathbf{a}_M] \in \mathbb{C}^{N \times 1}$ , and  $\tilde{\mathbf{H}}_2^H \mathbf{a}_M \sim \mathcal{CN}(\mathbf{0}, M \mathbf{I}_N)$ . Therefore, using the definition of the complex central Wishart distribution [67, (1)], we have

$$\mathbf{J}_n \mathbf{J}_n^H \sim \mathcal{CW}_M(\mathbf{I}_M, 1), 1 \leq n \leq N, \quad (82)$$

$$\tilde{\mathbf{H}}_2^H \tilde{\mathbf{H}}_2 \sim \mathcal{CW}_N(\mathbf{I}_N, M), \quad (83)$$

$$\tilde{\mathbf{H}}_2^H \mathbf{a}_M \mathbf{a}_M^H \tilde{\mathbf{H}}_2 \sim \mathcal{CW}_N(M \mathbf{I}_N, 1). \quad (84)$$

Then, by exploiting the properties of the complex Wishart distribution [67, Table 1], for deterministic matrices  $\mathbf{F} \in \mathbb{C}^{M \times M}$  and  $\mathbf{W} \in \mathbb{C}^{N \times N}$ , we have

$$\mathbb{E} \left\{ \mathbf{J}_n \mathbf{J}_n^H \mathbf{F} \mathbf{J}_n \mathbf{J}_n^H \right\} = \mathbf{F} + \text{Tr}\{\mathbf{F}\} \mathbf{I}_M, 1 \leq n \leq N, \quad (85)$$

$$\mathbb{E} \left\{ \tilde{\mathbf{H}}_2^H \tilde{\mathbf{H}}_2 \mathbf{W} \tilde{\mathbf{H}}_2^H \tilde{\mathbf{H}}_2 \right\} = M^2 \mathbf{W} + M \text{Tr}\{\mathbf{W}\} \mathbf{I}_N, \quad (86)$$

$$\mathbb{E} \left\{ \tilde{\mathbf{H}}_2^H \mathbf{a}_M \mathbf{a}_M^H \tilde{\mathbf{H}}_2 \mathbf{W} \tilde{\mathbf{H}}_2^H \mathbf{a}_M \mathbf{a}_M^H \tilde{\mathbf{H}}_2 \right\} = M^2 \mathbf{W} + M^2 \text{Tr}\{\mathbf{W}\} \mathbf{I}_N. \quad (87)$$

By letting  $\mathbf{F} = \mathbf{I}_M$ , we also have

$$\mathbb{E} \left\{ \|\mathbf{J}_n\|^4 \right\} = \text{Tr} \left\{ \mathbb{E} \left\{ \mathbf{J}_n \mathbf{J}_n^H \mathbf{J}_n \mathbf{J}_n^H \right\} \right\} = M^2 + M. \quad (88)$$

We can now move to the proof of the lemma. By invoking  $\mathbf{A}_k = a_{k3} \mathbf{a}_M \mathbf{a}_M^H + a_{k4} \mathbf{I}_M$ , we have

$$\begin{aligned} & \mathbb{E} \left\{ \tilde{\mathbf{H}}_2^H \mathbf{A}_k \tilde{\mathbf{H}}_2 \mathbf{W} \tilde{\mathbf{H}}_2^H \mathbf{A}_k \tilde{\mathbf{H}}_2 \right\} \\ &= \mathbb{E} \left\{ \left( a_{k3} \tilde{\mathbf{H}}_2^H \mathbf{a}_M \mathbf{a}_M^H \tilde{\mathbf{H}}_2 + a_{k4} \tilde{\mathbf{H}}_2^H \tilde{\mathbf{H}}_2 \right) \mathbf{W} \left( a_{k3} \tilde{\mathbf{H}}_2^H \mathbf{a}_M \mathbf{a}_M^H \tilde{\mathbf{H}}_2 + a_{k4} \tilde{\mathbf{H}}_2^H \tilde{\mathbf{H}}_2 \right) \right\} \\ &= a_{k3}^2 \mathbb{E} \left\{ \tilde{\mathbf{H}}_2^H \mathbf{a}_M \mathbf{a}_M^H \tilde{\mathbf{H}}_2 \mathbf{W} \tilde{\mathbf{H}}_2^H \mathbf{a}_M \mathbf{a}_M^H \tilde{\mathbf{H}}_2 \right\} + a_{k3} a_{k4} \mathbb{E} \left\{ \tilde{\mathbf{H}}_2^H \mathbf{a}_M \mathbf{a}_M^H \tilde{\mathbf{H}}_2 \mathbf{W} \tilde{\mathbf{H}}_2^H \tilde{\mathbf{H}}_2 \right\} \\ & \quad + a_{k3} a_{k4} \mathbb{E} \left\{ \tilde{\mathbf{H}}_2^H \tilde{\mathbf{H}}_2 \mathbf{W} \tilde{\mathbf{H}}_2^H \mathbf{a}_M \mathbf{a}_M^H \tilde{\mathbf{H}}_2 \right\} + a_{k4}^2 \mathbb{E} \left\{ \tilde{\mathbf{H}}_2^H \tilde{\mathbf{H}}_2 \mathbf{W} \tilde{\mathbf{H}}_2^H \tilde{\mathbf{H}}_2 \right\}. \end{aligned} \quad (89)$$

In the following, we calculate the four expectations in (89) one by one. Using (87), the first expectation is given by

$$\mathbb{E} \left\{ \tilde{\mathbf{H}}_2^H \mathbf{a}_M \mathbf{a}_M^H \tilde{\mathbf{H}}_2 \mathbf{W} \tilde{\mathbf{H}}_2^H \mathbf{a}_M \mathbf{a}_M^H \tilde{\mathbf{H}}_2 \right\} = M^2 \mathbf{W} + M^2 \text{Tr}\{\mathbf{W}\} \mathbf{I}_N. \quad (90)$$

As for the second expectation, its  $(n1, n2)$ -th entry can be expanded as

$$\begin{aligned} & \left[ \tilde{\mathbf{H}}_2^H \mathbf{a}_M \mathbf{a}_M^H \tilde{\mathbf{H}}_2 \mathbf{W} \tilde{\mathbf{H}}_2^H \tilde{\mathbf{H}}_2 \right]_{n1, n2} \\ &= \sum_{h=1}^N \sum_{m=1}^N \left[ \tilde{\mathbf{H}}_2^H \mathbf{a}_M \mathbf{a}_M^H \tilde{\mathbf{H}}_2 \right]_{n1, m} [\mathbf{W}]_{m, h} \left[ \tilde{\mathbf{H}}_2^H \tilde{\mathbf{H}}_2 \right]_{h, n2} \\ &= \sum_{h=1}^N \sum_{m=1}^N \mathbf{J}_{n1}^H \mathbf{a}_M \mathbf{a}_M^H \mathbf{J}_m [\mathbf{W}]_{m, h} \mathbf{J}_h^H \mathbf{J}_{n2}. \end{aligned} \quad (91)$$

Consider the non-diagonal entries, i.e., for  $n1 \neq n2$  in (91). Using Lemma 4 and Lemma 5, we can identify the non-zero expectation as follows

$$\mathbb{E} \left\{ \left[ \tilde{\mathbf{H}}_2^H \mathbf{a}_M \mathbf{a}_M^H \tilde{\mathbf{H}}_2 \mathbf{W} \tilde{\mathbf{H}}_2^H \tilde{\mathbf{H}}_2 \right]_{n1, n2} \right\} = [\mathbf{W}]_{n1, n2} \mathbb{E} \left\{ \mathbf{J}_{n1}^H \mathbf{a}_M \mathbf{a}_M^H \mathbf{J}_{n1} \right\} \mathbb{E} \left\{ \mathbf{J}_{n2}^H \mathbf{J}_{n2} \right\} = M^2 [\mathbf{W}]_{n1, n2}. \quad (92)$$

Then, consider the diagonal entries, i.e., for  $n1 = n2$  in (91). The expectation is

$$\begin{aligned} & \mathbb{E} \left\{ \left[ \tilde{\mathbf{H}}_2^H \mathbf{a}_M \mathbf{a}_M^H \tilde{\mathbf{H}}_2 \mathbf{W} \tilde{\mathbf{H}}_2^H \tilde{\mathbf{H}}_2 \right]_{n1, n1} \right\} \\ &= [\mathbf{W}]_{n1, n1} \text{Tr} \left\{ \mathbf{a}_M \mathbf{a}_M^H \mathbb{E} \left\{ \mathbf{J}_{n1} \mathbf{J}_{n1}^H \mathbf{J}_{n1} \mathbf{J}_{n1}^H \right\} \right\} \\ &+ \sum_{h=1, h \neq n1}^N [\mathbf{W}]_{h, h} \mathbb{E} \left\{ \mathbf{J}_{n1}^H \mathbf{a}_M \mathbf{a}_M^H \mathbb{E} \left\{ \mathbf{J}_h \mathbf{J}_h^H \right\} \mathbf{J}_{n1} \right\} \\ &\stackrel{(a)}{=} M^2 [\mathbf{W}]_{n1, n1} + M \text{Tr}\{\mathbf{W}\}. \end{aligned} \quad (93)$$

where (a) utilizes the (85). Combining (92) and (93), the expectation of the second term is

$$\mathbb{E} \left\{ \tilde{\mathbf{H}}_2^H \mathbf{a}_M \mathbf{a}_M^H \tilde{\mathbf{H}}_2 \mathbf{W} \tilde{\mathbf{H}}_2^H \tilde{\mathbf{H}}_2 \right\} = M^2 \mathbf{W} + M \text{Tr}\{\mathbf{W}\} \mathbf{I}_N. \quad (94)$$

Following a similar procedure as in the computation of the second term, we can derive the third expectation as follows

$$\mathbb{E} \left\{ \tilde{\mathbf{H}}_2^H \tilde{\mathbf{H}}_2 \mathbf{W} \tilde{\mathbf{H}}_2^H \mathbf{a}_M \mathbf{a}_M^H \tilde{\mathbf{H}}_2 \right\} = M^2 \mathbf{W} + M \text{Tr}\{\mathbf{W}\} \mathbf{I}_N. \quad (95)$$

The fourth expectation is given in (86), where

$$\mathbb{E} \left\{ \tilde{\mathbf{H}}_2^H \tilde{\mathbf{H}}_2 \mathbf{W} \tilde{\mathbf{H}}_2^H \tilde{\mathbf{H}}_2 \right\} = M^2 \mathbf{W} + M \text{Tr}\{\mathbf{W}\} \mathbf{I}_N. \quad (96)$$

The proof follows by substituting (90), (94), (95), and (96) into (89). ■



## APPENDIX B

Recalling the definition of  $\mathbf{q}_k$  in (10), where  $\tilde{\mathbf{H}}_2$ ,  $\tilde{\mathbf{h}}_k$ ,  $\tilde{\mathbf{d}}_k$ , and  $\mathbf{N}$  are independent of each other and composed of zero-mean entries, we have

$$\mathbb{E} \{ \mathbf{y}_p^k \} = \mathbb{E} \{ \mathbf{q}_k \} + \frac{1}{\sqrt{\tau p}} \mathbb{E} \{ \mathbf{N} \} \mathbf{s}_k = \mathbb{E} \{ \mathbf{q}_k \} = \sqrt{c_k \delta \varepsilon_k} \bar{\mathbf{H}}_2 \Phi \bar{\mathbf{h}}_k. \quad (97)$$

The covariance matrix between the unknown channel  $\mathbf{q}_k$  and the observation vector  $\mathbf{y}_p^k$  can be written as

$$\begin{aligned} \text{Cov} \{ \mathbf{q}_k, \mathbf{y}_p^k \} &= \mathbb{E} \left\{ (\mathbf{q}_k - \mathbb{E} \{ \mathbf{q}_k \}) (\mathbf{y}_p^k - \mathbb{E} \{ \mathbf{y}_p^k \})^H \right\} \\ &= \mathbb{E} \left\{ (\mathbf{q}_k - \mathbb{E} \{ \mathbf{q}_k \}) \left( \mathbf{q}_k + \frac{1}{\sqrt{\tau p}} \mathbf{N} \mathbf{s}_k - \mathbb{E} \{ \mathbf{q}_k \} \right)^H \right\} \\ &= \mathbb{E} \left\{ (\mathbf{q}_k - \mathbb{E} \{ \mathbf{q}_k \}) (\mathbf{q}_k - \mathbb{E} \{ \mathbf{q}_k \})^H \right\} \\ &= \text{Cov} \{ \mathbf{q}_k, \mathbf{q}_k \}, \end{aligned} \quad (98)$$

and

$$\text{Cov} \{ \mathbf{y}_p^k, \mathbf{q}_k \} = (\text{Cov} \{ \mathbf{q}_k, \mathbf{y}_p^k \})^H = (\text{Cov} \{ \mathbf{q}_k, \mathbf{q}_k \})^H = \text{Cov} \{ \mathbf{q}_k, \mathbf{q}_k \}. \quad (99)$$

Invoking the definition of  $\mathbf{q}_k$ , we obtain

$$\begin{aligned} \text{Cov} \{ \mathbf{q}_k, \mathbf{q}_k \} &= \mathbb{E} \left\{ (\mathbf{q}_k - \mathbb{E} \{ \mathbf{q}_k \}) (\mathbf{q}_k - \mathbb{E} \{ \mathbf{q}_k \})^H \right\} \\ &= \mathbb{E} \left\{ \begin{aligned} & \left( \sqrt{c_k \delta} \bar{\mathbf{H}}_2 \Phi \tilde{\mathbf{h}}_k + \sqrt{c_k \varepsilon_k} \tilde{\mathbf{H}}_2 \Phi \bar{\mathbf{h}}_k + \sqrt{c_k} \tilde{\mathbf{H}}_2 \Phi \tilde{\mathbf{h}}_k + \sqrt{\gamma_k} \tilde{\mathbf{d}}_k \right) \\ & \times \left( \sqrt{c_k \delta} \tilde{\mathbf{h}}_k^H \Phi^H \bar{\mathbf{H}}_2^H + \sqrt{c_k \varepsilon_k} \bar{\mathbf{h}}_k^H \Phi^H \tilde{\mathbf{H}}_2^H + \sqrt{c_k} \tilde{\mathbf{h}}_k^H \Phi^H \tilde{\mathbf{H}}_2^H + \sqrt{\gamma_k} \tilde{\mathbf{d}}_k^H \right) \end{aligned} \right\} \\ &= \mathbb{E} \left\{ c_k \delta \bar{\mathbf{H}}_2 \Phi \tilde{\mathbf{h}}_k \tilde{\mathbf{h}}_k^H \Phi^H \bar{\mathbf{H}}_2^H + c_k \varepsilon_k \tilde{\mathbf{H}}_2 \Phi \bar{\mathbf{h}}_k \bar{\mathbf{h}}_k^H \Phi^H \tilde{\mathbf{H}}_2^H + c_k \tilde{\mathbf{H}}_2 \Phi \tilde{\mathbf{h}}_k \tilde{\mathbf{h}}_k^H \Phi^H \tilde{\mathbf{H}}_2^H + \gamma_k \tilde{\mathbf{d}}_k \tilde{\mathbf{d}}_k^H \right\} \\ &\stackrel{(b)}{=} N c_k \delta \mathbf{a}_M \mathbf{a}_M^H + (N c_k (\varepsilon_k + 1) + \gamma_k) \mathbf{I}_M, \end{aligned} \quad (100)$$

where (b) exploits Lemma 4 and the mutual independence of  $\tilde{\mathbf{H}}_2$  and  $\tilde{\mathbf{h}}_k$ .

Similarly, we have

$$\begin{aligned} \text{Cov} \{ \mathbf{y}_p^k, \mathbf{y}_p^k \} &= \mathbb{E} \left\{ (\mathbf{y}_p^k - \mathbb{E} \{ \mathbf{y}_p^k \}) (\mathbf{y}_p^k - \mathbb{E} \{ \mathbf{y}_p^k \})^H \right\} \\ &= \mathbb{E} \left\{ \left( \mathbf{q}_k - \mathbb{E} \{ \mathbf{q}_k \} + \frac{1}{\sqrt{\tau p}} \mathbf{N} \mathbf{s}_k \right) \left( \mathbf{q}_k - \mathbb{E} \{ \mathbf{q}_k \} + \frac{1}{\sqrt{\tau p}} \mathbf{N} \mathbf{s}_k \right)^H \right\} \\ &= \mathbb{E} \left\{ (\mathbf{q}_k - \mathbb{E} \{ \mathbf{q}_k \}) (\mathbf{q}_k - \mathbb{E} \{ \mathbf{q}_k \})^H \right\} + \frac{1}{\tau p} \mathbb{E} \{ \mathbf{N} \mathbf{s}_k \mathbf{s}_k^H \mathbf{N}^H \} \\ &= \text{Cov} \{ \mathbf{q}_k, \mathbf{q}_k \} + \frac{\sigma^2}{\tau p} \mathbf{I}_M. \end{aligned} \quad (101)$$

Finally, by introducing the auxiliary variables of  $a_{k1} = N c_k \delta$  and  $a_{k2} = N c_k (\varepsilon_k + 1) + \gamma_k$ , the proof is completed.

## APPENDIX C

The LMMSE estimate of the channel  $\mathbf{q}_k$  based on the observation vector  $\mathbf{y}_p^k$  can be written as [68, Chapter 12.5]

$$\hat{\mathbf{q}}_k = \mathbb{E} \{ \mathbf{q}_k \} + \text{Cov} \{ \mathbf{q}_k, \mathbf{y}_p^k \} \text{Cov}^{-1} \{ \mathbf{y}_p^k, \mathbf{y}_p^k \} (\mathbf{y}_p^k - \mathbb{E} \{ \mathbf{y}_p^k \}), \quad (102)$$

where the mean and covariance matrices have been obtained in Lemma 1.

Let us compute  $\text{Cov}^{-1} \{ \mathbf{y}_p^k, \mathbf{y}_p^k \}$ . Using the Woodbury matrix identity [68, Page 571], we have

$$\begin{aligned} \text{Cov}^{-1} \{ \mathbf{y}_p^k, \mathbf{y}_p^k \} &= \left( a_{k1} \mathbf{a}_M \mathbf{a}_M^H + \left( a_{k2} + \frac{\sigma^2}{\tau p} \right) \mathbf{I}_M \right)^{-1} \\ &= \left( a_{k2} + \frac{\sigma^2}{\tau p} \right)^{-1} \mathbf{I}_M - \frac{a_{k1} \left( a_{k2} + \frac{\sigma^2}{\tau p} \right)^{-2}}{1 + M a_{k1} \left( a_{k2} + \frac{\sigma^2}{\tau p} \right)^{-1}} \mathbf{a}_M \mathbf{a}_M^H. \end{aligned} \quad (103)$$

As a result, we have

$$\begin{aligned} &\text{Cov} \{ \mathbf{q}_k, \mathbf{y}_p^k \} \text{Cov}^{-1} \{ \mathbf{y}_p^k, \mathbf{y}_p^k \} \\ &= (a_{k1} \mathbf{a}_M \mathbf{a}_M^H + a_{k2} \mathbf{I}_M) \left\{ \left( a_{k2} + \frac{\sigma^2}{\tau p} \right)^{-1} \mathbf{I}_M - \frac{a_{k1} \left( a_{k2} + \frac{\sigma^2}{\tau p} \right)^{-2}}{1 + M a_{k1} \left( a_{k2} + \frac{\sigma^2}{\tau p} \right)^{-1}} \mathbf{a}_M \mathbf{a}_M^H \right\} \\ &= \frac{a_{k1} \frac{\sigma^2}{\tau p}}{\left( a_{k2} + \frac{\sigma^2}{\tau p} \right) \left\{ \left( a_{k2} + \frac{\sigma^2}{\tau p} \right) + M a_{k1} \right\}} \mathbf{a}_M \mathbf{a}_M^H + \frac{a_{k2}}{a_{k2} + \frac{\sigma^2}{\tau p}} \mathbf{I}_M \\ &\triangleq a_{k3} \mathbf{a}_M \mathbf{a}_M^H + a_{k4} \mathbf{I}_M \triangleq \mathbf{A}_k = \mathbf{A}_k^H. \end{aligned} \quad (104)$$

Since we have  $\mathbb{E} \{ \mathbf{q}_k \} = \mathbb{E} \{ \mathbf{y}_p^k \} = \sqrt{c_k \delta \varepsilon_k} \bar{\mathbf{H}}_2 \Phi \bar{\mathbf{h}}_k$ , the LMMSE channel estimate in (102) is calculated as

$$\begin{aligned} \hat{\mathbf{q}}_k &= \sqrt{c_k \delta \varepsilon_k} \bar{\mathbf{H}}_2 \Phi \bar{\mathbf{h}}_k + \mathbf{A}_k (\mathbf{y}_p^k - \sqrt{c_k \delta \varepsilon_k} \bar{\mathbf{H}}_2 \Phi \bar{\mathbf{h}}_k) \\ &= \mathbf{A}_k \mathbf{y}_p^k + (\mathbf{I}_M - \mathbf{A}_k) \sqrt{c_k \delta \varepsilon_k} \bar{\mathbf{H}}_2 \Phi \bar{\mathbf{h}}_k \\ &\triangleq \mathbf{A}_k \mathbf{y}_p^k + \mathbf{B}_k. \end{aligned} \quad (105)$$

Additionally, we can expand the above linear expression and rewrite it as

$$\begin{aligned} \hat{\mathbf{q}}_k &= \mathbf{A}_k \left( \mathbf{q}_k + \frac{1}{\sqrt{\tau p}} \mathbf{N} \mathbf{s}_k \right) + \mathbf{B}_k \\ &= \mathbf{A}_k \left( \sum_{\omega=1}^4 \mathbf{q}_k^\omega + \sqrt{\gamma_k} \tilde{\mathbf{d}}_k + \frac{1}{\sqrt{\tau p}} \mathbf{N} \mathbf{s}_k \right) + (\mathbf{I}_M - \mathbf{A}_k) \mathbf{q}_k^1 \\ &= \mathbf{q}_k^1 + \sum_{\omega=2}^4 \mathbf{A}_k \mathbf{q}_k^\omega + \sqrt{\gamma_k} \mathbf{A}_k \tilde{\mathbf{d}}_k + \frac{1}{\sqrt{\tau p}} \mathbf{A}_k \mathbf{N} \mathbf{s}_k. \end{aligned} \quad (106)$$

Then, by exploiting the property  $\mathbf{A}_k \bar{\mathbf{H}}_2 = (a_{k3} \mathbf{a}_M \mathbf{a}_M^H + a_{k4} \mathbf{I}_M) \mathbf{a}_M \mathbf{a}_N^H = (M a_{k3} + a_{k4}) \bar{\mathbf{H}}_2$ , we arrive at (17).

Based on the estimate  $\hat{\mathbf{q}}_k$ , we can obtain the estimation error  $\mathbf{e}_k = \mathbf{q}_k - \hat{\mathbf{q}}_k$ . By direct inspection, the mean of  $\mathbf{e}_k$  is zero. Exploiting [68, Eq. (12.21)], Lemma 1 and (104), the MSE matrix of the estimation error can be calculated as

$$\begin{aligned}
\mathbf{MSE}_k &= \mathbb{E} \{ \mathbf{e}_k \mathbf{e}_k^H \} \\
&= \text{Cov} \{ \mathbf{q}_k, \mathbf{q}_k \} - \text{Cov} \{ \mathbf{q}_k, \mathbf{y}_p^k \} \text{Cov}^{-1} \{ \mathbf{y}_p^k, \mathbf{y}_p^k \} \text{Cov} \{ \mathbf{y}_p^k, \mathbf{q}_k \} \\
&= \text{Cov} \{ \mathbf{q}_k, \mathbf{q}_k \} - \mathbf{A}_k \text{Cov} \{ \mathbf{q}_k, \mathbf{q}_k \} \\
&= (\mathbf{I}_M - \mathbf{A}_k) \text{Cov} \{ \mathbf{q}_k, \mathbf{q}_k \} \\
&= ((1 - a_{k4}) \mathbf{I}_M - a_{k3} \mathbf{a}_M \mathbf{a}_M^H) (a_{k1} \mathbf{a}_M \mathbf{a}_M^H + a_{k2} \mathbf{I}_M) \\
&= (a_{k1} (1 - a_{k4}) - M a_{k1} a_{k3} - a_{k2} a_{k3}) \mathbf{a}_M \mathbf{a}_M^H + a_{k2} (1 - a_{k4}) \mathbf{I}_M \\
&\triangleq a_{k5} \mathbf{a}_M \mathbf{a}_M^H + a_{k6} \mathbf{I}_M,
\end{aligned} \tag{107}$$

where

$$\begin{aligned}
a_{k5} &= a_{k1} (1 - a_{k4}) - (M a_{k1} + a_{k2}) a_{k3} \\
&= a_{k1} \left( 1 - \frac{a_{k2}}{a_{k2} + \frac{\sigma^2}{\tau p}} \right) - (M a_{k1} + a_{k2}) \frac{a_{k1} \frac{\sigma^2}{\tau p}}{\left( a_{k2} + \frac{\sigma^2}{\tau p} \right) \left\{ \left( a_{k2} + \frac{\sigma^2}{\tau p} \right) + M a_{k1} \right\}} \\
&= \frac{a_{k1} \left( \frac{\sigma^2}{\tau p} \right)^2}{\left( a_{k2} + \frac{\sigma^2}{\tau p} \right) \left( a_{k2} + \frac{\sigma^2}{\tau p} + M a_{k1} \right)},
\end{aligned} \tag{108}$$

and

$$a_{k6} = a_{k2} (1 - a_{k4}) = a_{k2} \left( 1 - \frac{a_{k2}}{a_{k2} + \frac{\sigma^2}{\tau p}} \right) = \frac{a_{k2} \frac{\sigma^2}{\tau p}}{a_{k2} + \frac{\sigma^2}{\tau p}}. \tag{109}$$

Based on the MSE matrix, the NMSE of the estimation error can be expressed as [54, Eq. (3.20)]

$$\begin{aligned}
\text{NMSE}_k &= \frac{\text{Tr} \{ \mathbf{MSE}_k \}}{\text{Tr} \{ \text{Cov} \{ \mathbf{q}_k, \mathbf{q}_k \} \}} = \frac{M (a_{k5} + a_{k6})}{M (a_{k1} + a_{k2})} = \frac{a_{k5} + a_{k6}}{a_{k1} + a_{k2}} \\
&= \frac{\frac{\sigma^2}{\tau p} \left( M a_{k1} a_{k2} + a_{k2}^2 + (a_{k1} + a_{k2}) \frac{\sigma^2}{\tau p} \right)}{\left( a_{k2} + \frac{\sigma^2}{\tau p} \right) \left( a_{k2} + \frac{\sigma^2}{\tau p} + M a_{k1} \right) (a_{k1} + a_{k2})}.
\end{aligned} \tag{110}$$

Hence, the proof is completed.

## APPENDIX D

Recall that  $\mathbf{A}_k = a_{k3}\mathbf{a}_M\mathbf{a}_M^H + a_{k4}\mathbf{I}_M$ , and  $\bar{\mathbf{H}}_2 = \mathbf{a}_M\mathbf{a}_N^H$ . We can readily obtain

$$\begin{aligned}
\text{Tr}\{\mathbf{A}_k\} &= M(a_{k3} + a_{k4}) \triangleq Me_{k1}, \\
\mathbf{A}_k\bar{\mathbf{H}}_2 &= a_{k3}\mathbf{a}_M\mathbf{a}_M^H\mathbf{a}_M\mathbf{a}_N^H + a_{k4}\mathbf{I}_M\mathbf{a}_M\mathbf{a}_N^H = (Ma_{k3} + a_{k4})\bar{\mathbf{H}}_2 \triangleq e_{k2}\bar{\mathbf{H}}_2, \\
\mathbf{A}_k\mathbf{A}_k &= a_{k3}\mathbf{a}_M\mathbf{a}_M^H(a_{k3}\mathbf{a}_M\mathbf{a}_M^H + a_{k4}\mathbf{I}_M) + a_{k4}\mathbf{I}_M(a_{k3}\mathbf{a}_M\mathbf{a}_M^H + a_{k4}\mathbf{I}_M) \\
&= Ma_{k3}^2\mathbf{a}_M\mathbf{a}_M^H + 2a_{k3}a_{k4}\mathbf{a}_M\mathbf{a}_M^H + a_{k4}^2\mathbf{I}_M, \\
\text{Tr}\{\mathbf{A}_k\mathbf{A}_k\} &= M(Ma_{k3}^2 + 2a_{k3}a_{k4} + a_{k4}^2) \triangleq Me_{k3}.
\end{aligned} \tag{111}$$

By direct inspection of  $e_{k1}, e_{k2}, e_{k3}$ , we evince that they are composed of non-negative terms. Therefore, we have  $e_{k1}, e_{k2}, e_{k3} \geq 0$ . Then, we aim to prove  $e_{k1}, e_{k2}, e_{k3} \leq 1$ . We first focus on the parameter  $e_{k2}$ . Using the expressions of  $a_{k3}$  and  $a_{k4}$  in (20) and (21), we can expand  $e_{k2}$  as

$$\begin{aligned}
e_{k2} &= Ma_{k3} + a_{k4} = \frac{Ma_{k1}\frac{\sigma^2}{\tau p}}{\left(a_{k2} + \frac{\sigma^2}{\tau p}\right)\left(a_{k2} + \frac{\sigma^2}{\tau p} + Ma_{k1}\right)} + \frac{a_{k2}}{a_{k2} + \frac{\sigma^2}{\tau p}} \\
&= \frac{a_{k2}\left(a_{k2} + \frac{\sigma^2}{\tau p} + Ma_{k1}\right) + Ma_{k1}\frac{\sigma^2}{\tau p}}{a_{k2}\left(a_{k2} + \frac{\sigma^2}{\tau p} + Ma_{k1}\right) + Ma_{k1}\frac{\sigma^2}{\tau p} + \frac{\sigma^2}{\tau p}\left(a_{k2} + \frac{\sigma^2}{\tau p}\right)}.
\end{aligned} \tag{112}$$

It is clear that the numerator in (112) is smaller than the denominator. Therefore, we proved that  $e_{k2} \leq 1$ . Then, we can directly obtain

$$e_{k1} \leq e_{k2} \leq 1, \tag{113}$$

$$e_{k3} \leq e_{k2}^2 \leq e_{k2} \leq 1. \tag{114}$$

Finally, when  $\tau p \rightarrow \infty$  or  $N \rightarrow \infty$ , we have  $a_{k3} \rightarrow 0$  and  $a_{k4} \rightarrow 1$ , which implies that  $e_{k1} = e_{k2} = e_{k3} \rightarrow 1$ . When  $\tau p \rightarrow 0$ , we have  $a_{k3}, a_{k4} \rightarrow 0$ , which gives  $e_{k1} = e_{k2} = e_{k3} \rightarrow 0$ . This completes the proof.

## APPENDIX E

### A. Signal Term and Noise Term

According to the orthogonality property of the LMMSE estimator, we have  $\mathbb{E}\{\mathbf{e}_k(\mathbf{y}_p^k)^H\} = \mathbf{0}$ . Besides, since  $\mathbf{e}_k$  has zero mean, we obtain  $\mathbb{E}\{\hat{\mathbf{q}}_k^H\mathbf{e}_k\} = \mathbb{E}\{(\mathbf{A}_k\mathbf{y}_p^k + \mathbf{B}_k)^H\mathbf{e}_k\} = 0$ . Therefore, we have

$$\mathbb{E}\{\hat{\mathbf{q}}_k^H\mathbf{q}_k\} = \mathbb{E}\{\hat{\mathbf{q}}_k^H\hat{\mathbf{q}}_k\} + \mathbb{E}\{\hat{\mathbf{q}}_k^H\mathbf{e}_k\} = \mathbb{E}\{\|\hat{\mathbf{q}}_k\|^2\}. \tag{115}$$

Denote the signal term of (35) as  $|\mathbb{E}\{\hat{\mathbf{q}}_k^H \mathbf{q}_k\}|^2 \triangleq E_k^{(\text{signal})}(\Phi)$ , and denote the noise term of (35) as  $\mathbb{E}\{\|\hat{\mathbf{q}}_k\|^2\} \triangleq E_k^{(\text{noise})}(\Phi)$ . Then, from (115), we obtain

$$E_k^{(\text{signal})}(\Phi) = \left(E_k^{(\text{noise})}(\Phi)\right)^2 = \left(\mathbb{E}\{\hat{\mathbf{q}}_k^H \mathbf{q}_k\}\right)^2. \quad (116)$$

Let us now derive  $E_k^{(\text{noise})}(\Phi)$ . Recall the expressions in (10) and (17). Since  $\tilde{\mathbf{H}}_2$ ,  $\tilde{\mathbf{h}}_k$ ,  $\tilde{\mathbf{d}}_k$  and  $\mathbf{N}$  are independent of each other and they all have a zero mean, we can derive the term  $\mathbb{E}\{\hat{\mathbf{q}}_k^H \mathbf{q}_k\}$  by selecting the non-zero terms in the expansion as

$$\begin{aligned} E_k^{(\text{noise})}(\Phi) &= \mathbb{E}\{\hat{\mathbf{q}}_k^H \mathbf{q}_k\} \\ &= \mathbb{E}\left\{\left(\sum_{\omega=1}^4 \hat{\mathbf{q}}_k^\omega + \sqrt{\gamma_k} \mathbf{A}_k \tilde{\mathbf{d}}_k + \frac{1}{\sqrt{\tau p}} \mathbf{A}_k \mathbf{N} \mathbf{s}_k\right)^H \left(\sum_{\psi=1}^4 \mathbf{q}_k^\psi + \sqrt{\gamma_k} \tilde{\mathbf{d}}_k\right)\right\} \\ &= \sum_{\omega=1}^4 \mathbb{E}\left\{(\hat{\mathbf{q}}_k^\omega)^H \mathbf{q}_k^\omega\right\} + \gamma_k \mathbb{E}\left\{\tilde{\mathbf{d}}_k^H \mathbf{A}_k^H \tilde{\mathbf{d}}_k\right\} \\ &= c_k \delta \varepsilon_k \bar{\mathbf{h}}_k^H \Phi^H \bar{\mathbf{H}}_2^H \bar{\mathbf{H}}_2 \Phi \bar{\mathbf{h}}_k + e_{k2} c_k \delta \mathbb{E}\left\{\tilde{\mathbf{h}}_k^H \Phi^H \bar{\mathbf{H}}_2^H \bar{\mathbf{H}}_2 \Phi \tilde{\mathbf{h}}_k\right\} \\ &\quad + c_k \varepsilon_k \bar{\mathbf{h}}_k^H \Phi^H \mathbb{E}\left\{\tilde{\mathbf{H}}_2^H \mathbf{A}_k^H \tilde{\mathbf{H}}_2\right\} \Phi \bar{\mathbf{h}}_k + c_k \mathbb{E}\left\{\tilde{\mathbf{h}}_k^H \Phi^H \mathbb{E}\left\{\tilde{\mathbf{H}}_2^H \mathbf{A}_k^H \tilde{\mathbf{H}}_2\right\} \Phi \tilde{\mathbf{h}}_k\right\} + \gamma_k \text{Tr}\{\mathbf{A}_k^H\} \\ &\stackrel{(c)}{=} c_k \delta \varepsilon_k M |f_k(\Phi)|^2 + c_k \delta M N e_{k2} + c_k \varepsilon_k M N e_{k1} + c_k M N e_{k1} + \gamma_k M e_{k1} \\ &= M \left\{|f_k(\Phi)|^2 c_k \delta \varepsilon_k + N c_k \delta e_{k2} + (N c_k (\varepsilon_k + 1) + \gamma_k) e_{k1}\right\}, \end{aligned} \quad (117)$$

where (c) applies Lemma 4 and exploits the identities  $\text{Tr}\{\mathbf{A}_k\} = M e_{k1}$ ,  $\Phi^H \Phi = \mathbf{I}_N$ , and  $\text{Tr}\{\bar{\mathbf{H}}_2^H \bar{\mathbf{H}}_2\} = M N$ . Substituting (117) into (116), we complete the calculation of  $E_k^{(\text{signal})}(\Phi)$  and  $E_k^{(\text{noise})}(\Phi)$ .

We conclude this subsection by deriving some useful results that are obtained by using a procedure similar to that used for obtaining (117). To be specific, we aim to derive  $\mathbb{E}\{\mathbf{q}_k^H \mathbf{q}_k\}$ ,  $\mathbb{E}\{\hat{\mathbf{q}}_k^H \hat{\mathbf{q}}_k\}$ ,  $\mathbb{E}\{\mathbf{q}_k^H \mathbf{A}_k \mathbf{A}_k^H \mathbf{q}_k\}$ ,  $\mathbb{E}\{\mathbf{q}_i^H \mathbf{A}_k \mathbf{A}_k^H \mathbf{q}_i\}$ , and  $\mathbb{E}\{\hat{\mathbf{q}}_k^H \mathbf{q}_k\}$ .

Firstly, when  $\mathbf{A}_k = \mathbf{I}_M$  and  $\tau \rightarrow \infty$ , the imperfect estimate  $\hat{\mathbf{q}}_k$  becomes the perfect estimate  $\mathbf{q}_k$ . Therefore, substituting  $\mathbf{A}_k = \mathbf{I}_M$  and  $\tau \rightarrow \infty$  into (117), we have

$$\mathbb{E}\{\mathbf{q}_k^H \mathbf{q}_k\} = M \left\{|f_k(\Phi)|^2 c_k \delta \varepsilon_k + N c_k (\delta + \varepsilon_k + 1) + \gamma_k\right\}. \quad (118)$$

Secondly, by using the expression of  $\hat{\mathbf{q}}_k$  in (17), we have

$$\begin{aligned} \mathbb{E}\{\hat{\mathbf{q}}_k^H \hat{\mathbf{q}}_k\} &= \mathbb{E}\left\{\sum_{\omega=1}^4 \sum_{\psi=1}^4 \left(\hat{\mathbf{q}}_k^\omega\right)^H \hat{\mathbf{q}}_k^\psi\right\} = \sum_{\omega=1}^4 \mathbb{E}\left\{\left\|\hat{\mathbf{q}}_k^\omega\right\|^2\right\} \\ &\stackrel{(d)}{=} M \left\{|f_k(\Phi)|^2 c_k \delta \varepsilon_k + N c_k \delta e_{k2}^2 + N c_k (\varepsilon_k + 1) e_{k3}\right\}, \end{aligned} \quad (119)$$

where (d) follows by applying the identity  $\text{Tr}\{\mathbf{A}_k^H \mathbf{A}_k\} = M e_{k3}$ .

Thirdly, using  $\mathbf{A}_k^H = \mathbf{A}_k$  and  $\mathbf{A}_k \bar{\mathbf{H}}_2 = e_{k2} \bar{\mathbf{H}}_2$ , we have

$$\begin{aligned} \mathbb{E} \left\{ \mathbf{q}_k^H \mathbf{A}_k \mathbf{A}_k^H \mathbf{q}_k \right\} &= \mathbb{E} \left\{ \sum_{\omega=1}^4 \sum_{\psi=1}^4 (\mathbf{A}_k \mathbf{q}_k^\omega)^H (\mathbf{A}_k \mathbf{q}_k^\psi) \right\} \\ &= \left\| \sqrt{c_k \delta \varepsilon_k} \mathbf{A}_k \bar{\mathbf{H}}_2 \Phi \bar{\mathbf{h}}_k \right\|^2 + \sum_{\omega=2}^4 \mathbb{E} \left\{ \|\hat{\mathbf{q}}_k^\omega\|^2 \right\} \\ &= M \left\{ |f_k(\Phi)|^2 c_k \delta \varepsilon_k e_{k2}^2 + N c_k \delta e_{k2}^2 + N c_k (\varepsilon_k + 1) e_{k3} \right\}. \end{aligned} \quad (120)$$

Also, for  $i \neq k$ , we have

$$\mathbb{E} \left\{ \mathbf{q}_i^H \mathbf{A}_k \mathbf{A}_k^H \mathbf{q}_i \right\} = M \left\{ |f_i(\Phi)|^2 c_i \delta \varepsilon_i e_{k2}^2 + N c_i \delta e_{k2}^2 + N c_i (\varepsilon_i + 1) e_{k3} \right\}. \quad (121)$$

Finally, by substituting  $\gamma_k = 0$  into (117), we arrive at

$$\mathbb{E} \left\{ \hat{\mathbf{q}}_k^H \mathbf{q}_k \right\} = M \left\{ |f_k(\Phi)|^2 c_k \delta \varepsilon_k + N c_k \delta e_{k2} + N c_k (\varepsilon_k + 1) e_{k1} \right\}. \quad (122)$$

### B. Interference Term

In this subsection, we derive the interference term of (35). The interference term is denoted by  $\mathbb{E} \left\{ |\hat{\mathbf{q}}_k^H \mathbf{q}_i|^2 \right\} \triangleq I_{ki}(\Phi)$ . First, it is worth noting that the derivation of the interference term in the presence of imperfect CSI and double-Rician channels in RIS-aided massive MIMO systems has two main differences compared to conventional massive MIMO systems. Firstly, the channel  $\mathbf{q}_k$  and  $\mathbf{q}_i$  are not independent, since different users experience the same RIS-BS channel. This can be readily validated by examining that  $\mathbb{E} \left\{ \mathbf{q}_k^H \mathbf{q}_i \right\} \neq \mathbb{E} \left\{ \mathbf{q}_k^H \right\} \mathbb{E} \left\{ \mathbf{q}_i \right\}$ . Secondly, the LMMSE error  $\mathbf{e}_k$  is uncorrelated with but dependent on the estimate  $\hat{\mathbf{q}}_k$ , since the cascaded channel is not Gaussian distributed. To tackle these two challenges, we derive the interference term by decomposing it as

$$\begin{aligned} I_{ki}(\Phi) &= \mathbb{E} \left\{ |\hat{\mathbf{q}}_k^H \mathbf{q}_i|^2 \right\} = \mathbb{E} \left\{ \left| \left( \hat{\mathbf{q}}_k + \mathbf{A}_k \mathbf{d}_k + \frac{1}{\sqrt{\tau p}} \mathbf{A}_k \mathbf{N} \mathbf{s}_k \right)^H (\mathbf{q}_i + \mathbf{d}_i) \right|^2 \right\} \\ &= \mathbb{E} \left\{ \left| \hat{\mathbf{q}}_k^H \mathbf{q}_i + \hat{\mathbf{q}}_k^H \mathbf{d}_i + \mathbf{d}_k^H \mathbf{A}_k^H \mathbf{q}_i + \mathbf{d}_k^H \mathbf{A}_k^H \mathbf{d}_i + \frac{1}{\sqrt{\tau p}} \mathbf{s}_k^H \mathbf{N}^H \mathbf{A}_k^H \mathbf{q}_i + \frac{1}{\sqrt{\tau p}} \mathbf{s}_k^H \mathbf{N}^H \mathbf{A}_k^H \mathbf{d}_i \right|^2 \right\} \\ &= \mathbb{E} \left\{ |\hat{\mathbf{q}}_k^H \mathbf{q}_i|^2 \right\} + \mathbb{E} \left\{ |\hat{\mathbf{q}}_k^H \mathbf{d}_i|^2 \right\} + \mathbb{E} \left\{ |\mathbf{d}_k^H \mathbf{A}_k^H \mathbf{q}_i|^2 \right\} + \mathbb{E} \left\{ |\mathbf{d}_k^H \mathbf{A}_k^H \mathbf{d}_i|^2 \right\} \\ &\quad + \frac{1}{\tau p} \mathbb{E} \left\{ |\mathbf{s}_k^H \mathbf{N}^H \mathbf{A}_k^H \mathbf{q}_i|^2 \right\} + \frac{1}{\tau p} \mathbb{E} \left\{ |\mathbf{s}_k^H \mathbf{N}^H \mathbf{A}_k^H \mathbf{d}_i|^2 \right\}. \end{aligned} \quad (123)$$

We aim to derive the six expectations in (123) one by one, but the first one  $\mathbb{E} \left\{ |\hat{\mathbf{q}}_k^H \mathbf{q}_i|^2 \right\}$  will be derived last. The second term in (123) is

$$\mathbb{E} \left\{ |\hat{\mathbf{q}}_k^H \mathbf{d}_i|^2 \right\} = \mathbb{E} \left\{ \hat{\mathbf{q}}_k^H \mathbf{d}_i \mathbf{d}_i^H \hat{\mathbf{q}}_k \right\} = \mathbb{E} \left\{ \hat{\mathbf{q}}_k^H \mathbb{E} \left\{ \mathbf{d}_i \mathbf{d}_i^H \right\} \hat{\mathbf{q}}_k \right\} = \gamma_i \mathbb{E} \left\{ \hat{\mathbf{q}}_k^H \hat{\mathbf{q}}_k \right\}, \quad (124)$$

where  $\mathbb{E} \left\{ \hat{\mathbf{q}}_k^H \hat{\mathbf{q}}_k \right\}$  is given in (119).

The third term in (123) is

$$\mathbb{E} \left\{ \left| \mathbf{d}_k^H \mathbf{A}_k^H \underline{\mathbf{q}}_i \right|^2 \right\} = \mathbb{E} \left\{ \underline{\mathbf{q}}_i^H \mathbf{A}_k \mathbb{E} \left\{ \mathbf{d}_k \mathbf{d}_k^H \right\} \mathbf{A}_k^H \underline{\mathbf{q}}_i \right\} = \gamma_k \mathbb{E} \left\{ \underline{\mathbf{q}}_i^H \mathbf{A}_k \mathbf{A}_k^H \underline{\mathbf{q}}_i \right\}, \quad (125)$$

where  $\mathbb{E} \left\{ \underline{\mathbf{q}}_i^H \mathbf{A}_k \mathbf{A}_k^H \underline{\mathbf{q}}_i \right\}$  is given in (121).

The fourth term in (123) is

$$\begin{aligned} \mathbb{E} \left\{ \left| \mathbf{d}_k^H \mathbf{A}_k^H \mathbf{d}_i \right|^2 \right\} &= \mathbb{E} \left\{ \mathbf{d}_k^H \mathbf{A}_k^H \mathbb{E} \left\{ \mathbf{d}_i \mathbf{d}_i^H \right\} \mathbf{A}_k \mathbf{d}_k \right\} \\ &= \gamma_i \mathbb{E} \left\{ \mathbf{d}_k^H \mathbf{A}_k^H \mathbf{A}_k \mathbf{d}_k \right\} = \gamma_k \gamma_i \text{Tr} \left\{ \mathbf{A}_k^H \mathbf{A}_k \right\} \\ &= \gamma_k \gamma_i M e_{k3}. \end{aligned} \quad (126)$$

The fifth term in (123) is

$$\frac{1}{\tau p} \mathbb{E} \left\{ \left| \mathbf{s}_k^H \mathbf{N}^H \mathbf{A}_k^H \underline{\mathbf{q}}_i \right|^2 \right\} = \frac{1}{\tau p} \mathbb{E} \left\{ \underline{\mathbf{q}}_i^H \mathbf{A}_k \mathbb{E} \left\{ \mathbf{N} \mathbf{s}_k \mathbf{s}_k^H \mathbf{N}^H \right\} \mathbf{A}_k^H \underline{\mathbf{q}}_i \right\} = \frac{\sigma^2}{\tau p} \mathbb{E} \left\{ \underline{\mathbf{q}}_i^H \mathbf{A}_k \mathbf{A}_k^H \underline{\mathbf{q}}_i \right\}, \quad (127)$$

where  $\mathbb{E} \left\{ \underline{\mathbf{q}}_i^H \mathbf{A}_k \mathbf{A}_k^H \underline{\mathbf{q}}_i \right\}$  is given in (121).

The sixth term in (123) is

$$\frac{1}{\tau p} \mathbb{E} \left\{ \left| \mathbf{s}_k^H \mathbf{N}^H \mathbf{A}_k^H \mathbf{d}_i \right|^2 \right\} = \frac{\sigma^2}{\tau p} \gamma_i \text{Tr} \left\{ \mathbf{A}_k^H \mathbf{A}_k \right\} = \frac{\sigma^2}{\tau p} \gamma_i M e_{k3}. \quad (128)$$

Finally, we derive the first term  $\mathbb{E} \left\{ \left| \hat{\mathbf{q}}_k^H \underline{\mathbf{q}}_i \right|^2 \right\}$ , which can be expanded as

$$\begin{aligned} \mathbb{E} \left\{ \left| \hat{\mathbf{q}}_k^H \underline{\mathbf{q}}_i \right|^2 \right\} &= \mathbb{E} \left\{ \left| \sum_{\omega=1}^4 \sum_{\psi=1}^4 (\hat{\mathbf{q}}_k^\omega)^H \mathbf{q}_i^\psi \right|^2 \right\} \\ &= \sum_{\omega=1}^4 \sum_{\psi=1}^4 \mathbb{E} \left\{ \left| (\hat{\mathbf{q}}_k^\omega)^H \mathbf{q}_i^\psi \right|^2 \right\} + \sum_{\substack{\omega 1, \psi 1, \omega 2, \psi 2, \\ (\omega 1, \psi 1) \neq (\omega 2, \psi 2)}}^4 \mathbb{E} \left\{ \left( (\hat{\mathbf{q}}_k^{\omega 1})^H \mathbf{q}_i^{\psi 1} \right) \left( (\hat{\mathbf{q}}_k^{\omega 2})^H \mathbf{q}_i^{\psi 2} \right)^H \right\}, \end{aligned} \quad (129)$$

where  $\mathbf{q}_k^1 - \mathbf{q}_k^4$  are defined in (10), and  $\hat{\mathbf{q}}_k^1 - \hat{\mathbf{q}}_k^4$  are defined in (17).

Equation (129) can be derived by calculating the expectations of the 16 modulus-square terms and the expectations of the other cross-terms. We first calculate the former 16 modulus-square terms in (129) one by one. The derivation utilizes Lemma 4, Lemma 6, and the independence between  $\tilde{\mathbf{H}}_2$ ,  $\tilde{\mathbf{h}}_k$ , and  $\tilde{\mathbf{h}}_i$ .

Firstly, we consider the terms with  $\omega = 1$ . When  $\psi = 1$ , we have

$$\begin{aligned} &\mathbb{E} \left\{ \left| \sqrt{c_k \delta \varepsilon_k} \sqrt{c_i \delta \varepsilon_i} \bar{\mathbf{h}}_k^H \Phi^H \bar{\mathbf{H}}_2^H \bar{\mathbf{H}}_2 \Phi \bar{\mathbf{h}}_i \right|^2 \right\} \\ &= c_k c_i \delta^2 \varepsilon_k \varepsilon_i \bar{\mathbf{h}}_k^H \Phi^H \mathbf{a}_N \mathbf{a}_M^H \mathbf{a}_M \mathbf{a}_N^H \Phi \bar{\mathbf{h}}_i \bar{\mathbf{h}}_i^H \Phi^H \mathbf{a}_N \mathbf{a}_M^H \mathbf{a}_M \mathbf{a}_N^H \Phi \bar{\mathbf{h}}_k \\ &= c_k c_i \delta^2 \varepsilon_k \varepsilon_i M^2 |f_k(\Phi)|^2 |f_i(\Phi)|^2. \end{aligned} \quad (130)$$

When  $\psi = 2$ , we have

$$\begin{aligned}
& \mathbb{E} \left\{ \left| \sqrt{c_k \delta \varepsilon_k} \sqrt{c_i \delta} \bar{\mathbf{h}}_k^H \boldsymbol{\Phi}^H \bar{\mathbf{H}}_2^H \bar{\mathbf{H}}_2 \boldsymbol{\Phi} \tilde{\mathbf{h}}_i \right|^2 \right\} \\
&= c_k c_i \delta^2 \varepsilon_k \bar{\mathbf{h}}_k^H \boldsymbol{\Phi}^H \mathbf{a}_N \mathbf{a}_M^H \mathbf{a}_M \mathbf{a}_N^H \boldsymbol{\Phi} \mathbb{E} \left\{ \tilde{\mathbf{h}}_i \tilde{\mathbf{h}}_i^H \right\} \boldsymbol{\Phi}^H \mathbf{a}_N \mathbf{a}_M^H \mathbf{a}_M \mathbf{a}_N^H \boldsymbol{\Phi} \bar{\mathbf{h}}_k \\
&= c_k c_i \delta^2 \varepsilon_k M^2 N |f_k(\boldsymbol{\Phi})|^2.
\end{aligned} \tag{131}$$

When  $\psi = 3$ , using Lemma 4, we arrive at

$$\begin{aligned}
& \mathbb{E} \left\{ \left| \sqrt{c_k \delta \varepsilon_k} \sqrt{c_i \varepsilon_i} \bar{\mathbf{h}}_k^H \boldsymbol{\Phi}^H \bar{\mathbf{H}}_2^H \tilde{\mathbf{H}}_2 \boldsymbol{\Phi} \bar{\mathbf{h}}_i \right|^2 \right\} \\
&= c_k c_i \delta \varepsilon_k \varepsilon_i \bar{\mathbf{h}}_k^H \boldsymbol{\Phi}^H \bar{\mathbf{H}}_2^H \mathbb{E} \left\{ \tilde{\mathbf{H}}_2 \boldsymbol{\Phi} \bar{\mathbf{h}}_i \bar{\mathbf{h}}_i^H \boldsymbol{\Phi}^H \tilde{\mathbf{H}}_2^H \right\} \bar{\mathbf{H}}_2 \boldsymbol{\Phi} \bar{\mathbf{h}}_k \\
&= c_k c_i \delta \varepsilon_k \varepsilon_i N \bar{\mathbf{h}}_k^H \boldsymbol{\Phi}^H \bar{\mathbf{H}}_2^H \bar{\mathbf{H}}_2 \boldsymbol{\Phi} \bar{\mathbf{h}}_k \\
&= c_k c_i \delta \varepsilon_k \varepsilon_i M N |f_k(\boldsymbol{\Phi})|^2.
\end{aligned} \tag{132}$$

When  $\psi = 4$ , we have

$$\begin{aligned}
& \mathbb{E} \left\{ \left| \sqrt{c_k \delta \varepsilon_k} \sqrt{c_i} \bar{\mathbf{h}}_k^H \boldsymbol{\Phi}^H \bar{\mathbf{H}}_2^H \tilde{\mathbf{H}}_2 \boldsymbol{\Phi} \tilde{\mathbf{h}}_i \right|^2 \right\} \\
&= c_k c_i \delta \varepsilon_k \bar{\mathbf{h}}_k^H \boldsymbol{\Phi}^H \bar{\mathbf{H}}_2^H \mathbb{E} \left\{ \tilde{\mathbf{H}}_2 \boldsymbol{\Phi} \mathbb{E} \left\{ \tilde{\mathbf{h}}_i \tilde{\mathbf{h}}_i^H \right\} \boldsymbol{\Phi}^H \tilde{\mathbf{H}}_2^H \right\} \bar{\mathbf{H}}_2 \boldsymbol{\Phi} \bar{\mathbf{h}}_k \\
&= c_k c_i \delta \varepsilon_k \bar{\mathbf{h}}_k^H \boldsymbol{\Phi}^H \bar{\mathbf{H}}_2^H \mathbb{E} \left\{ \tilde{\mathbf{H}}_2 \tilde{\mathbf{H}}_2^H \right\} \bar{\mathbf{H}}_2 \boldsymbol{\Phi} \bar{\mathbf{h}}_k \\
&= c_k c_i \delta \varepsilon_k M N |f_k(\boldsymbol{\Phi})|^2.
\end{aligned} \tag{133}$$

Secondly, we consider the terms with  $\omega = 2$ . When  $\psi = 1$ , we have

$$\begin{aligned}
& \mathbb{E} \left\{ \left| e_{k2} \sqrt{c_k \delta} \sqrt{c_i \delta \varepsilon_i} \tilde{\mathbf{h}}_k^H \boldsymbol{\Phi}^H \bar{\mathbf{H}}_2^H \bar{\mathbf{H}}_2 \boldsymbol{\Phi} \bar{\mathbf{h}}_i \right|^2 \right\} \\
&= e_{k2}^2 c_k c_i \delta^2 \varepsilon_i \mathbb{E} \left\{ \tilde{\mathbf{h}}_k^H \boldsymbol{\Phi}^H \bar{\mathbf{H}}_2^H \bar{\mathbf{H}}_2 \boldsymbol{\Phi} \bar{\mathbf{h}}_i \bar{\mathbf{h}}_i^H \boldsymbol{\Phi}^H \bar{\mathbf{H}}_2^H \bar{\mathbf{H}}_2 \boldsymbol{\Phi} \tilde{\mathbf{h}}_k \right\} \\
&= e_{k2}^2 c_k c_i \delta^2 \varepsilon_i \text{Tr} \left\{ \bar{\mathbf{H}}_2^H \bar{\mathbf{H}}_2 \boldsymbol{\Phi} \bar{\mathbf{h}}_i \bar{\mathbf{h}}_i^H \boldsymbol{\Phi}^H \bar{\mathbf{H}}_2^H \bar{\mathbf{H}}_2 \right\} \\
&= e_{k2}^2 c_k c_i \delta^2 \varepsilon_i \text{Tr} \left\{ \mathbf{a}_N^H \boldsymbol{\Phi} \bar{\mathbf{h}}_i \bar{\mathbf{h}}_i^H \boldsymbol{\Phi}^H \mathbf{a}_N \mathbf{a}_M^H \mathbf{a}_M \mathbf{a}_N^H \mathbf{a}_N \mathbf{a}_M^H \mathbf{a}_M \right\} \\
&= e_{k2}^2 c_k c_i \delta^2 \varepsilon_i M^2 N |f_i(\boldsymbol{\Phi})|^2.
\end{aligned} \tag{134}$$

When  $\psi = 2$ , we arrive at

$$\begin{aligned}
& \mathbb{E} \left\{ \left| e_{k2} \sqrt{c_k \delta} \sqrt{c_i \delta} \tilde{\mathbf{h}}_k^H \boldsymbol{\Phi}^H \bar{\mathbf{H}}_2^H \bar{\mathbf{H}}_2 \boldsymbol{\Phi} \tilde{\mathbf{h}}_i \right|^2 \right\} \\
&= e_{k2}^2 c_k c_i \delta^2 \mathbb{E} \left\{ \tilde{\mathbf{h}}_k^H \boldsymbol{\Phi}^H \bar{\mathbf{H}}_2^H \bar{\mathbf{H}}_2 \boldsymbol{\Phi} \mathbb{E} \left\{ \tilde{\mathbf{h}}_i \tilde{\mathbf{h}}_i^H \right\} \boldsymbol{\Phi}^H \bar{\mathbf{H}}_2^H \bar{\mathbf{H}}_2 \boldsymbol{\Phi} \tilde{\mathbf{h}}_k \right\} \\
&= e_{k2}^2 c_k c_i \delta^2 \text{Tr} \left\{ \bar{\mathbf{H}}_2^H \bar{\mathbf{H}}_2 \bar{\mathbf{H}}_2^H \bar{\mathbf{H}}_2 \right\} \\
&= e_{k2}^2 c_k c_i \delta^2 M^2 N^2.
\end{aligned} \tag{135}$$



When  $\psi = 3$ , we get

$$\begin{aligned}
& \mathbb{E} \left\{ \left| e_{k2} \sqrt{c_k} \delta \sqrt{c_i} \tilde{\mathbf{h}}_k^H \Phi^H \bar{\mathbf{H}}_2^H \tilde{\mathbf{H}}_2 \Phi \tilde{\mathbf{h}}_i \right|^2 \right\} \\
&= e_{k2}^2 c_k c_i \delta \varepsilon_i \mathbb{E} \left\{ \tilde{\mathbf{h}}_k^H \Phi^H \bar{\mathbf{H}}_2^H \mathbb{E} \left\{ \tilde{\mathbf{H}}_2 \Phi \tilde{\mathbf{h}}_i \tilde{\mathbf{h}}_i^H \Phi^H \tilde{\mathbf{H}}_2^H \right\} \bar{\mathbf{H}}_2 \Phi \tilde{\mathbf{h}}_k \right\} \\
&= e_{k2}^2 c_k c_i \delta \varepsilon_i N \mathbb{E} \left\{ \tilde{\mathbf{h}}_k^H \Phi^H \bar{\mathbf{H}}_2^H \bar{\mathbf{H}}_2 \Phi \tilde{\mathbf{h}}_k \right\} \\
&= e_{k2}^2 c_k c_i \delta \varepsilon_i N \text{Tr} \left\{ \bar{\mathbf{H}}_2^H \bar{\mathbf{H}}_2 \right\} \\
&= e_{k2}^2 c_k c_i \delta \varepsilon_i M N^2.
\end{aligned} \tag{136}$$

When  $\psi = 4$ , we have

$$\begin{aligned}
& \mathbb{E} \left\{ \left| e_{k2} \sqrt{c_k} \delta \sqrt{c_i} \tilde{\mathbf{h}}_k^H \Phi^H \bar{\mathbf{H}}_2^H \tilde{\mathbf{H}}_2 \Phi \tilde{\mathbf{h}}_i \right|^2 \right\} \\
&= e_{k2}^2 c_k c_i \delta \mathbb{E} \left\{ \tilde{\mathbf{h}}_k^H \Phi^H \bar{\mathbf{H}}_2^H \mathbb{E} \left\{ \tilde{\mathbf{H}}_2 \Phi \mathbb{E} \left\{ \tilde{\mathbf{h}}_i \tilde{\mathbf{h}}_i^H \right\} \Phi^H \tilde{\mathbf{H}}_2^H \right\} \bar{\mathbf{H}}_2 \Phi \tilde{\mathbf{h}}_k \right\} \\
&= e_{k2}^2 c_k c_i \delta \mathbb{E} \left\{ \tilde{\mathbf{h}}_k^H \Phi^H \bar{\mathbf{H}}_2^H \mathbb{E} \left\{ \tilde{\mathbf{H}}_2 \tilde{\mathbf{H}}_2^H \right\} \bar{\mathbf{H}}_2 \Phi \tilde{\mathbf{h}}_k \right\} \\
&= e_{k2}^2 c_k c_i \delta N \text{Tr} \left\{ \bar{\mathbf{H}}_2^H \bar{\mathbf{H}}_2 \right\} \\
&= e_{k2}^2 c_k c_i \delta M N^2.
\end{aligned} \tag{137}$$

Thirdly, we consider the terms with  $\omega = 3$ . When  $\psi = 1$ , using  $\mathbf{A}_k \bar{\mathbf{H}}_2 = e_{k2} \bar{\mathbf{H}}_2$ , we have

$$\begin{aligned}
& \mathbb{E} \left\{ \left| \sqrt{c_k} \varepsilon_k \sqrt{c_i} \delta \varepsilon_i \bar{\mathbf{h}}_k^H \Phi^H \tilde{\mathbf{H}}_2^H \mathbf{A}_k^H \bar{\mathbf{H}}_2 \Phi \tilde{\mathbf{h}}_i \right|^2 \right\} \\
&= c_k c_i \delta \varepsilon_k \varepsilon_i \bar{\mathbf{h}}_k^H \Phi^H \mathbb{E} \left\{ \tilde{\mathbf{H}}_2^H \mathbf{A}_k^H \bar{\mathbf{H}}_2 \Phi \tilde{\mathbf{h}}_i \tilde{\mathbf{h}}_i^H \Phi^H \bar{\mathbf{H}}_2^H \mathbf{A}_k \tilde{\mathbf{H}}_2 \right\} \Phi \bar{\mathbf{h}}_k \\
&= c_k c_i \delta \varepsilon_k \varepsilon_i \bar{\mathbf{h}}_k^H \Phi^H \text{Tr} \left\{ e_{k2} \bar{\mathbf{H}}_2 \Phi \tilde{\mathbf{h}}_i \tilde{\mathbf{h}}_i^H \Phi^H \bar{\mathbf{H}}_2^H e_{k2} \right\} \Phi \bar{\mathbf{h}}_k \\
&= e_{k2}^2 c_k c_i \delta \varepsilon_k \varepsilon_i M |f_i(\Phi)|^2 \bar{\mathbf{h}}_k^H \Phi^H \Phi \bar{\mathbf{h}}_k \\
&= e_{k2}^2 c_k c_i \delta \varepsilon_k \varepsilon_i M N |f_i(\Phi)|^2.
\end{aligned} \tag{138}$$

When  $\psi = 2$ , we arrive at

$$\begin{aligned}
& \mathbb{E} \left\{ \left| \sqrt{c_k} \varepsilon_k \sqrt{c_i} \delta \bar{\mathbf{h}}_k^H \Phi^H \tilde{\mathbf{H}}_2^H \mathbf{A}_k^H \bar{\mathbf{H}}_2 \Phi \tilde{\mathbf{h}}_i \right|^2 \right\} \\
&= c_k c_i \delta \varepsilon_k \bar{\mathbf{h}}_k^H \Phi^H \mathbb{E} \left\{ \tilde{\mathbf{H}}_2^H \mathbf{A}_k^H \bar{\mathbf{H}}_2 \Phi \mathbb{E} \left\{ \tilde{\mathbf{h}}_i \tilde{\mathbf{h}}_i^H \right\} \Phi^H \bar{\mathbf{H}}_2^H \mathbf{A}_k \tilde{\mathbf{H}}_2 \right\} \Phi \bar{\mathbf{h}}_k \\
&= e_{k2}^2 c_k c_i \delta \varepsilon_k \bar{\mathbf{h}}_k^H \Phi^H \text{Tr} \left\{ \bar{\mathbf{H}}_2 \bar{\mathbf{H}}_2^H \right\} \Phi \bar{\mathbf{h}}_k \\
&= e_{k2}^2 c_k c_i \delta \varepsilon_k M N^2.
\end{aligned} \tag{139}$$

When  $\psi = 3$ , using Lemma 6, we have

$$\begin{aligned}
& \mathbb{E} \left\{ \left| \sqrt{c_k \varepsilon_k} \sqrt{c_i \varepsilon_i} \bar{\mathbf{h}}_k^H \Phi^H \tilde{\mathbf{H}}_2^H \mathbf{A}_k^H \tilde{\mathbf{H}}_2 \Phi \bar{\mathbf{h}}_i \right|^2 \right\} \\
&= c_k c_i \varepsilon_k \varepsilon_i \bar{\mathbf{h}}_k^H \Phi^H \mathbb{E} \left\{ \tilde{\mathbf{H}}_2^H \mathbf{A}_k^H \tilde{\mathbf{H}}_2 \Phi \bar{\mathbf{h}}_i \bar{\mathbf{h}}_i^H \Phi^H \tilde{\mathbf{H}}_2^H \mathbf{A}_k \tilde{\mathbf{H}}_2 \right\} \Phi \bar{\mathbf{h}}_k \\
&= c_k c_i \varepsilon_k \varepsilon_i \bar{\mathbf{h}}_k^H \Phi^H \left( e_{k1}^2 M^2 \Phi \bar{\mathbf{h}}_i \bar{\mathbf{h}}_i^H \Phi^H + e_{k3} M \text{Tr} \left\{ \Phi \bar{\mathbf{h}}_i \bar{\mathbf{h}}_i^H \Phi^H \right\} \mathbf{I}_N \right) \Phi \bar{\mathbf{h}}_k \quad (140) \\
&= c_k c_i \varepsilon_k \varepsilon_i \left( e_{k1}^2 M^2 \bar{\mathbf{h}}_k^H \bar{\mathbf{h}}_i \bar{\mathbf{h}}_i^H \bar{\mathbf{h}}_k + e_{k3} M \text{Tr} \left\{ \bar{\mathbf{h}}_i \bar{\mathbf{h}}_i^H \right\} \bar{\mathbf{h}}_k^H \bar{\mathbf{h}}_k \right) \\
&= c_k c_i \varepsilon_k \varepsilon_i \left( e_{k1}^2 M^2 \left| \bar{\mathbf{h}}_k^H \bar{\mathbf{h}}_i \right|^2 + e_{k3} M N^2 \right).
\end{aligned}$$

When  $\psi = 4$ , using Lemma 6 with  $\mathbf{W} = \mathbf{I}_N$ , we get

$$\begin{aligned}
& \mathbb{E} \left\{ \left| \sqrt{c_k \varepsilon_k} \sqrt{c_i} \bar{\mathbf{h}}_k^H \Phi^H \tilde{\mathbf{H}}_2^H \mathbf{A}_k^H \tilde{\mathbf{H}}_2 \Phi \bar{\mathbf{h}}_i \right|^2 \right\} \\
&= c_k c_i \varepsilon_k \bar{\mathbf{h}}_k^H \Phi^H \mathbb{E} \left\{ \tilde{\mathbf{H}}_2^H \mathbf{A}_k^H \tilde{\mathbf{H}}_2 \Phi \mathbb{E} \left\{ \tilde{\mathbf{h}}_i \tilde{\mathbf{h}}_i^H \right\} \Phi^H \tilde{\mathbf{H}}_2^H \mathbf{A}_k \tilde{\mathbf{H}}_2 \right\} \Phi \bar{\mathbf{h}}_k \\
&= c_k c_i \varepsilon_k \bar{\mathbf{h}}_k^H \Phi^H \mathbb{E} \left\{ \tilde{\mathbf{H}}_2^H \mathbf{A}_k^H \tilde{\mathbf{H}}_2 \tilde{\mathbf{H}}_2^H \mathbf{A}_k \tilde{\mathbf{H}}_2 \right\} \Phi \bar{\mathbf{h}}_k \quad (141) \\
&= c_k c_i \varepsilon_k (e_{k1}^2 M^2 + e_{k3} M N) \bar{\mathbf{h}}_k^H \Phi^H \mathbf{I}_N \Phi \bar{\mathbf{h}}_k \\
&= c_k c_i \varepsilon_k (e_{k1}^2 M^2 + e_{k3} M N) N.
\end{aligned}$$

Fourthly, we consider the terms with  $\omega = 4$ . When  $\psi = 1$ , we have

$$\begin{aligned}
& \mathbb{E} \left\{ \left| \sqrt{c_k} \sqrt{c_i \delta \varepsilon_i} \tilde{\mathbf{h}}_k^H \Phi^H \tilde{\mathbf{H}}_2^H \mathbf{A}_k^H \bar{\mathbf{H}}_2 \Phi \bar{\mathbf{h}}_i \right|^2 \right\} \\
&= c_k c_i \delta \varepsilon_i \mathbb{E} \left\{ \tilde{\mathbf{h}}_k^H \Phi^H \mathbb{E} \left\{ \tilde{\mathbf{H}}_2^H \mathbf{A}_k^H \bar{\mathbf{H}}_2 \Phi \bar{\mathbf{h}}_i \bar{\mathbf{h}}_i^H \Phi^H \bar{\mathbf{H}}_2^H \mathbf{A}_k \tilde{\mathbf{H}}_2 \right\} \Phi \tilde{\mathbf{h}}_k \right\} \\
&= e_{k2}^2 c_k c_i \delta \varepsilon_i \mathbb{E} \left\{ \tilde{\mathbf{h}}_k^H \Phi^H \text{Tr} \left\{ \bar{\mathbf{H}}_2 \Phi \bar{\mathbf{h}}_i \bar{\mathbf{h}}_i^H \Phi^H \bar{\mathbf{H}}_2^H \right\} \Phi \tilde{\mathbf{h}}_k \right\} \quad (142) \\
&= e_{k2}^2 c_k c_i \delta \varepsilon_i M |f_i(\Phi)|^2 \mathbb{E} \left\{ \tilde{\mathbf{h}}_k^H \tilde{\mathbf{h}}_k \right\} \\
&= e_{k2}^2 c_k c_i \delta \varepsilon_i M N |f_i(\Phi)|^2.
\end{aligned}$$

When  $\psi = 2$ , we have

$$\begin{aligned}
& \mathbb{E} \left\{ \left| \sqrt{c_k} \sqrt{c_i \delta} \tilde{\mathbf{h}}_k^H \Phi^H \tilde{\mathbf{H}}_2^H \mathbf{A}_k^H \bar{\mathbf{H}}_2 \Phi \bar{\mathbf{h}}_i \right|^2 \right\} \\
&= c_k c_i \delta \mathbb{E} \left\{ \tilde{\mathbf{h}}_k^H \Phi^H \mathbb{E} \left\{ \tilde{\mathbf{H}}_2^H \mathbf{A}_k^H \bar{\mathbf{H}}_2 \Phi \mathbb{E} \left\{ \tilde{\mathbf{h}}_i \tilde{\mathbf{h}}_i^H \right\} \Phi^H \bar{\mathbf{H}}_2^H \mathbf{A}_k \tilde{\mathbf{H}}_2 \right\} \Phi \tilde{\mathbf{h}}_k \right\} \\
&= e_{k2}^2 c_k c_i \delta \mathbb{E} \left\{ \tilde{\mathbf{h}}_k^H \Phi^H \mathbb{E} \left\{ \tilde{\mathbf{H}}_2^H \bar{\mathbf{H}}_2 \bar{\mathbf{H}}_2^H \tilde{\mathbf{H}}_2 \right\} \Phi \tilde{\mathbf{h}}_k \right\} \quad (143) \\
&= e_{k2}^2 c_k c_i \delta M N \mathbb{E} \left\{ \tilde{\mathbf{h}}_k^H \tilde{\mathbf{h}}_k \right\} \\
&= e_{k2}^2 c_k c_i \delta M N^2.
\end{aligned}$$

When  $\psi = 3$ , we have

$$\begin{aligned}
& \mathbb{E} \left\{ \left| \sqrt{c_k} \sqrt{c_i \varepsilon_i} \tilde{\mathbf{h}}_k^H \Phi^H \tilde{\mathbf{H}}_2^H \mathbf{A}_k^H \tilde{\mathbf{H}}_2 \Phi \bar{\mathbf{h}}_i \right|^2 \right\} \\
&= c_k c_i \varepsilon_i \mathbb{E} \left\{ \tilde{\mathbf{h}}_k^H \Phi^H \mathbb{E} \left\{ \tilde{\mathbf{H}}_2^H \mathbf{A}_k^H \tilde{\mathbf{H}}_2 \Phi \bar{\mathbf{h}}_i \bar{\mathbf{h}}_i^H \Phi^H \tilde{\mathbf{H}}_2^H \mathbf{A}_k \tilde{\mathbf{H}}_2 \right\} \Phi \tilde{\mathbf{h}}_k \right\} \\
&= c_k c_i \varepsilon_i \mathbb{E} \left\{ \tilde{\mathbf{h}}_k^H \Phi^H \left( e_{k1}^2 M^2 \Phi \bar{\mathbf{h}}_i \bar{\mathbf{h}}_i^H \Phi^H + e_{k3} M \text{Tr} \left\{ \Phi \bar{\mathbf{h}}_i \bar{\mathbf{h}}_i^H \Phi^H \right\} \mathbf{I}_N \right) \Phi \tilde{\mathbf{h}}_k \right\} \\
&= c_k c_i \varepsilon_i \mathbb{E} \left\{ e_{k1}^2 M^2 \tilde{\mathbf{h}}_k^H \bar{\mathbf{h}}_i \bar{\mathbf{h}}_i^H \tilde{\mathbf{h}}_k + e_{k3} M N \tilde{\mathbf{h}}_k^H \tilde{\mathbf{h}}_k \right\} \\
&= c_k c_i \varepsilon_i (e_{k1}^2 M^2 N + e_{k3} M N^2).
\end{aligned} \tag{144}$$

When  $\psi = 4$ , we get

$$\begin{aligned}
& \mathbb{E} \left\{ \left| \sqrt{c_k} \sqrt{c_i} \tilde{\mathbf{h}}_k^H \Phi^H \tilde{\mathbf{H}}_2^H \mathbf{A}_k^H \tilde{\mathbf{H}}_2 \Phi \tilde{\mathbf{h}}_i \right|^2 \right\} \\
&= c_k c_i \mathbb{E} \left\{ \tilde{\mathbf{h}}_k^H \Phi^H \mathbb{E} \left\{ \tilde{\mathbf{H}}_2^H \mathbf{A}_k^H \tilde{\mathbf{H}}_2 \Phi \mathbb{E} \left\{ \tilde{\mathbf{h}}_i \tilde{\mathbf{h}}_i^H \right\} \Phi^H \tilde{\mathbf{H}}_2^H \mathbf{A}_k \tilde{\mathbf{H}}_2 \right\} \Phi \tilde{\mathbf{h}}_k \right\} \\
&= c_k c_i \mathbb{E} \left\{ \tilde{\mathbf{h}}_k^H \Phi^H \mathbb{E} \left\{ \tilde{\mathbf{H}}_2^H \mathbf{A}_k^H \tilde{\mathbf{H}}_2 \tilde{\mathbf{H}}_2^H \mathbf{A}_k \tilde{\mathbf{H}}_2 \right\} \Phi \tilde{\mathbf{h}}_k \right\} \\
&= c_k c_i \mathbb{E} \left\{ (e_{k1}^2 M^2 + e_{k3} M N) \tilde{\mathbf{h}}_k^H \tilde{\mathbf{h}}_k \right\} \\
&= c_k c_i (e_{k1}^2 M^2 N + e_{k3} M N^2).
\end{aligned} \tag{145}$$

The calculation of the expectations of the 16 modulus-square terms in (129) is completed. Then, we focus on the remaining cross-terms in (129). Even though the total number of cross-terms is  $16 \times 15$ , only a few terms are non-zero. To help identify the non-zero cross-terms, we expand  $\hat{\mathbf{q}}_k^H \mathbf{q}_i$  as

$$\begin{aligned}
\hat{\mathbf{q}}_k^H \mathbf{q}_i &= \sum_{\omega=1}^4 \sum_{\psi=1}^4 (\hat{\mathbf{q}}_k^\omega)^H \mathbf{q}_i^\psi \\
&= \eta_{11} \bar{\mathbf{h}}_k^H \Phi^H \bar{\mathbf{H}}_2^H \bar{\mathbf{H}}_2 \Phi \bar{\mathbf{h}}_i + \eta_{12} \bar{\mathbf{h}}_k^H \Phi^H \bar{\mathbf{H}}_2^H \bar{\mathbf{H}}_2 \Phi \tilde{\mathbf{h}}_i + \eta_{13} \bar{\mathbf{h}}_k^H \Phi^H \bar{\mathbf{H}}_2^H \tilde{\mathbf{H}}_2 \Phi \bar{\mathbf{h}}_i + \eta_{14} \bar{\mathbf{h}}_k^H \Phi^H \bar{\mathbf{H}}_2^H \tilde{\mathbf{H}}_2 \Phi \tilde{\mathbf{h}}_i \\
&+ \eta_{21} \tilde{\mathbf{h}}_k^H \Phi^H \bar{\mathbf{H}}_2^H \bar{\mathbf{H}}_2 \Phi \bar{\mathbf{h}}_i + \eta_{22} \tilde{\mathbf{h}}_k^H \Phi^H \bar{\mathbf{H}}_2^H \bar{\mathbf{H}}_2 \Phi \tilde{\mathbf{h}}_i + \eta_{23} \tilde{\mathbf{h}}_k^H \Phi^H \bar{\mathbf{H}}_2^H \tilde{\mathbf{H}}_2 \Phi \bar{\mathbf{h}}_i + \eta_{24} \tilde{\mathbf{h}}_k^H \Phi^H \bar{\mathbf{H}}_2^H \tilde{\mathbf{H}}_2 \Phi \tilde{\mathbf{h}}_i \\
&+ \eta_{31} \bar{\mathbf{h}}_k^H \Phi^H \tilde{\mathbf{H}}_2^H \mathbf{A}_k^H \bar{\mathbf{H}}_2 \Phi \bar{\mathbf{h}}_i + \eta_{32} \bar{\mathbf{h}}_k^H \Phi^H \tilde{\mathbf{H}}_2^H \mathbf{A}_k^H \bar{\mathbf{H}}_2 \Phi \tilde{\mathbf{h}}_i \\
&+ \eta_{33} \bar{\mathbf{h}}_k^H \Phi^H \tilde{\mathbf{H}}_2^H \mathbf{A}_k^H \tilde{\mathbf{H}}_2 \Phi \bar{\mathbf{h}}_i + \eta_{34} \bar{\mathbf{h}}_k^H \Phi^H \tilde{\mathbf{H}}_2^H \mathbf{A}_k^H \tilde{\mathbf{H}}_2 \Phi \tilde{\mathbf{h}}_i \\
&+ \eta_{41} \tilde{\mathbf{h}}_k^H \Phi^H \tilde{\mathbf{H}}_2^H \mathbf{A}_k^H \bar{\mathbf{H}}_2 \Phi \bar{\mathbf{h}}_i + \eta_{42} \tilde{\mathbf{h}}_k^H \Phi^H \tilde{\mathbf{H}}_2^H \mathbf{A}_k^H \bar{\mathbf{H}}_2 \Phi \tilde{\mathbf{h}}_i \\
&+ \eta_{43} \tilde{\mathbf{h}}_k^H \Phi^H \tilde{\mathbf{H}}_2^H \mathbf{A}_k^H \tilde{\mathbf{H}}_2 \Phi \bar{\mathbf{h}}_i + \eta_{44} \tilde{\mathbf{h}}_k^H \Phi^H \tilde{\mathbf{H}}_2^H \mathbf{A}_k^H \tilde{\mathbf{H}}_2 \Phi \tilde{\mathbf{h}}_i.
\end{aligned} \tag{146}$$

For brevity, we use the notation  $\eta_{11} - \eta_{44}$  to identify the coefficients (path-loss factors and Rician factors) in front of the product of vectors and matrices, since these coefficients are deterministic and do not determine whether the expectations of the cross-terms are zero or not. Then, we can calculate the cross-terms in (129) by calculating the expectation of the product of

one term in (146) with the conjugate transpose of another term in (146). Therefore, by exploiting Lemma 5, the independence and the zero-mean properties of  $\tilde{\mathbf{H}}_2$ ,  $\tilde{\mathbf{h}}_k$  and  $\tilde{\mathbf{h}}_i$ , we find that only 8 cross-terms have a non-zero expectation. They can be combined as

$$\begin{aligned} & \sum_{\substack{\omega 1, \psi 1, \omega 2, \psi 2, \\ (\omega 1, \psi 1) \neq (\omega 2, \psi 2)}}^4 \mathbb{E} \left\{ \left( (\hat{\mathbf{q}}_k^{\omega 1})^H \mathbf{q}_i^{\psi 1} \right) \left( (\hat{\mathbf{q}}_k^{\omega 2})^H \mathbf{q}_i^{\psi 2} \right)^H \right\} \\ &= 2 \operatorname{Re} \left\{ \mathbb{E} \left\{ \left( (\hat{\mathbf{q}}_k^1)^H \mathbf{q}_i^1 \right) \left( (\hat{\mathbf{q}}_k^3)^H \mathbf{q}_i^3 \right)^H \right\} \right\} + 2 \operatorname{Re} \left\{ \mathbb{E} \left\{ \left( (\hat{\mathbf{q}}_k^1)^H \mathbf{q}_i^2 \right) \left( (\hat{\mathbf{q}}_k^3)^H \mathbf{q}_i^4 \right)^H \right\} \right\} \\ &+ 2 \operatorname{Re} \left\{ \mathbb{E} \left\{ \left( (\hat{\mathbf{q}}_k^2)^H \mathbf{q}_i^1 \right) \left( (\hat{\mathbf{q}}_k^4)^H \mathbf{q}_i^3 \right)^H \right\} \right\} + 2 \operatorname{Re} \left\{ \mathbb{E} \left\{ \left( (\hat{\mathbf{q}}_k^2)^H \mathbf{q}_i^2 \right) \left( (\hat{\mathbf{q}}_k^4)^H \mathbf{q}_i^4 \right)^H \right\} \right\}. \end{aligned} \quad (147)$$

Then, we calculate these 4 terms in (147) one by one. Using  $\operatorname{Tr} \{\mathbf{A}_k\} = M e_{k1}$ , the first cross-term is derived as

$$\begin{aligned} & 2 \operatorname{Re} \left\{ \mathbb{E} \left\{ \left( (\hat{\mathbf{q}}_k^1)^H \mathbf{q}_i^1 \right) \left( (\hat{\mathbf{q}}_k^3)^H \mathbf{q}_i^3 \right)^H \right\} \right\} \\ &= 2 \operatorname{Re} \left\{ \mathbb{E} \left\{ \sqrt{c_k \delta \varepsilon_k} \sqrt{c_i \delta \varepsilon_i} \bar{\mathbf{h}}_k^H \Phi^H \bar{\mathbf{H}}_2^H \bar{\mathbf{H}}_2 \Phi \bar{\mathbf{h}}_i \left( \sqrt{c_k \varepsilon_k} \sqrt{c_i \varepsilon_i} \bar{\mathbf{h}}_k^H \Phi^H \tilde{\mathbf{H}}_2^H \mathbf{A}_k^H \tilde{\mathbf{H}}_2 \Phi \bar{\mathbf{h}}_i \right)^H \right\} \right\} \\ &= 2 c_k c_i \delta \varepsilon_k \varepsilon_i \operatorname{Re} \left\{ \bar{\mathbf{h}}_k^H \Phi^H \bar{\mathbf{H}}_2^H \bar{\mathbf{H}}_2 \Phi \bar{\mathbf{h}}_i \bar{\mathbf{h}}_i^H \Phi^H \mathbb{E} \left\{ \tilde{\mathbf{H}}_2^H \mathbf{A}_k \tilde{\mathbf{H}}_2 \right\} \Phi \bar{\mathbf{h}}_k \right\} \\ &= 2 c_k c_i \delta \varepsilon_k \varepsilon_i e_{k1} M \operatorname{Re} \left\{ \bar{\mathbf{h}}_k^H \Phi^H \bar{\mathbf{H}}_2^H \bar{\mathbf{H}}_2 \Phi \bar{\mathbf{h}}_i \bar{\mathbf{h}}_i^H \bar{\mathbf{h}}_k \right\} \\ &= 2 c_k c_i \delta \varepsilon_k \varepsilon_i e_{k1} M \operatorname{Re} \left\{ \bar{\mathbf{h}}_k^H \Phi^H \mathbf{a}_N \mathbf{a}_M^H \mathbf{a}_M \mathbf{a}_N^H \Phi \bar{\mathbf{h}}_i \bar{\mathbf{h}}_i^H \bar{\mathbf{h}}_k \right\} \\ &= 2 c_k c_i \delta \varepsilon_k \varepsilon_i e_{k1} M^2 \operatorname{Re} \left\{ f_k^H(\Phi) f_i(\Phi) \bar{\mathbf{h}}_i^H \bar{\mathbf{h}}_k \right\}. \end{aligned} \quad (148)$$

Note that the real operator  $\operatorname{Re} \{\cdot\}$  will be omitted for the calculation of the 2nd, 3rd, and 4th cross-terms, since the results derived show that they only have real parts. Then, the second cross-term is

$$\begin{aligned} & 2 \operatorname{Re} \left\{ \mathbb{E} \left\{ \left( (\hat{\mathbf{q}}_k^1)^H \mathbf{q}_i^2 \right) \left( (\hat{\mathbf{q}}_k^3)^H \mathbf{q}_i^4 \right)^H \right\} \right\} \\ &= 2 \mathbb{E} \left\{ \sqrt{c_k \delta \varepsilon_k} \sqrt{c_i \delta \varepsilon_i} \bar{\mathbf{h}}_k^H \Phi^H \bar{\mathbf{H}}_2^H \bar{\mathbf{H}}_2 \Phi \tilde{\mathbf{h}}_i \left( \sqrt{c_k \varepsilon_k} \sqrt{c_i} \bar{\mathbf{h}}_k^H \Phi^H \tilde{\mathbf{H}}_2^H \mathbf{A}_k^H \tilde{\mathbf{H}}_2 \Phi \tilde{\mathbf{h}}_i \right)^H \right\} \\ &= 2 c_k c_i \delta \varepsilon_k \bar{\mathbf{h}}_k^H \Phi^H \bar{\mathbf{H}}_2^H \bar{\mathbf{H}}_2 \Phi \mathbb{E} \left\{ \tilde{\mathbf{h}}_i \tilde{\mathbf{h}}_i^H \right\} \Phi^H \mathbb{E} \left\{ \tilde{\mathbf{H}}_2^H \mathbf{A}_k \tilde{\mathbf{H}}_2 \right\} \Phi \bar{\mathbf{h}}_k \\ &= 2 c_k c_i \delta \varepsilon_k e_{k1} M \bar{\mathbf{h}}_k^H \Phi^H \bar{\mathbf{H}}_2^H \bar{\mathbf{H}}_2 \Phi \bar{\mathbf{h}}_k \\ &= 2 c_k c_i \delta \varepsilon_k e_{k1} M^2 |f_k(\Phi)|^2. \end{aligned} \quad (149)$$

The third cross-term is

$$\begin{aligned}
& 2 \operatorname{Re} \left\{ \mathbb{E} \left\{ \left( (\hat{\mathbf{q}}_k^2)^H \mathbf{q}_i^1 \right) \left( (\hat{\mathbf{q}}_k^4)^H \mathbf{q}_i^3 \right)^H \right\} \right\} \\
&= 2 \mathbb{E} \left\{ e_{k2} \sqrt{c_k} \delta \sqrt{c_i} \delta \varepsilon_i \tilde{\mathbf{h}}_k^H \boldsymbol{\Phi}^H \bar{\mathbf{H}}_2^H \bar{\mathbf{H}}_2 \boldsymbol{\Phi} \tilde{\mathbf{h}}_i \left( \sqrt{c_k} \sqrt{c_i} \varepsilon_i \tilde{\mathbf{h}}_k^H \boldsymbol{\Phi}^H \tilde{\mathbf{H}}_2^H \mathbf{A}_k^H \tilde{\mathbf{H}}_2 \boldsymbol{\Phi} \tilde{\mathbf{h}}_i \right)^H \right\} \\
&= 2 c_k c_i \delta \varepsilon_i e_{k2} \mathbb{E} \left\{ \tilde{\mathbf{h}}_k^H \boldsymbol{\Phi}^H \bar{\mathbf{H}}_2^H \bar{\mathbf{H}}_2 \boldsymbol{\Phi} \tilde{\mathbf{h}}_i \tilde{\mathbf{h}}_i^H \boldsymbol{\Phi}^H \mathbb{E} \left\{ \tilde{\mathbf{H}}_2^H \mathbf{A}_k \tilde{\mathbf{H}}_2 \right\} \boldsymbol{\Phi} \tilde{\mathbf{h}}_k \right\} \\
&= 2 c_k c_i \delta \varepsilon_i e_{k1} e_{k2} M \mathbb{E} \left\{ \tilde{\mathbf{h}}_k^H \boldsymbol{\Phi}^H \bar{\mathbf{H}}_2^H \bar{\mathbf{H}}_2 \boldsymbol{\Phi} \tilde{\mathbf{h}}_i \tilde{\mathbf{h}}_i^H \tilde{\mathbf{h}}_k \right\} \\
&= 2 c_k c_i \delta \varepsilon_i e_{k1} e_{k2} M \operatorname{Tr} \left\{ \tilde{\mathbf{h}}_i^H \boldsymbol{\Phi}^H \bar{\mathbf{H}}_2^H \bar{\mathbf{H}}_2 \boldsymbol{\Phi} \tilde{\mathbf{h}}_i \right\} \\
&= 2 c_k c_i \delta \varepsilon_i e_{k1} e_{k2} M^2 |f_i(\boldsymbol{\Phi})|^2.
\end{aligned} \tag{150}$$

The fourth cross-term is

$$\begin{aligned}
& 2 \operatorname{Re} \left\{ \mathbb{E} \left\{ \left( (\hat{\mathbf{q}}_k^2)^H \mathbf{q}_i^2 \right) \left( (\hat{\mathbf{q}}_k^4)^H \mathbf{q}_i^4 \right)^H \right\} \right\} \\
&= 2 \mathbb{E} \left\{ e_{k2} \sqrt{c_k} \delta \sqrt{c_i} \delta \tilde{\mathbf{h}}_k^H \boldsymbol{\Phi}^H \bar{\mathbf{H}}_2^H \bar{\mathbf{H}}_2 \boldsymbol{\Phi} \tilde{\mathbf{h}}_i \left( \sqrt{c_k} \sqrt{c_i} \tilde{\mathbf{h}}_k^H \boldsymbol{\Phi}^H \tilde{\mathbf{H}}_2^H \mathbf{A}_k^H \tilde{\mathbf{H}}_2 \boldsymbol{\Phi} \tilde{\mathbf{h}}_i \right)^H \right\} \\
&= 2 c_k c_i \delta e_{k2} \mathbb{E} \left\{ \tilde{\mathbf{h}}_k^H \boldsymbol{\Phi}^H \bar{\mathbf{H}}_2^H \bar{\mathbf{H}}_2 \boldsymbol{\Phi} \mathbb{E} \left\{ \tilde{\mathbf{h}}_i \tilde{\mathbf{h}}_i^H \right\} \boldsymbol{\Phi}^H \mathbb{E} \left\{ \tilde{\mathbf{H}}_2^H \mathbf{A}_k \tilde{\mathbf{H}}_2 \right\} \boldsymbol{\Phi} \tilde{\mathbf{h}}_k \right\} \\
&= 2 c_k c_i \delta e_{k1} e_{k2} M \mathbb{E} \left\{ \tilde{\mathbf{h}}_k^H \boldsymbol{\Phi}^H \bar{\mathbf{H}}_2^H \bar{\mathbf{H}}_2 \boldsymbol{\Phi} \tilde{\mathbf{h}}_k \right\} \\
&= 2 c_k c_i \delta e_{k1} e_{k2} M^2 N.
\end{aligned} \tag{151}$$

We have completed the calculation of the expectation of 8 cross-terms. Finally, the interference term  $I_{ki}(\boldsymbol{\Phi})$  is obtained by combining (124) - (128), (130) - (145) and (148) - (151) to (123) with some direct simplifications.

### C. Signal Leakage

In this subsection, we derive the signal leakage term of (35) as

$$E_k^{(\text{leakage})}(\boldsymbol{\Phi}) = \mathbb{E} \left\{ |\hat{\mathbf{q}}_k^H \mathbf{q}_k|^2 \right\} - \left| \mathbb{E} \left\{ \hat{\mathbf{q}}_k^H \mathbf{q}_k \right\} \right|^2, \tag{152}$$

where  $\mathbb{E} \left\{ \hat{\mathbf{q}}_k^H \mathbf{q}_k \right\}$  is given in (117). Therefore, we only need to derive the expectation  $\mathbb{E} \left\{ |\hat{\mathbf{q}}_k^H \mathbf{q}_k|^2 \right\}$ . By exploiting the zero-mean properties of  $\mathbf{d}_k$  and  $\mathbf{N}$ , and exploiting the independence between

the cascaded channel, the direct channel, and the noise, we can expand this term and remove the terms with zero expectation as

$$\begin{aligned}
\mathbb{E} \left\{ \left| \hat{\mathbf{q}}_k^H \mathbf{q}_k \right|^2 \right\} &= \mathbb{E} \left\{ \left| \left( \hat{\mathbf{q}}_k^H + \mathbf{d}_k^H \mathbf{A}_k^H + \frac{1}{\sqrt{\tau p}} \mathbf{s}_k^H \mathbf{N}^H \mathbf{A}_k^H \right) (\mathbf{q}_k + \mathbf{d}_k) \right|^2 \right\} \\
&= \mathbb{E} \left\{ \left| \hat{\mathbf{q}}_k^H \mathbf{q}_k + \hat{\mathbf{q}}_k^H \mathbf{d}_k + \mathbf{d}_k^H \mathbf{A}_k^H \mathbf{q}_k + \mathbf{d}_k^H \mathbf{A}_k^H \mathbf{d}_k + \frac{1}{\sqrt{\tau p}} \mathbf{s}_k^H \mathbf{N}^H \mathbf{A}_k^H \mathbf{q}_k + \frac{1}{\sqrt{\tau p}} \mathbf{s}_k^H \mathbf{N}^H \mathbf{A}_k^H \mathbf{d}_k \right|^2 \right\} \\
&\stackrel{(d)}{=} \mathbb{E} \left\{ \left| \hat{\mathbf{q}}_k^H \mathbf{q}_k \right|^2 \right\} + \mathbb{E} \left\{ \left| \hat{\mathbf{q}}_k^H \mathbf{d}_k \right|^2 \right\} + \mathbb{E} \left\{ \left| \mathbf{d}_k^H \mathbf{A}_k^H \mathbf{q}_k \right|^2 \right\} + \mathbb{E} \left\{ \left| \mathbf{d}_k^H \mathbf{A}_k^H \mathbf{d}_k \right|^2 \right\} \\
&+ \mathbb{E} \left\{ \left| \frac{1}{\sqrt{\tau p}} \mathbf{s}_k^H \mathbf{N}^H \mathbf{A}_k^H \mathbf{q}_k \right|^2 \right\} + \mathbb{E} \left\{ \left| \frac{1}{\sqrt{\tau p}} \mathbf{s}_k^H \mathbf{N}^H \mathbf{A}_k^H \mathbf{d}_k \right|^2 \right\} + 2 \operatorname{Re} \left\{ \mathbb{E} \left\{ \hat{\mathbf{q}}_k^H \mathbf{q}_k (\mathbf{d}_k^H \mathbf{A}_k^H \mathbf{d}_k)^H \right\} \right\},
\end{aligned} \tag{153}$$

where in (d) the cross-term  $\mathbb{E} \left\{ \hat{\mathbf{q}}_k^H \mathbf{d}_k (\mathbf{d}_k^H \mathbf{A}_k^H \mathbf{q}_k)^H \right\}$  is zero due to Lemma 5, and the cross-term  $\mathbb{E} \left\{ \hat{\mathbf{q}}_k^H \mathbf{d}_k (\mathbf{d}_k^H \mathbf{A}_k^H \mathbf{d}_k)^H \right\}$  is zero because the odd-order central moments of a zero-mean Gaussian variable are zero [69, Eq. (12)].

Next, we derive the 2nd - 7th terms in (153), but the first term in (153) is calculated at the end. The second term in (153) is

$$\mathbb{E} \left\{ \left| \hat{\mathbf{q}}_k^H \mathbf{d}_k \right|^2 \right\} = \mathbb{E} \left\{ \hat{\mathbf{q}}_k^H \mathbb{E} \left\{ \mathbf{d}_k \mathbf{d}_k^H \right\} \hat{\mathbf{q}}_k \right\} = \gamma_k \mathbb{E} \left\{ \hat{\mathbf{q}}_k^H \hat{\mathbf{q}}_k \right\}, \tag{154}$$

where  $\mathbb{E} \left\{ \hat{\mathbf{q}}_k^H \hat{\mathbf{q}}_k \right\}$  is given in (119).

The third term in (153) is

$$\mathbb{E} \left\{ \left| \mathbf{d}_k^H \mathbf{A}_k^H \mathbf{q}_k \right|^2 \right\} = \mathbb{E} \left\{ \mathbf{q}_k^H \mathbf{A}_k \mathbb{E} \left\{ \mathbf{d}_k \mathbf{d}_k^H \right\} \mathbf{A}_k^H \mathbf{q}_k \right\} = \gamma_k \mathbb{E} \left\{ \mathbf{q}_k^H \mathbf{A}_k \mathbf{A}_k^H \mathbf{q}_k \right\}, \tag{155}$$

where  $\mathbb{E} \left\{ \mathbf{q}_k^H \mathbf{A}_k \mathbf{A}_k^H \mathbf{q}_k \right\}$  is given in (120).

Since  $\tilde{\mathbf{d}}_k \tilde{\mathbf{d}}_k^H \sim \mathcal{CW}_M(\mathbf{I}_M, 1)$ , using the property of the Wishart distribution (85), the fourth term in (153) can be obtained as

$$\begin{aligned}
\mathbb{E} \left\{ \left| \mathbf{d}_k^H \mathbf{A}_k^H \mathbf{d}_k \right|^2 \right\} &= \mathbb{E} \left\{ \mathbf{d}_k^H \mathbf{A}_k^H \mathbf{d}_k \mathbf{d}_k^H \mathbf{A}_k \mathbf{d}_k \right\} \\
&= \operatorname{Tr} \left\{ \mathbb{E} \left\{ \mathbf{A}_k^H \mathbf{d}_k \mathbf{d}_k^H \mathbf{A}_k \mathbf{d}_k \mathbf{d}_k^H \right\} \right\} \\
&= \gamma_k^2 \operatorname{Tr} \left\{ \mathbf{A}_k^H (\mathbf{A}_k + \operatorname{Tr} \left\{ \mathbf{A}_k \right\} \mathbf{I}_M) \right\} \\
&= \gamma_k^2 \operatorname{Tr} \left\{ \mathbf{A}_k^H \mathbf{A}_k \right\} + \gamma_k^2 (\operatorname{Tr} \left\{ \mathbf{A}_k \right\})^2 \\
&= \gamma_k^2 M e_{k3} + \gamma_k^2 M^2 e_{k1}^2.
\end{aligned} \tag{156}$$

The fifth term in (153) is calculated as

$$\mathbb{E} \left\{ \left| \frac{1}{\sqrt{\tau p}} \mathbf{s}_k^H \mathbf{N}^H \mathbf{A}_k^H \mathbf{q}_k \right|^2 \right\} = \frac{1}{\tau p} \mathbb{E} \left\{ \mathbf{q}_k^H \mathbf{A}_k \mathbb{E} \left\{ \mathbf{N} \mathbf{s}_k \mathbf{s}_k^H \mathbf{N}^H \right\} \mathbf{A}_k^H \mathbf{q}_k \right\} = \frac{\sigma^2}{\tau p} \mathbb{E} \left\{ \mathbf{q}_k^H \mathbf{A}_k \mathbf{A}_k^H \mathbf{q}_k \right\}, \tag{157}$$

where  $\mathbb{E} \left\{ \underline{\mathbf{q}}_k^H \mathbf{A}_k \mathbf{A}_k^H \underline{\mathbf{q}}_k \right\}$  is given in (120).

The sixth term in (153) is

$$\begin{aligned} \mathbb{E} \left\{ \left| \frac{1}{\sqrt{\tau p}} \mathbf{s}_k^H \mathbf{N}^H \mathbf{A}_k^H \mathbf{d}_k \right|^2 \right\} &= \frac{1}{\tau p} \mathbb{E} \left\{ \mathbf{d}_k^H \mathbf{A}_k \mathbb{E} \left\{ \mathbf{N} \mathbf{s}_k \mathbf{s}_k^H \mathbf{N}^H \right\} \mathbf{A}_k^H \mathbf{d}_k \right\} \\ &= \frac{\sigma^2}{\tau p} \gamma_k \text{Tr} \left\{ \mathbf{A}_k \mathbf{A}_k^H \right\} = \frac{\sigma^2}{\tau p} \gamma_k M e_{k3}. \end{aligned} \quad (158)$$

The seventh term in (153) is

$$\begin{aligned} 2 \text{Re} \left\{ \mathbb{E} \left\{ \hat{\underline{\mathbf{q}}}_k^H \underline{\mathbf{q}}_k \left( \mathbf{d}_k^H \mathbf{A}_k^H \mathbf{d}_k \right)^H \right\} \right\} &= 2 \text{Re} \left\{ \mathbb{E} \left\{ \hat{\underline{\mathbf{q}}}_k^H \underline{\mathbf{q}}_k \right\} \mathbb{E} \left\{ \mathbf{d}_k^H \mathbf{A}_k \mathbf{d}_k \right\} \right\} \\ &= 2 \gamma_k M e_{k1} \text{Re} \left\{ \mathbb{E} \left\{ \hat{\underline{\mathbf{q}}}_k^H \underline{\mathbf{q}}_k \right\} \right\} = 2 \gamma_k M e_{k1} \mathbb{E} \left\{ \hat{\underline{\mathbf{q}}}_k^H \underline{\mathbf{q}}_k \right\}, \end{aligned} \quad (159)$$

where  $\mathbb{E} \left\{ \hat{\underline{\mathbf{q}}}_k^H \underline{\mathbf{q}}_k \right\}$  is given in (122).

Finally, we derive the first term  $\mathbb{E} \left\{ \left| \hat{\underline{\mathbf{q}}}_k^H \underline{\mathbf{q}}_k \right|^2 \right\}$  in (153), which can be expanded as

$$\begin{aligned} \mathbb{E} \left\{ \left| \hat{\underline{\mathbf{q}}}_k^H \underline{\mathbf{q}}_k \right|^2 \right\} &= \mathbb{E} \left\{ \left| \sum_{\omega=1}^4 \sum_{\psi=1}^4 (\hat{\underline{\mathbf{q}}}_k^\omega)^H \mathbf{q}_k^\psi \right|^2 \right\} \\ &= \sum_{\omega=1}^4 \sum_{\psi=1}^4 \mathbb{E} \left\{ \left| (\hat{\underline{\mathbf{q}}}_k^\omega)^H \mathbf{q}_k^\psi \right|^2 \right\} + \sum_{\substack{\omega 1, \psi 1, \omega 2, \psi 2 \\ (\omega 1, \psi 1) \neq (\omega 2, \psi 2)}}^4 \mathbb{E} \left\{ \left( (\hat{\underline{\mathbf{q}}}_k^{\omega 1})^H \mathbf{q}_k^{\psi 1} \right) \left( (\hat{\underline{\mathbf{q}}}_k^{\omega 2})^H \mathbf{q}_k^{\psi 2} \right)^H \right\}. \end{aligned} \quad (160)$$

In the following, we first calculate the 16 modulus-square terms in (160), and then calculate the remaining cross-terms.

Firstly, we consider the terms with  $\omega = 1$ . When  $\psi = 1$ , we have

$$\begin{aligned} &\mathbb{E} \left\{ \left| \sqrt{c_k \delta \varepsilon_k} \sqrt{c_k \delta \varepsilon_k} \bar{\mathbf{h}}_k^H \boldsymbol{\Phi}^H \bar{\mathbf{H}}_2^H \bar{\mathbf{H}}_2 \boldsymbol{\Phi} \bar{\mathbf{h}}_k \right|^2 \right\} \\ &= c_k^2 \delta^2 \varepsilon_k^2 \left| \left( \bar{\mathbf{h}}_k^H \boldsymbol{\Phi}^H \mathbf{a}_N \right) \mathbf{a}_M^H \mathbf{a}_M \left( \mathbf{a}_N^H \boldsymbol{\Phi} \bar{\mathbf{h}}_k \right) \right|^2 \\ &= c_k^2 \delta^2 \varepsilon_k^2 M^2 |f_k(\boldsymbol{\Phi})|^4. \end{aligned} \quad (161)$$

When  $\psi = 2$ , we arrive at

$$\begin{aligned} &\mathbb{E} \left\{ \left| \sqrt{c_k \delta \varepsilon_k} \sqrt{c_k \delta \varepsilon_k} \bar{\mathbf{h}}_k^H \boldsymbol{\Phi}^H \bar{\mathbf{H}}_2^H \bar{\mathbf{H}}_2 \boldsymbol{\Phi} \tilde{\mathbf{h}}_k \right|^2 \right\} \\ &= c_k^2 \delta^2 \varepsilon_k^2 \bar{\mathbf{h}}_k^H \boldsymbol{\Phi}^H \bar{\mathbf{H}}_2^H \bar{\mathbf{H}}_2 \boldsymbol{\Phi} \mathbb{E} \left\{ \tilde{\mathbf{h}}_k \tilde{\mathbf{h}}_k^H \right\} \boldsymbol{\Phi}^H \bar{\mathbf{H}}_2^H \bar{\mathbf{H}}_2 \boldsymbol{\Phi} \bar{\mathbf{h}}_k \\ &= c_k^2 \delta^2 \varepsilon_k^2 \bar{\mathbf{h}}_k^H \boldsymbol{\Phi}^H \bar{\mathbf{H}}_2^H \bar{\mathbf{H}}_2 \bar{\mathbf{H}}_2^H \bar{\mathbf{H}}_2 \boldsymbol{\Phi} \bar{\mathbf{h}}_k \\ &= c_k^2 \delta^2 \varepsilon_k^2 \bar{\mathbf{h}}_k^H \boldsymbol{\Phi}^H \mathbf{a}_N \mathbf{a}_M^H \mathbf{a}_M \mathbf{a}_N^H \mathbf{a}_M \mathbf{a}_N^H \boldsymbol{\Phi} \bar{\mathbf{h}}_k \\ &= c_k^2 \delta^2 \varepsilon_k^2 M^2 N \bar{\mathbf{h}}_k^H \boldsymbol{\Phi}^H \mathbf{a}_N \mathbf{a}_N^H \boldsymbol{\Phi} \bar{\mathbf{h}}_k \\ &= c_k^2 \delta^2 \varepsilon_k^2 M^2 N |f_k(\boldsymbol{\Phi})|^2. \end{aligned} \quad (162)$$

When  $\psi = 3$ , we have

$$\begin{aligned}
& \mathbb{E} \left\{ \left| \sqrt{c_k \delta \varepsilon_k} \sqrt{c_k \varepsilon_k} \bar{\mathbf{h}}_k^H \boldsymbol{\Phi}^H \bar{\mathbf{H}}_2^H \tilde{\mathbf{H}}_2 \boldsymbol{\Phi} \bar{\mathbf{h}}_k \right|^2 \right\} \\
&= c_k^2 \delta \varepsilon_k^2 \bar{\mathbf{h}}_k^H \boldsymbol{\Phi}^H \bar{\mathbf{H}}_2^H \mathbb{E} \left\{ \tilde{\mathbf{H}}_2 \boldsymbol{\Phi} \bar{\mathbf{h}}_k \bar{\mathbf{h}}_k^H \boldsymbol{\Phi}^H \tilde{\mathbf{H}}_2^H \right\} \bar{\mathbf{H}}_2 \boldsymbol{\Phi} \bar{\mathbf{h}}_k \\
&= c_k^2 \delta \varepsilon_k^2 N \bar{\mathbf{h}}_k^H \boldsymbol{\Phi}^H \bar{\mathbf{H}}_2^H \bar{\mathbf{H}}_2 \boldsymbol{\Phi} \bar{\mathbf{h}}_k \\
&= c_k^2 \delta \varepsilon_k^2 M N |f_k(\boldsymbol{\Phi})|^2.
\end{aligned} \tag{163}$$

When  $\psi = 4$ , we get

$$\begin{aligned}
& \mathbb{E} \left\{ \left| \sqrt{c_k \delta \varepsilon_k} \sqrt{c_k} \bar{\mathbf{h}}_k^H \boldsymbol{\Phi}^H \bar{\mathbf{H}}_2^H \tilde{\mathbf{H}}_2 \boldsymbol{\Phi} \tilde{\mathbf{h}}_k \right|^2 \right\} \\
&= c_k^2 \delta \varepsilon_k \bar{\mathbf{h}}_k^H \boldsymbol{\Phi}^H \bar{\mathbf{H}}_2^H \mathbb{E} \left\{ \tilde{\mathbf{H}}_2 \boldsymbol{\Phi} \mathbb{E} \left\{ \tilde{\mathbf{h}}_k \tilde{\mathbf{h}}_k^H \right\} \boldsymbol{\Phi}^H \tilde{\mathbf{H}}_2^H \right\} \bar{\mathbf{H}}_2 \boldsymbol{\Phi} \bar{\mathbf{h}}_k \\
&= c_k^2 \delta \varepsilon_k M N |f_k(\boldsymbol{\Phi})|^2.
\end{aligned} \tag{164}$$

Secondly, we consider the terms with  $\omega = 2$ . When  $\psi = 1$ , we have

$$\begin{aligned}
& \mathbb{E} \left\{ \left| e_{k2} \sqrt{c_k \delta} \sqrt{c_k \delta \varepsilon_k} \tilde{\mathbf{h}}_k^H \boldsymbol{\Phi}^H \bar{\mathbf{H}}_2^H \bar{\mathbf{H}}_2 \boldsymbol{\Phi} \bar{\mathbf{h}}_k \right|^2 \right\} \\
&= c_k^2 \delta^2 \varepsilon_k e_{k2}^2 \mathbb{E} \left\{ \tilde{\mathbf{h}}_k^H \boldsymbol{\Phi}^H \bar{\mathbf{H}}_2^H \bar{\mathbf{H}}_2 \boldsymbol{\Phi} \bar{\mathbf{h}}_k \bar{\mathbf{h}}_k^H \boldsymbol{\Phi}^H \bar{\mathbf{H}}_2^H \bar{\mathbf{H}}_2 \boldsymbol{\Phi} \tilde{\mathbf{h}}_k \right\} \\
&= c_k^2 \delta^2 \varepsilon_k e_{k2}^2 \text{Tr} \left\{ \bar{\mathbf{H}}_2^H \bar{\mathbf{H}}_2 \boldsymbol{\Phi} \bar{\mathbf{h}}_k \bar{\mathbf{h}}_k^H \boldsymbol{\Phi}^H \bar{\mathbf{H}}_2^H \bar{\mathbf{H}}_2 \right\} \\
&= c_k^2 \delta^2 \varepsilon_k e_{k2}^2 \text{Tr} \left\{ \mathbf{a}_M^H \mathbf{a}_M \left( \mathbf{a}_N^H \boldsymbol{\Phi} \bar{\mathbf{h}}_k \bar{\mathbf{h}}_k^H \boldsymbol{\Phi}^H \mathbf{a}_N \right) \mathbf{a}_M^H \mathbf{a}_M \mathbf{a}_N^H \mathbf{a}_N \right\} \\
&= c_k^2 \delta^2 \varepsilon_k e_{k2}^2 M^2 N |f_k(\boldsymbol{\Phi})|^2.
\end{aligned} \tag{165}$$

Since  $\tilde{\mathbf{h}}_k \tilde{\mathbf{h}}_k^H \sim \mathcal{CW}_N(\mathbf{I}_N, 1)$ , using (85), when  $\psi = 2$ , we arrive at

$$\begin{aligned}
& \mathbb{E} \left\{ \left| e_{k2} \sqrt{c_k \delta} \sqrt{c_k \delta} \tilde{\mathbf{h}}_k^H \boldsymbol{\Phi}^H \bar{\mathbf{H}}_2^H \bar{\mathbf{H}}_2 \boldsymbol{\Phi} \tilde{\mathbf{h}}_k \right|^2 \right\} \\
&= c_k^2 \delta^2 e_{k2}^2 \mathbb{E} \left\{ \tilde{\mathbf{h}}_k^H \boldsymbol{\Phi}^H \bar{\mathbf{H}}_2^H \bar{\mathbf{H}}_2 \boldsymbol{\Phi} \tilde{\mathbf{h}}_k \tilde{\mathbf{h}}_k^H \boldsymbol{\Phi}^H \bar{\mathbf{H}}_2^H \bar{\mathbf{H}}_2 \boldsymbol{\Phi} \tilde{\mathbf{h}}_k \right\} \\
&= c_k^2 \delta^2 e_{k2}^2 \text{Tr} \left\{ \boldsymbol{\Phi}^H \bar{\mathbf{H}}_2^H \bar{\mathbf{H}}_2 \boldsymbol{\Phi} \mathbb{E} \left\{ \tilde{\mathbf{h}}_k \tilde{\mathbf{h}}_k^H \boldsymbol{\Phi}^H \bar{\mathbf{H}}_2^H \bar{\mathbf{H}}_2 \boldsymbol{\Phi} \tilde{\mathbf{h}}_k \tilde{\mathbf{h}}_k^H \right\} \right\} \\
&= c_k^2 \delta^2 e_{k2}^2 \text{Tr} \left\{ \boldsymbol{\Phi}^H \bar{\mathbf{H}}_2^H \bar{\mathbf{H}}_2 \boldsymbol{\Phi} \left( \boldsymbol{\Phi}^H \bar{\mathbf{H}}_2^H \bar{\mathbf{H}}_2 \boldsymbol{\Phi} + \text{Tr} \left\{ \boldsymbol{\Phi}^H \bar{\mathbf{H}}_2^H \bar{\mathbf{H}}_2 \boldsymbol{\Phi} \right\} \mathbf{I}_N \right) \right\} \\
&= c_k^2 \delta^2 e_{k2}^2 \text{Tr} \left\{ \boldsymbol{\Phi}^H \bar{\mathbf{H}}_2^H \bar{\mathbf{H}}_2 \boldsymbol{\Phi} \boldsymbol{\Phi}^H \bar{\mathbf{H}}_2^H \bar{\mathbf{H}}_2 \boldsymbol{\Phi} + M N \boldsymbol{\Phi}^H \bar{\mathbf{H}}_2^H \bar{\mathbf{H}}_2 \boldsymbol{\Phi} \right\} \\
&= c_k^2 \delta^2 e_{k2}^2 \left( \text{Tr} \left\{ \mathbf{a}_N \mathbf{a}_M^H \mathbf{a}_M \mathbf{a}_N^H \mathbf{a}_N \mathbf{a}_M^H \mathbf{a}_M \mathbf{a}_N^H \right\} + \text{Tr} \left\{ M N \mathbf{a}_N \mathbf{a}_M^H \mathbf{a}_M \mathbf{a}_N^H \right\} \right) \\
&= 2 c_k^2 \delta^2 e_{k2}^2 M^2 N^2.
\end{aligned} \tag{166}$$



When  $\psi = 3$ , we have

$$\begin{aligned}
& \mathbb{E} \left\{ \left| e_{k2} \sqrt{c_k \delta} \sqrt{c_k \varepsilon_k} \tilde{\mathbf{h}}_k^H \Phi^H \bar{\mathbf{H}}_2^H \tilde{\mathbf{H}}_2 \Phi \bar{\mathbf{h}}_k \right|^2 \right\} \\
&= c_k^2 \delta \varepsilon_k e_{k2}^2 \mathbb{E} \left\{ \tilde{\mathbf{h}}_k^H \Phi^H \bar{\mathbf{H}}_2^H \mathbb{E} \left\{ \tilde{\mathbf{H}}_2 \Phi \bar{\mathbf{h}}_k \bar{\mathbf{h}}_k^H \Phi^H \tilde{\mathbf{H}}_2^H \right\} \bar{\mathbf{H}}_2 \Phi \tilde{\mathbf{h}}_k \right\} \\
&= c_k^2 \delta \varepsilon_k e_{k2}^2 N \mathbb{E} \left\{ \tilde{\mathbf{h}}_k^H \Phi^H \bar{\mathbf{H}}_2^H \bar{\mathbf{H}}_2 \Phi \tilde{\mathbf{h}}_k \right\} \\
&= c_k^2 \delta \varepsilon_k e_{k2}^2 M N^2.
\end{aligned} \tag{167}$$

When  $\psi = 4$ , we arrive at

$$\begin{aligned}
& \mathbb{E} \left\{ \left| e_{k2} \sqrt{c_k \delta} \sqrt{c_k} \tilde{\mathbf{h}}_k^H \Phi^H \bar{\mathbf{H}}_2^H \tilde{\mathbf{H}}_2 \Phi \tilde{\mathbf{h}}_k \right|^2 \right\} \\
&= c_k^2 \delta e_{k2}^2 \mathbb{E} \left\{ \tilde{\mathbf{h}}_k^H \Phi^H \bar{\mathbf{H}}_2^H \tilde{\mathbf{H}}_2 \Phi \tilde{\mathbf{h}}_k \tilde{\mathbf{h}}_k^H \Phi^H \tilde{\mathbf{H}}_2^H \bar{\mathbf{H}}_2 \Phi \tilde{\mathbf{h}}_k \right\} \\
&\stackrel{(e)}{=} c_k^2 \delta e_{k2}^2 \mathbb{E}_{\tilde{\mathbf{h}}_k} \left\{ \tilde{\mathbf{h}}_k^H \Phi^H \bar{\mathbf{H}}_2^H \mathbb{E}_{\tilde{\mathbf{H}}_2} \left\{ \tilde{\mathbf{H}}_2 \Phi \tilde{\mathbf{h}}_k \tilde{\mathbf{h}}_k^H \Phi^H \tilde{\mathbf{H}}_2^H \right\} \bar{\mathbf{H}}_2 \Phi \tilde{\mathbf{h}}_k \mid \tilde{\mathbf{h}}_k \right\} \\
&= c_k^2 \delta e_{k2}^2 \mathbb{E}_{\tilde{\mathbf{h}}_k} \left\{ \tilde{\mathbf{h}}_k^H \Phi^H \bar{\mathbf{H}}_2^H \text{Tr} \left\{ \tilde{\mathbf{h}}_k \tilde{\mathbf{h}}_k^H \right\} \bar{\mathbf{H}}_2 \Phi \tilde{\mathbf{h}}_k \mid \tilde{\mathbf{h}}_k \right\} \\
&\stackrel{(f)}{=} c_k^2 \delta e_{k2}^2 \mathbb{E} \left\{ \tilde{\mathbf{h}}_k^H \Phi^H \bar{\mathbf{H}}_2^H \bar{\mathbf{H}}_2 \Phi \tilde{\mathbf{h}}_k \left( \tilde{\mathbf{h}}_k^H \tilde{\mathbf{h}}_k \right) \right\} \\
&= c_k^2 \delta e_{k2}^2 \text{Tr} \left\{ \Phi^H \bar{\mathbf{H}}_2^H \bar{\mathbf{H}}_2 \Phi \mathbb{E} \left\{ \tilde{\mathbf{h}}_k \tilde{\mathbf{h}}_k^H \tilde{\mathbf{h}}_k \tilde{\mathbf{h}}_k^H \right\} \right\} \\
&\stackrel{(g)}{=} c_k^2 \delta e_{k2}^2 \text{Tr} \left\{ \Phi^H \bar{\mathbf{H}}_2^H \bar{\mathbf{H}}_2 \Phi (N+1) \mathbf{I}_N \right\} \\
&= c_k^2 \delta e_{k2}^2 M N (N+1),
\end{aligned} \tag{168}$$

where (e) utilizes the law of total expectation, which calculates the conditional expectation of  $\tilde{\mathbf{H}}_2$  given  $\tilde{\mathbf{h}}_k$ , and then calculates the expectation of  $\tilde{\mathbf{h}}_k$ . Since  $\tilde{\mathbf{H}}_2$  is independent of  $\tilde{\mathbf{h}}_k$ , the conditional expectation of  $\tilde{\mathbf{H}}_2$  given  $\tilde{\mathbf{h}}_k$  is the same as its unconditional expectation; (f) comes from  $\text{Tr} \left\{ \tilde{\mathbf{h}}_k \tilde{\mathbf{h}}_k^H \right\} = \tilde{\mathbf{h}}_k^H \tilde{\mathbf{h}}_k$  which is a scalar number and its place can be arbitrarily moved; and (g) applies a special case of (85).

Thirdly, we consider the terms with  $\omega = 3$ . When  $\psi = 1$ , we have

$$\begin{aligned}
& \mathbb{E} \left\{ \left| \sqrt{c_k \varepsilon_k} \sqrt{c_k \delta \varepsilon_k} \bar{\mathbf{h}}_k^H \Phi^H \tilde{\mathbf{H}}_2^H \mathbf{A}_k^H \bar{\mathbf{H}}_2 \Phi \bar{\mathbf{h}}_k \right|^2 \right\} \\
&= c_k^2 \delta \varepsilon_k^2 \bar{\mathbf{h}}_k^H \Phi^H \mathbb{E} \left\{ \tilde{\mathbf{H}}_2^H \mathbf{A}_k^H \bar{\mathbf{H}}_2 \Phi \bar{\mathbf{h}}_k \bar{\mathbf{h}}_k^H \Phi^H \tilde{\mathbf{H}}_2^H \mathbf{A}_k \tilde{\mathbf{H}}_2 \right\} \Phi \bar{\mathbf{h}}_k \\
&= c_k^2 \delta \varepsilon_k^2 \bar{\mathbf{h}}_k^H \Phi^H \text{Tr} \left\{ \mathbf{A}_k^H \bar{\mathbf{H}}_2 \Phi \bar{\mathbf{h}}_k \bar{\mathbf{h}}_k^H \Phi^H \bar{\mathbf{H}}_2^H \mathbf{A}_k \right\} \Phi \bar{\mathbf{h}}_k \\
&= c_k^2 \delta \varepsilon_k^2 e_{k2}^2 \bar{\mathbf{h}}_k^H \Phi^H \text{Tr} \left\{ \mathbf{a}_N^H \Phi \bar{\mathbf{h}}_k \bar{\mathbf{h}}_k^H \Phi^H \mathbf{a}_N \mathbf{a}_M^H \mathbf{a}_M \right\} \Phi \bar{\mathbf{h}}_k \\
&= c_k^2 \delta \varepsilon_k^2 e_{k2}^2 M N |f_k(\Phi)|^2.
\end{aligned} \tag{169}$$

When  $\psi = 2$ , we have

$$\begin{aligned}
& \mathbb{E} \left\{ \left| \sqrt{c_k \varepsilon_k} \sqrt{c_k \delta} \bar{\mathbf{h}}_k^H \Phi^H \tilde{\mathbf{H}}_2^H \mathbf{A}_k^H \bar{\mathbf{H}}_2 \Phi \tilde{\mathbf{h}}_k \right|^2 \right\} \\
&= c_k^2 \delta \varepsilon_k \bar{\mathbf{h}}_k^H \Phi^H \mathbb{E} \left\{ \tilde{\mathbf{H}}_2^H \mathbf{A}_k^H \bar{\mathbf{H}}_2 \Phi \mathbb{E} \left\{ \tilde{\mathbf{h}}_k \tilde{\mathbf{h}}_k^H \right\} \Phi^H \bar{\mathbf{H}}_2^H \mathbf{A}_k \tilde{\mathbf{H}}_2 \right\} \Phi \bar{\mathbf{h}}_k \\
&= c_k^2 \delta \varepsilon_k \bar{\mathbf{h}}_k^H \Phi^H \text{Tr} \left\{ \mathbf{A}_k^H \bar{\mathbf{H}}_2 \bar{\mathbf{H}}_2^H \mathbf{A}_k \right\} \Phi \bar{\mathbf{h}}_k \\
&= c_k^2 \delta \varepsilon_k e_{k2}^2 M N^2.
\end{aligned} \tag{170}$$

When  $\psi = 3$ , using Lemma 6, we have

$$\begin{aligned}
& \mathbb{E} \left\{ \left| \sqrt{c_k \varepsilon_k} \sqrt{c_k \varepsilon_k} \bar{\mathbf{h}}_k^H \Phi^H \tilde{\mathbf{H}}_2^H \mathbf{A}_k^H \tilde{\mathbf{H}}_2 \Phi \bar{\mathbf{h}}_k \right|^2 \right\} \\
&= c_k^2 \varepsilon_k^2 \bar{\mathbf{h}}_k^H \Phi^H \mathbb{E} \left\{ \tilde{\mathbf{H}}_2^H \mathbf{A}_k^H \tilde{\mathbf{H}}_2 \Phi \bar{\mathbf{h}}_k \bar{\mathbf{h}}_k^H \Phi^H \tilde{\mathbf{H}}_2^H \mathbf{A}_k \tilde{\mathbf{H}}_2 \right\} \Phi \bar{\mathbf{h}}_k \\
&= c_k^2 \varepsilon_k^2 \bar{\mathbf{h}}_k^H \Phi^H \left( e_{k1}^2 M^2 \Phi \bar{\mathbf{h}}_k \bar{\mathbf{h}}_k^H \Phi^H + e_{k3} M \text{Tr} \left\{ \Phi \bar{\mathbf{h}}_k \bar{\mathbf{h}}_k^H \Phi^H \right\} \mathbf{I}_N \right) \Phi \bar{\mathbf{h}}_k \\
&= c_k^2 \varepsilon_k^2 \left( e_{k1}^2 M^2 \bar{\mathbf{h}}_k^H \bar{\mathbf{h}}_k \bar{\mathbf{h}}_k^H \bar{\mathbf{h}}_k + e_{k3} M N \bar{\mathbf{h}}_k^H \bar{\mathbf{h}}_k \right) \\
&= c_k^2 \varepsilon_k^2 (e_{k1}^2 M^2 N^2 + e_{k3} M N^2).
\end{aligned} \tag{171}$$

When  $\psi = 4$ , using Lemma 6 with  $\mathbf{W} = \mathbf{I}_N$ , we have

$$\begin{aligned}
& \mathbb{E} \left\{ \left| \sqrt{c_k \varepsilon_k} \sqrt{c_k} \bar{\mathbf{h}}_k^H \Phi^H \tilde{\mathbf{H}}_2^H \mathbf{A}_k^H \tilde{\mathbf{H}}_2 \Phi \tilde{\mathbf{h}}_k \right|^2 \right\} \\
&= c_k^2 \varepsilon_k \bar{\mathbf{h}}_k^H \Phi^H \mathbb{E} \left\{ \tilde{\mathbf{H}}_2^H \mathbf{A}_k^H \tilde{\mathbf{H}}_2 \Phi \mathbb{E} \left\{ \tilde{\mathbf{h}}_k \tilde{\mathbf{h}}_k^H \right\} \Phi^H \tilde{\mathbf{H}}_2^H \mathbf{A}_k \tilde{\mathbf{H}}_2 \right\} \Phi \bar{\mathbf{h}}_k \\
&= c_k^2 \varepsilon_k \bar{\mathbf{h}}_k^H \Phi^H \mathbb{E} \left\{ \tilde{\mathbf{H}}_2^H \mathbf{A}_k^H \tilde{\mathbf{H}}_2 \tilde{\mathbf{H}}_2^H \mathbf{A}_k \tilde{\mathbf{H}}_2 \right\} \Phi \bar{\mathbf{h}}_k \\
&= c_k^2 \varepsilon_k (e_{k1}^2 M^2 + e_{k3} M N) \bar{\mathbf{h}}_k^H \Phi^H \mathbf{I}_N \Phi \bar{\mathbf{h}}_k \\
&= c_k^2 \varepsilon_k (e_{k1}^2 M^2 N + e_{k3} M N^2).
\end{aligned} \tag{172}$$

Fourthly, we consider the terms with  $\omega = 4$ . When  $\psi = 1$ , we have

$$\begin{aligned}
& \mathbb{E} \left\{ \left| \sqrt{c_k} \sqrt{c_k \delta \varepsilon_k} \tilde{\mathbf{h}}_k^H \Phi^H \tilde{\mathbf{H}}_2^H \mathbf{A}_k^H \bar{\mathbf{H}}_2 \Phi \bar{\mathbf{h}}_k \right|^2 \right\} \\
&= c_k^2 \delta \varepsilon_k \mathbb{E} \left\{ \tilde{\mathbf{h}}_k^H \Phi^H \mathbb{E} \left\{ \tilde{\mathbf{H}}_2^H \mathbf{A}_k^H \bar{\mathbf{H}}_2 \Phi \bar{\mathbf{h}}_k \bar{\mathbf{h}}_k^H \Phi^H \bar{\mathbf{H}}_2^H \mathbf{A}_k \tilde{\mathbf{H}}_2 \right\} \Phi \tilde{\mathbf{h}}_k \right\} \\
&= c_k^2 \delta \varepsilon_k e_{k2}^2 \mathbb{E} \left\{ \tilde{\mathbf{h}}_k^H \Phi^H \text{Tr} \left\{ \bar{\mathbf{H}}_2 \Phi \bar{\mathbf{h}}_k \bar{\mathbf{h}}_k^H \Phi^H \bar{\mathbf{H}}_2^H \right\} \Phi \tilde{\mathbf{h}}_k \right\} \\
&= c_k^2 \delta \varepsilon_k e_{k2}^2 M |f_k(\Phi)|^2 \mathbb{E} \left\{ \tilde{\mathbf{h}}_k^H \tilde{\mathbf{h}}_k \right\} \\
&= c_k^2 \delta \varepsilon_k e_{k2}^2 M N |f_k(\Phi)|^2.
\end{aligned} \tag{173}$$

When  $\psi = 2$ , we have

$$\begin{aligned}
& \mathbb{E} \left\{ \left| \sqrt{c_k} \sqrt{c_k} \tilde{\mathbf{h}}_k^H \Phi^H \tilde{\mathbf{H}}_2^H \mathbf{A}_k^H \bar{\mathbf{H}}_2 \Phi \tilde{\mathbf{h}}_k \right|^2 \right\} \\
&= c_k^2 \delta \mathbb{E}_{\tilde{\mathbf{h}}_k} \left\{ \tilde{\mathbf{h}}_k^H \Phi^H \mathbb{E}_{\tilde{\mathbf{H}}_2} \left\{ \tilde{\mathbf{H}}_2^H \mathbf{A}_k^H \bar{\mathbf{H}}_2 \Phi \tilde{\mathbf{h}}_k \tilde{\mathbf{h}}_k^H \Phi^H \bar{\mathbf{H}}_2^H \mathbf{A}_k \tilde{\mathbf{H}}_2 \right\} \Phi \tilde{\mathbf{h}}_k \mid \tilde{\mathbf{h}}_k \right\} \\
&= c_k^2 \delta e_{k2}^2 \mathbb{E} \left\{ \tilde{\mathbf{h}}_k^H \Phi^H \text{Tr} \left\{ \bar{\mathbf{H}}_2 \Phi \tilde{\mathbf{h}}_k \tilde{\mathbf{h}}_k^H \Phi^H \bar{\mathbf{H}}_2^H \right\} \Phi \tilde{\mathbf{h}}_k \right\} \\
&\stackrel{(h)}{=} c_k^2 \delta e_{k2}^2 \mathbb{E} \left\{ \tilde{\mathbf{h}}_k^H \Phi^H \Phi \tilde{\mathbf{h}}_k \left( \tilde{\mathbf{h}}_k^H \Phi^H \bar{\mathbf{H}}_2^H \bar{\mathbf{H}}_2 \Phi \tilde{\mathbf{h}}_k \right) \right\} \\
&= c_k^2 \delta e_{k2}^2 \text{Tr} \left\{ \mathbb{E} \left\{ \tilde{\mathbf{h}}_k \tilde{\mathbf{h}}_k^H \Phi^H \bar{\mathbf{H}}_2^H \bar{\mathbf{H}}_2 \Phi \tilde{\mathbf{h}}_k \tilde{\mathbf{h}}_k^H \right\} \right\} \\
&= c_k^2 \delta e_{k2}^2 \text{Tr} \left\{ \Phi^H \bar{\mathbf{H}}_2^H \bar{\mathbf{H}}_2 \Phi + \text{Tr} \left\{ \Phi^H \bar{\mathbf{H}}_2^H \bar{\mathbf{H}}_2 \Phi \right\} \mathbf{I}_N \right\} \\
&= c_k^2 \delta e_{k2}^2 \text{Tr} \left\{ \bar{\mathbf{H}}_2^H \bar{\mathbf{H}}_2 + MN \mathbf{I}_N \right\} \\
&= c_k^2 \delta e_{k2}^2 (MN + MN^2),
\end{aligned} \tag{174}$$

where (h) comes from  $\text{Tr} \left\{ \bar{\mathbf{H}}_2 \Phi \tilde{\mathbf{h}}_k \tilde{\mathbf{h}}_k^H \Phi^H \bar{\mathbf{H}}_2^H \right\} = \tilde{\mathbf{h}}_k^H \Phi^H \bar{\mathbf{H}}_2^H \bar{\mathbf{H}}_2 \Phi \tilde{\mathbf{h}}_k$ , which is a  $1 \times 1$  number and can be moved to the end of the equation.

When  $\psi = 3$ , using Lemma 4 and Lemma 6, we have

$$\begin{aligned}
& \mathbb{E} \left\{ \left| \sqrt{c_k} \sqrt{c_k} \tilde{\mathbf{h}}_k^H \Phi^H \tilde{\mathbf{H}}_2^H \mathbf{A}_k^H \tilde{\mathbf{H}}_2 \Phi \tilde{\mathbf{h}}_k \right|^2 \right\} \\
&= c_k^2 \varepsilon_k \mathbb{E} \left\{ \tilde{\mathbf{h}}_k^H \Phi^H \mathbb{E} \left\{ \tilde{\mathbf{H}}_2^H \mathbf{A}_k^H \tilde{\mathbf{H}}_2 \Phi \tilde{\mathbf{h}}_k \tilde{\mathbf{h}}_k^H \Phi^H \tilde{\mathbf{H}}_2^H \mathbf{A}_k \tilde{\mathbf{H}}_2 \right\} \Phi \tilde{\mathbf{h}}_k \right\} \\
&= c_k^2 \varepsilon_k \mathbb{E} \left\{ \tilde{\mathbf{h}}_k^H \Phi^H \left( e_{k1}^2 M^2 \Phi \tilde{\mathbf{h}}_k \tilde{\mathbf{h}}_k^H \Phi^H + e_{k3} M \text{Tr} \left\{ \Phi \tilde{\mathbf{h}}_k \tilde{\mathbf{h}}_k^H \Phi^H \right\} \mathbf{I}_N \right) \Phi \tilde{\mathbf{h}}_k \right\} \\
&= c_k^2 \varepsilon_k \mathbb{E} \left\{ e_{k1}^2 M^2 \tilde{\mathbf{h}}_k^H \Phi^H \Phi \tilde{\mathbf{h}}_k \tilde{\mathbf{h}}_k^H \Phi^H \Phi \tilde{\mathbf{h}}_k + e_{k3} MN \tilde{\mathbf{h}}_k^H \Phi^H \Phi \tilde{\mathbf{h}}_k \right\} \\
&= c_k^2 \varepsilon_k \mathbb{E} \left\{ e_{k1}^2 M^2 \tilde{\mathbf{h}}_k^H \tilde{\mathbf{h}}_k \tilde{\mathbf{h}}_k^H \tilde{\mathbf{h}}_k + e_{k3} MN \tilde{\mathbf{h}}_k^H \tilde{\mathbf{h}}_k \right\} \\
&= c_k^2 \varepsilon_k (e_{k1}^2 M^2 N + e_{k3} MN^2).
\end{aligned} \tag{175}$$

When  $\psi = 4$ , we get

$$\begin{aligned}
& \mathbb{E} \left\{ \left| \sqrt{c_k} \sqrt{c_k} \tilde{\mathbf{h}}_k^H \Phi^H \tilde{\mathbf{H}}_2^H \mathbf{A}_k^H \tilde{\mathbf{H}}_2 \Phi \tilde{\mathbf{h}}_k \right|^2 \right\} \\
&= c_k^2 \mathbb{E}_{\tilde{\mathbf{h}}_k} \left\{ \tilde{\mathbf{h}}_k^H \Phi^H \mathbb{E}_{\tilde{\mathbf{H}}_2} \left\{ \tilde{\mathbf{H}}_2^H \mathbf{A}_k^H \tilde{\mathbf{H}}_2 \Phi \tilde{\mathbf{h}}_k \tilde{\mathbf{h}}_k^H \Phi^H \tilde{\mathbf{H}}_2^H \mathbf{A}_k \tilde{\mathbf{H}}_2 \right\} \Phi \tilde{\mathbf{h}}_k \mid \tilde{\mathbf{h}}_k \right\} \\
&= c_k^2 \mathbb{E}_{\tilde{\mathbf{h}}_k} \left\{ \tilde{\mathbf{h}}_k^H \Phi^H \left( e_{k1}^2 M^2 \Phi \tilde{\mathbf{h}}_k \tilde{\mathbf{h}}_k^H \Phi^H + e_{k3} M \text{Tr} \left\{ \Phi \tilde{\mathbf{h}}_k \tilde{\mathbf{h}}_k^H \Phi^H \right\} \mathbf{I}_N \right) \Phi \tilde{\mathbf{h}}_k \right\} \\
&= c_k^2 \mathbb{E} \left\{ e_{k1}^2 M^2 \tilde{\mathbf{h}}_k^H \tilde{\mathbf{h}}_k \tilde{\mathbf{h}}_k^H \tilde{\mathbf{h}}_k + e_{k3} M \tilde{\mathbf{h}}_k^H \tilde{\mathbf{h}}_k \tilde{\mathbf{h}}_k^H \tilde{\mathbf{h}}_k \right\} \\
&\stackrel{(i)}{=} c_k^2 \{ e_{k1}^2 M^2 N(N+1) + e_{k3} MN(N+1) \},
\end{aligned} \tag{176}$$

where (i) uses (88).

Herein, the calculation of the 16 modulus-square terms are completed. Now, we focus on the expectation of the remaining cross-terms. To better understand the form of the cross-terms, we give the expansion of  $\hat{\mathbf{q}}_k^H \mathbf{q}_k$  as

$$\begin{aligned}
\hat{\mathbf{q}}_k^H \mathbf{q}_k &= \sum_{\omega=1}^4 \sum_{\psi=1}^4 (\hat{\mathbf{q}}_k^\omega)^H \mathbf{q}_k^\psi \\
&= \eta^{11} \bar{\mathbf{h}}_k^H \Phi^H \bar{\mathbf{H}}_2^H \bar{\mathbf{H}}_2 \Phi \bar{\mathbf{h}}_k + \eta^{12} \bar{\mathbf{h}}_k^H \Phi^H \bar{\mathbf{H}}_2^H \bar{\mathbf{H}}_2 \Phi \tilde{\mathbf{h}}_k + \eta^{13} \bar{\mathbf{h}}_k^H \Phi^H \bar{\mathbf{H}}_2^H \tilde{\mathbf{H}}_2 \Phi \bar{\mathbf{h}}_k + \eta^{14} \bar{\mathbf{h}}_k^H \Phi^H \bar{\mathbf{H}}_2^H \tilde{\mathbf{H}}_2 \Phi \tilde{\mathbf{h}}_k \\
&+ \eta^{21} \tilde{\mathbf{h}}_k^H \Phi^H \bar{\mathbf{H}}_2^H \bar{\mathbf{H}}_2 \Phi \bar{\mathbf{h}}_k + \eta^{22} \tilde{\mathbf{h}}_k^H \Phi^H \bar{\mathbf{H}}_2^H \bar{\mathbf{H}}_2 \Phi \tilde{\mathbf{h}}_k + \eta^{23} \tilde{\mathbf{h}}_k^H \Phi^H \bar{\mathbf{H}}_2^H \tilde{\mathbf{H}}_2 \Phi \bar{\mathbf{h}}_k + \eta^{24} \tilde{\mathbf{h}}_k^H \Phi^H \bar{\mathbf{H}}_2^H \tilde{\mathbf{H}}_2 \Phi \tilde{\mathbf{h}}_k \\
&+ \eta^{31} \bar{\mathbf{h}}_k^H \Phi^H \tilde{\mathbf{H}}_2^H \mathbf{A}_k^H \bar{\mathbf{H}}_2 \Phi \bar{\mathbf{h}}_k + \eta^{32} \bar{\mathbf{h}}_k^H \Phi^H \tilde{\mathbf{H}}_2^H \mathbf{A}_k^H \bar{\mathbf{H}}_2 \Phi \tilde{\mathbf{h}}_k \\
&+ \eta^{33} \bar{\mathbf{h}}_k^H \Phi^H \tilde{\mathbf{H}}_2^H \mathbf{A}_k^H \tilde{\mathbf{H}}_2 \Phi \bar{\mathbf{h}}_k + \eta^{34} \bar{\mathbf{h}}_k^H \Phi^H \tilde{\mathbf{H}}_2^H \mathbf{A}_k^H \tilde{\mathbf{H}}_2 \Phi \tilde{\mathbf{h}}_k \\
&+ \eta^{41} \tilde{\mathbf{h}}_k^H \Phi^H \tilde{\mathbf{H}}_2^H \mathbf{A}_k^H \bar{\mathbf{H}}_2 \Phi \bar{\mathbf{h}}_k + \eta^{42} \tilde{\mathbf{h}}_k^H \Phi^H \tilde{\mathbf{H}}_2^H \mathbf{A}_k^H \bar{\mathbf{H}}_2 \Phi \tilde{\mathbf{h}}_k \\
&+ \eta^{43} \tilde{\mathbf{h}}_k^H \Phi^H \tilde{\mathbf{H}}_2^H \mathbf{A}_k^H \tilde{\mathbf{H}}_2 \Phi \bar{\mathbf{h}}_k + \eta^{44} \tilde{\mathbf{h}}_k^H \Phi^H \tilde{\mathbf{H}}_2^H \mathbf{A}_k^H \tilde{\mathbf{H}}_2 \Phi \tilde{\mathbf{h}}_k.
\end{aligned} \tag{177}$$

We use the notation  $\eta^{11} - \eta^{44}$  to identify the coefficients in front of the product of vectors and matrices. We can calculate the cross-terms in (160) by calculating the expectation of the product of one term in (177) with the conjugate transpose of another term in (177). There exist  $16 \times 15$  cross-terms, but only 20 of them are non-zero. Using Lemma 5, the independence and zero-mean properties of  $\tilde{\mathbf{H}}_2$  and  $\tilde{\mathbf{h}}_k$ , we can filter the 20 non-zero cross-terms, and combine them into the following 10 terms:

$$\begin{aligned}
&\sum_{\substack{\omega 1, \psi 1, \omega 2, \psi 2, \\ (\omega 1, \psi 1) \neq (\omega 2, \psi 2)}}^4 \mathbb{E} \left\{ \left( (\hat{\mathbf{q}}_k^{\omega 1})^H \mathbf{q}_k^{\psi 1} \right) \left( (\hat{\mathbf{q}}_k^{\omega 2})^H \mathbf{q}_k^{\psi 2} \right)^H \right\} \\
&= 2 \operatorname{Re} \left\{ \mathbb{E} \left\{ \left( (\hat{\mathbf{q}}_k^1)^H \mathbf{q}_k^1 \right) \left( (\hat{\mathbf{q}}_k^2)^H \mathbf{q}_k^2 \right)^H \right\} \right\} + 2 \operatorname{Re} \left\{ \mathbb{E} \left\{ \left( (\hat{\mathbf{q}}_k^1)^H \mathbf{q}_k^1 \right) \left( (\hat{\mathbf{q}}_k^3)^H \mathbf{q}_k^3 \right)^H \right\} \right\} \\
&+ 2 \operatorname{Re} \left\{ \mathbb{E} \left\{ \left( (\hat{\mathbf{q}}_k^1)^H \mathbf{q}_k^1 \right) \left( (\hat{\mathbf{q}}_k^4)^H \mathbf{q}_k^4 \right)^H \right\} \right\} + 2 \operatorname{Re} \left\{ \mathbb{E} \left\{ \left( (\hat{\mathbf{q}}_k^1)^H \mathbf{q}_k^2 \right) \left( (\hat{\mathbf{q}}_k^3)^H \mathbf{q}_k^4 \right)^H \right\} \right\} \\
&+ 2 \operatorname{Re} \left\{ \mathbb{E} \left\{ \left( (\hat{\mathbf{q}}_k^1)^H \mathbf{q}_k^3 \right) \left( (\hat{\mathbf{q}}_k^2)^H \mathbf{q}_k^4 \right)^H \right\} \right\} + 2 \operatorname{Re} \left\{ \mathbb{E} \left\{ \left( (\hat{\mathbf{q}}_k^2)^H \mathbf{q}_k^1 \right) \left( (\hat{\mathbf{q}}_k^4)^H \mathbf{q}_k^3 \right)^H \right\} \right\} \\
&+ 2 \operatorname{Re} \left\{ \mathbb{E} \left\{ \left( (\hat{\mathbf{q}}_k^2)^H \mathbf{q}_k^2 \right) \left( (\hat{\mathbf{q}}_k^3)^H \mathbf{q}_k^3 \right)^H \right\} \right\} + 2 \operatorname{Re} \left\{ \mathbb{E} \left\{ \left( (\hat{\mathbf{q}}_k^2)^H \mathbf{q}_k^2 \right) \left( (\hat{\mathbf{q}}_k^4)^H \mathbf{q}_k^4 \right)^H \right\} \right\} \\
&+ 2 \operatorname{Re} \left\{ \mathbb{E} \left\{ \left( (\hat{\mathbf{q}}_k^3)^H \mathbf{q}_k^1 \right) \left( (\hat{\mathbf{q}}_k^4)^H \mathbf{q}_k^2 \right)^H \right\} \right\} + 2 \operatorname{Re} \left\{ \mathbb{E} \left\{ \left( (\hat{\mathbf{q}}_k^3)^H \mathbf{q}_k^3 \right) \left( (\hat{\mathbf{q}}_k^4)^H \mathbf{q}_k^4 \right)^H \right\} \right\}.
\end{aligned} \tag{178}$$

Now, we derive these 10 terms in sequence. Note that the real operator  $\operatorname{Re} \{ \cdot \}$  is omitted, since the results show that they only have real parts.

Let us begin with the calculation of the first term as follows

$$\begin{aligned}
& 2\mathbb{E} \left\{ \sqrt{c_k \delta \varepsilon_k} \sqrt{c_k \delta \varepsilon_k} \bar{\mathbf{h}}_k^H \Phi^H \bar{\mathbf{H}}_2^H \bar{\mathbf{H}}_2 \Phi \bar{\mathbf{h}}_k \left( e_{k2} \sqrt{c_k \delta} \sqrt{c_k \delta} \tilde{\mathbf{h}}_k^H \Phi^H \bar{\mathbf{H}}_2^H \bar{\mathbf{H}}_2 \Phi \tilde{\mathbf{h}}_k \right)^H \right\} \\
&= 2c_k^2 \delta^2 \varepsilon_k e_{k2} \bar{\mathbf{h}}_k^H \Phi^H \bar{\mathbf{H}}_2^H \bar{\mathbf{H}}_2 \Phi \bar{\mathbf{h}}_k \mathbb{E} \left\{ \tilde{\mathbf{h}}_k^H \Phi^H \bar{\mathbf{H}}_2^H \bar{\mathbf{H}}_2 \Phi \tilde{\mathbf{h}}_k \right\} \\
&= 2c_k^2 \delta^2 \varepsilon_k e_{k2} \left( \bar{\mathbf{h}}_k^H \Phi^H \mathbf{a}_N \right) \mathbf{a}_M^H \mathbf{a}_M \left( \mathbf{a}_N^H \Phi \bar{\mathbf{h}}_k \right) \text{Tr} \left\{ \Phi^H \mathbf{a}_N \mathbf{a}_M^H \mathbf{a}_M \mathbf{a}_N^H \Phi \right\} \\
&= 2c_k^2 \delta^2 \varepsilon_k e_{k2} M^2 N |f_k(\Phi)|^2.
\end{aligned} \tag{179}$$

The second term is

$$\begin{aligned}
& 2\mathbb{E} \left\{ \sqrt{c_k \delta \varepsilon_k} \sqrt{c_k \delta \varepsilon_k} \bar{\mathbf{h}}_k^H \Phi^H \bar{\mathbf{H}}_2^H \bar{\mathbf{H}}_2 \Phi \bar{\mathbf{h}}_k \left( \sqrt{c_k \varepsilon_k} \sqrt{c_k \varepsilon_k} \bar{\mathbf{h}}_k^H \Phi^H \tilde{\mathbf{H}}_2^H \mathbf{A}_k^H \tilde{\mathbf{H}}_2 \Phi \bar{\mathbf{h}}_k \right)^H \right\} \\
&= 2c_k^2 \delta \varepsilon_k^2 \bar{\mathbf{h}}_k^H \Phi^H \bar{\mathbf{H}}_2^H \bar{\mathbf{H}}_2 \Phi \bar{\mathbf{h}}_k \bar{\mathbf{h}}_k^H \Phi^H \mathbb{E} \left\{ \tilde{\mathbf{H}}_2^H \mathbf{A}_k \tilde{\mathbf{H}}_2 \right\} \Phi \bar{\mathbf{h}}_k \\
&= 2c_k^2 \delta \varepsilon_k^2 e_{k1} M \left( \bar{\mathbf{h}}_k^H \Phi^H \mathbf{a}_N \right) \mathbf{a}_M^H \mathbf{a}_M \left( \mathbf{a}_N^H \Phi \bar{\mathbf{h}}_k \right) \bar{\mathbf{h}}_k^H \bar{\mathbf{h}}_k \\
&= 2c_k^2 \delta \varepsilon_k^2 e_{k1} M^2 N |f_k(\Phi)|^2.
\end{aligned} \tag{180}$$

The third term is

$$\begin{aligned}
& 2\mathbb{E} \left\{ \sqrt{c_k \delta \varepsilon_k} \sqrt{c_k \delta \varepsilon_k} \bar{\mathbf{h}}_k^H \Phi^H \bar{\mathbf{H}}_2^H \bar{\mathbf{H}}_2 \Phi \bar{\mathbf{h}}_k \left( \sqrt{c_k} \sqrt{c_k} \tilde{\mathbf{h}}_k^H \Phi^H \tilde{\mathbf{H}}_2^H \mathbf{A}_k^H \tilde{\mathbf{H}}_2 \Phi \tilde{\mathbf{h}}_k \right)^H \right\} \\
&= 2c_k^2 \delta \varepsilon_k \bar{\mathbf{h}}_k^H \Phi^H \bar{\mathbf{H}}_2^H \bar{\mathbf{H}}_2 \Phi \bar{\mathbf{h}}_k \mathbb{E} \left\{ \tilde{\mathbf{h}}_k^H \Phi^H \mathbb{E} \left\{ \tilde{\mathbf{H}}_2^H \mathbf{A}_k \tilde{\mathbf{H}}_2 \right\} \Phi \tilde{\mathbf{h}}_k \right\} \\
&= 2c_k^2 \delta \varepsilon_k e_{k1} M \left( \bar{\mathbf{h}}_k^H \Phi^H \mathbf{a}_N \right) \mathbf{a}_M^H \mathbf{a}_M \left( \mathbf{a}_N^H \Phi \bar{\mathbf{h}}_k \right) \mathbb{E} \left\{ \tilde{\mathbf{h}}_k^H \tilde{\mathbf{h}}_k \right\} \\
&= 2c_k^2 \delta \varepsilon_k e_{k1} M^2 N |f_k(\Phi)|^2.
\end{aligned} \tag{181}$$

The fourth term is

$$\begin{aligned}
& 2\mathbb{E} \left\{ \sqrt{c_k \delta \varepsilon_k} \sqrt{c_k \delta} \bar{\mathbf{h}}_k^H \Phi^H \bar{\mathbf{H}}_2^H \bar{\mathbf{H}}_2 \Phi \tilde{\mathbf{h}}_k \left( \sqrt{c_k \varepsilon_k} \sqrt{c_k} \bar{\mathbf{h}}_k^H \Phi^H \tilde{\mathbf{H}}_2^H \mathbf{A}_k^H \tilde{\mathbf{H}}_2 \Phi \tilde{\mathbf{h}}_k \right)^H \right\} \\
&= 2c_k^2 \delta \varepsilon_k \bar{\mathbf{h}}_k^H \Phi^H \bar{\mathbf{H}}_2^H \bar{\mathbf{H}}_2 \Phi \mathbb{E} \left\{ \tilde{\mathbf{h}}_k \tilde{\mathbf{h}}_k^H \right\} \Phi^H \mathbb{E} \left\{ \tilde{\mathbf{H}}_2^H \mathbf{A}_k \tilde{\mathbf{H}}_2 \right\} \Phi \bar{\mathbf{h}}_k \\
&= 2c_k^2 \delta \varepsilon_k e_{k1} M \bar{\mathbf{h}}_k^H \Phi^H \bar{\mathbf{H}}_2^H \bar{\mathbf{H}}_2 \Phi \bar{\mathbf{h}}_k \\
&= 2c_k^2 \delta \varepsilon_k e_{k1} M^2 |f_k(\Phi)|^2.
\end{aligned} \tag{182}$$

The fifth term is

$$\begin{aligned}
& 2\mathbb{E} \left\{ \sqrt{c_k \delta \varepsilon_k} \sqrt{c_k \varepsilon_k} \bar{\mathbf{h}}_k^H \Phi^H \bar{\mathbf{H}}_2^H \tilde{\mathbf{H}}_2 \Phi \bar{\mathbf{h}}_k \left( e_{k2} \sqrt{c_k \delta} \sqrt{c_k} \tilde{\mathbf{h}}_k^H \Phi^H \bar{\mathbf{H}}_2^H \tilde{\mathbf{H}}_2 \Phi \tilde{\mathbf{h}}_k \right)^H \right\} \\
&= 2c_k^2 \delta \varepsilon_k e_{k2} \bar{\mathbf{h}}_k^H \Phi^H \bar{\mathbf{H}}_2^H \mathbb{E} \left\{ \tilde{\mathbf{H}}_2 \Phi \bar{\mathbf{h}}_k \tilde{\mathbf{h}}_k^H \Phi^H \bar{\mathbf{H}}_2^H \Phi \tilde{\mathbf{h}}_k \right\} \\
&= 2c_k^2 \delta \varepsilon_k e_{k2} \bar{\mathbf{h}}_k^H \Phi^H \bar{\mathbf{H}}_2^H \mathbb{E}_{\tilde{\mathbf{h}}_k} \left\{ \mathbb{E}_{\tilde{\mathbf{H}}_2} \left\{ \tilde{\mathbf{H}}_2 \Phi \bar{\mathbf{h}}_k \tilde{\mathbf{h}}_k^H \Phi^H \tilde{\mathbf{H}}_2^H \right\} \bar{\mathbf{H}}_2 \Phi \tilde{\mathbf{h}}_k \mid \tilde{\mathbf{h}}_k \right\} \\
&= 2c_k^2 \delta \varepsilon_k e_{k2} \bar{\mathbf{h}}_k^H \Phi^H \bar{\mathbf{H}}_2^H \mathbb{E} \left\{ \text{Tr} \left\{ \Phi \bar{\mathbf{h}}_k \tilde{\mathbf{h}}_k^H \Phi^H \right\} \bar{\mathbf{H}}_2 \Phi \tilde{\mathbf{h}}_k \right\} \\
&\stackrel{(j)}{=} 2c_k^2 \delta \varepsilon_k e_{k2} \bar{\mathbf{h}}_k^H \Phi^H \bar{\mathbf{H}}_2^H \mathbb{E} \left\{ \bar{\mathbf{H}}_2 \Phi \tilde{\mathbf{h}}_k \left( \tilde{\mathbf{h}}_k^H \bar{\mathbf{h}}_k \right) \right\} \\
&= 2c_k^2 \delta \varepsilon_k e_{k2} \bar{\mathbf{h}}_k^H \Phi^H \bar{\mathbf{H}}_2^H \bar{\mathbf{H}}_2 \Phi \mathbb{E} \left\{ \tilde{\mathbf{h}}_k \tilde{\mathbf{h}}_k^H \right\} \bar{\mathbf{h}}_k \\
&= 2c_k^2 \delta \varepsilon_k e_{k2} \bar{\mathbf{h}}_k^H \Phi^H \bar{\mathbf{H}}_2^H \bar{\mathbf{H}}_2 \Phi \bar{\mathbf{h}}_k \\
&= 2c_k^2 \delta \varepsilon_k e_{k2} M |f_k(\Phi)|^2,
\end{aligned} \tag{183}$$

where (j) uses  $\text{Tr} \left\{ \Phi \bar{\mathbf{h}}_k \tilde{\mathbf{h}}_k^H \Phi^H \right\} = \tilde{\mathbf{h}}_k^H \bar{\mathbf{h}}_k$  and then places it at the end of the equation.

The sixth term is

$$\begin{aligned}
& 2\mathbb{E} \left\{ e_{k2} \sqrt{c_k \delta} \sqrt{c_k \delta \varepsilon_k} \tilde{\mathbf{h}}_k^H \Phi^H \bar{\mathbf{H}}_2^H \bar{\mathbf{H}}_2 \Phi \bar{\mathbf{h}}_k \left( \sqrt{c_k} \sqrt{c_k \varepsilon_k} \tilde{\mathbf{h}}_k^H \Phi^H \tilde{\mathbf{H}}_2^H \mathbf{A}_k^H \tilde{\mathbf{H}}_2 \Phi \bar{\mathbf{h}}_k \right)^H \right\} \\
&= 2c_k^2 \delta \varepsilon_k e_{k2} \mathbb{E} \left\{ \tilde{\mathbf{h}}_k^H \Phi^H \bar{\mathbf{H}}_2^H \bar{\mathbf{H}}_2 \Phi \bar{\mathbf{h}}_k \bar{\mathbf{h}}_k^H \Phi^H \mathbb{E} \left\{ \tilde{\mathbf{H}}_2^H \mathbf{A}_k \tilde{\mathbf{H}}_2 \right\} \Phi \tilde{\mathbf{h}}_k \right\} \\
&= 2c_k^2 \delta \varepsilon_k e_{k1} e_{k2} M \mathbb{E} \left\{ \tilde{\mathbf{h}}_k^H \Phi^H \bar{\mathbf{H}}_2^H \bar{\mathbf{H}}_2 \Phi \bar{\mathbf{h}}_k \bar{\mathbf{h}}_k^H \tilde{\mathbf{h}}_k \right\} \\
&= 2c_k^2 \delta \varepsilon_k e_{k1} e_{k2} M \text{Tr} \left\{ \bar{\mathbf{h}}_k^H \Phi^H \mathbf{a}_N \mathbf{a}_M^H \mathbf{a}_M \mathbf{a}_N^H \Phi \bar{\mathbf{h}}_k \right\} \\
&= 2c_k^2 \delta \varepsilon_k e_{k1} e_{k2} M^2 |f_k(\Phi)|^2.
\end{aligned} \tag{184}$$

The seventh term is

$$\begin{aligned}
& 2\mathbb{E} \left\{ e_{k2} \sqrt{c_k \delta} \sqrt{c_k \delta} \tilde{\mathbf{h}}_k^H \Phi^H \bar{\mathbf{H}}_2^H \bar{\mathbf{H}}_2 \Phi \tilde{\mathbf{h}}_k \left( \sqrt{c_k \varepsilon_k} \sqrt{c_k \varepsilon_k} \bar{\mathbf{h}}_k^H \Phi^H \tilde{\mathbf{H}}_2^H \mathbf{A}_k^H \tilde{\mathbf{H}}_2 \Phi \bar{\mathbf{h}}_k \right)^H \right\} \\
&= 2c_k^2 \delta \varepsilon_k e_{k2} \mathbb{E} \left\{ \tilde{\mathbf{h}}_k^H \Phi^H \bar{\mathbf{H}}_2^H \bar{\mathbf{H}}_2 \Phi \tilde{\mathbf{h}}_k \right\} \bar{\mathbf{h}}_k^H \Phi^H \mathbb{E} \left\{ \tilde{\mathbf{H}}_2^H \mathbf{A}_k \tilde{\mathbf{H}}_2 \right\} \Phi \bar{\mathbf{h}}_k \\
&= 2c_k^2 \delta \varepsilon_k e_{k1} e_{k2} M \mathbb{E} \left\{ \tilde{\mathbf{h}}_k^H \Phi^H \bar{\mathbf{H}}_2^H \bar{\mathbf{H}}_2 \Phi \tilde{\mathbf{h}}_k \right\} \bar{\mathbf{h}}_k^H \bar{\mathbf{h}}_k \\
&= 2c_k^2 \delta \varepsilon_k e_{k1} e_{k2} M \text{Tr} \left\{ \bar{\mathbf{H}}_2^H \bar{\mathbf{H}}_2 \right\} \bar{\mathbf{h}}_k^H \bar{\mathbf{h}}_k \\
&= 2c_k^2 \delta \varepsilon_k e_{k1} e_{k2} M^2 N^2.
\end{aligned} \tag{185}$$

The eighth term is

$$\begin{aligned}
& 2\mathbb{E} \left\{ e_{k2} \sqrt{c_k \delta} \sqrt{c_k \delta} \tilde{\mathbf{h}}_k^H \Phi^H \bar{\mathbf{H}}_2^H \bar{\mathbf{H}}_2 \Phi \tilde{\mathbf{h}}_k \left( \sqrt{c_k} \sqrt{c_k} \tilde{\mathbf{h}}_k^H \Phi^H \tilde{\mathbf{H}}_2^H \mathbf{A}_k^H \tilde{\mathbf{H}}_2 \Phi \tilde{\mathbf{h}}_k \right)^H \right\} \\
&= 2c_k^2 \delta e_{k2} \mathbb{E} \left\{ \tilde{\mathbf{h}}_k^H \Phi^H \bar{\mathbf{H}}_2^H \bar{\mathbf{H}}_2 \Phi \tilde{\mathbf{h}}_k \tilde{\mathbf{h}}_k^H \Phi^H \mathbb{E} \left\{ \tilde{\mathbf{H}}_2^H \mathbf{A}_k \tilde{\mathbf{H}}_2 \right\} \Phi \tilde{\mathbf{h}}_k \right\} \\
&= 2c_k^2 \delta e_{k1} e_{k2} M \mathbb{E} \left\{ \tilde{\mathbf{h}}_k^H \Phi^H \bar{\mathbf{H}}_2^H \bar{\mathbf{H}}_2 \Phi \tilde{\mathbf{h}}_k \tilde{\mathbf{h}}_k^H \tilde{\mathbf{h}}_k \right\} \\
&= 2c_k^2 \delta e_{k1} e_{k2} M \text{Tr} \left\{ \Phi^H \bar{\mathbf{H}}_2^H \bar{\mathbf{H}}_2 \Phi \mathbb{E} \left\{ \tilde{\mathbf{h}}_k \tilde{\mathbf{h}}_k^H \tilde{\mathbf{h}}_k \tilde{\mathbf{h}}_k^H \right\} \right\} \\
&= 2c_k^2 \delta e_{k1} e_{k2} M \text{Tr} \left\{ \Phi^H \bar{\mathbf{H}}_2^H \bar{\mathbf{H}}_2 \Phi (N+1) \mathbf{I}_N \right\} \\
&= 2c_k^2 \delta e_{k1} e_{k2} M^2 N (N+1).
\end{aligned} \tag{186}$$

The ninth term is

$$\begin{aligned}
& 2\mathbb{E} \left\{ \sqrt{c_k \varepsilon_k} \sqrt{c_k \delta \varepsilon_k} \bar{\mathbf{h}}_k^H \Phi^H \tilde{\mathbf{H}}_2^H \mathbf{A}_k^H \bar{\mathbf{H}}_2 \Phi \bar{\mathbf{h}}_k \left( \sqrt{c_k} \sqrt{c_k \delta} \tilde{\mathbf{h}}_k^H \Phi^H \tilde{\mathbf{H}}_2^H \mathbf{A}_k^H \bar{\mathbf{H}}_2 \Phi \tilde{\mathbf{h}}_k \right)^H \right\} \\
&= 2c_k^2 \delta \varepsilon_k \bar{\mathbf{h}}_k^H \Phi^H \mathbb{E}_{\tilde{\mathbf{h}}_k} \left\{ \mathbb{E}_{\tilde{\mathbf{H}}_2} \left\{ \tilde{\mathbf{H}}_2^H \mathbf{A}_k^H \bar{\mathbf{H}}_2 \Phi \bar{\mathbf{h}}_k \tilde{\mathbf{h}}_k^H \Phi^H \tilde{\mathbf{H}}_2^H \mathbf{A}_k \tilde{\mathbf{H}}_2 \right\} \Phi \tilde{\mathbf{h}}_k \mid \tilde{\mathbf{h}}_k \right\} \\
&= 2c_k^2 \delta \varepsilon_k \bar{\mathbf{h}}_k^H \Phi^H \mathbb{E} \left\{ \text{Tr} \left\{ \mathbf{A}_k^H \bar{\mathbf{H}}_2 \Phi \bar{\mathbf{h}}_k \tilde{\mathbf{h}}_k^H \Phi^H \bar{\mathbf{H}}_2^H \mathbf{A}_k \right\} \Phi \tilde{\mathbf{h}}_k \right\} \\
&= 2c_k^2 \delta \varepsilon_k e_{k2}^2 \bar{\mathbf{h}}_k^H \Phi^H \mathbb{E} \left\{ \text{Tr} \left\{ \bar{\mathbf{H}}_2 \Phi \bar{\mathbf{h}}_k \tilde{\mathbf{h}}_k^H \Phi^H \bar{\mathbf{H}}_2^H \right\} \Phi \tilde{\mathbf{h}}_k \right\} \\
&= 2c_k^2 \delta \varepsilon_k e_{k2}^2 \bar{\mathbf{h}}_k^H \Phi^H \mathbb{E} \left\{ \Phi \tilde{\mathbf{h}}_k \left( \tilde{\mathbf{h}}_k^H \Phi^H \bar{\mathbf{H}}_2^H \bar{\mathbf{H}}_2 \Phi \bar{\mathbf{h}}_k \right) \right\} \\
&= 2c_k^2 \delta \varepsilon_k e_{k2}^2 \bar{\mathbf{h}}_k^H \Phi^H \Phi \mathbb{E} \left\{ \tilde{\mathbf{h}}_k \tilde{\mathbf{h}}_k^H \right\} \Phi^H \bar{\mathbf{H}}_2^H \bar{\mathbf{H}}_2 \Phi \bar{\mathbf{h}}_k \\
&= 2c_k^2 \delta \varepsilon_k e_{k2}^2 \bar{\mathbf{h}}_k^H \Phi^H \bar{\mathbf{H}}_2^H \bar{\mathbf{H}}_2 \Phi \bar{\mathbf{h}}_k \\
&= 2c_k^2 \delta \varepsilon_k e_{k2}^2 M |f_k(\Phi)|^2.
\end{aligned} \tag{187}$$

The tenth term is

$$\begin{aligned}
& 2\mathbb{E} \left\{ \sqrt{c_k \varepsilon_k} \sqrt{c_k \varepsilon_k} \bar{\mathbf{h}}_k^H \Phi^H \tilde{\mathbf{H}}_2^H \mathbf{A}_k^H \tilde{\mathbf{H}}_2 \Phi \bar{\mathbf{h}}_k \left( \sqrt{c_k} \sqrt{c_k} \tilde{\mathbf{h}}_k^H \Phi^H \tilde{\mathbf{H}}_2^H \mathbf{A}_k^H \tilde{\mathbf{H}}_2 \Phi \tilde{\mathbf{h}}_k \right)^H \right\} \\
&= 2c_k^2 \varepsilon_k \bar{\mathbf{h}}_k^H \Phi^H \mathbb{E}_{\tilde{\mathbf{h}}_k} \left\{ \mathbb{E}_{\tilde{\mathbf{H}}_2} \left\{ \tilde{\mathbf{H}}_2^H \mathbf{A}_k^H \tilde{\mathbf{H}}_2 \Phi \bar{\mathbf{h}}_k \tilde{\mathbf{h}}_k^H \Phi^H \tilde{\mathbf{H}}_2^H \mathbf{A}_k \tilde{\mathbf{H}}_2 \right\} \Phi \tilde{\mathbf{h}}_k \mid \tilde{\mathbf{h}}_k \right\} \\
&= 2c_k^2 \varepsilon_k \bar{\mathbf{h}}_k^H \Phi^H \mathbb{E} \left\{ \left( e_{k1}^2 M^2 \Phi \bar{\mathbf{h}}_k \tilde{\mathbf{h}}_k^H \Phi^H + e_{k3} M \text{Tr} \left\{ \Phi \bar{\mathbf{h}}_k \tilde{\mathbf{h}}_k^H \Phi^H \right\} \mathbf{I}_N \right) \Phi \tilde{\mathbf{h}}_k \right\} \\
&= 2c_k^2 \varepsilon_k \mathbb{E} \left\{ e_{k1}^2 M^2 \bar{\mathbf{h}}_k^H \bar{\mathbf{h}}_k \tilde{\mathbf{h}}_k^H \tilde{\mathbf{h}}_k + e_{k3} M \bar{\mathbf{h}}_k^H \tilde{\mathbf{h}}_k \left( \tilde{\mathbf{h}}_k^H \bar{\mathbf{h}}_k \right) \right\} \\
&= 2c_k^2 \varepsilon_k (e_{k1}^2 M^2 N^2 + e_{k3} M N).
\end{aligned} \tag{188}$$

Thus, we have completed the calculation of 10 cross-terms. After some direct simplifications, we can obtain  $\mathbb{E} \left\{ \left| \hat{\mathbf{q}}_k^H \mathbf{q}_k \right|^2 \right\}$  by combining (154) - (159), (161) - (176) and (179) - (188) with (153). With the aid of  $\mathbb{E} \left\{ \left| \hat{\mathbf{q}}_k^H \mathbf{q}_k \right|^2 \right\}$  and (117), we can complete the calculation of the signal leakage  $E_k^{(\text{leakage})}(\Phi)$  using (152).

## APPENDIX F

Recall the definition of  $f_k(\Phi)$  in (43). If  $N = 1$ , we have  $\zeta_1^k = 0$ . Then, for any design of  $\theta_1$ , we have  $|f_k(\Phi)| = |e^{j\theta_1}| = 1$ .

If  $N > 1$ , we aim to prove that  $0 \leq |f_k(\Phi)| \leq N$ . Firstly, by invoking the triangle inequality, we have

$$|f_k(\Phi)| = \left| \sum_{n=1}^N e^{j(\zeta_n^k + \theta_n)} \right| \leq \sum_{n=1}^N \left| e^{j(\zeta_n^k + \theta_n)} \right| = N. \quad (189)$$

The equality holds if the phase shifts of all the RIS elements are aligned as

$$\theta_n = -\zeta_n^k + C_0, \forall n, \quad (190)$$

where  $C_0$  is an arbitrary constant.

Next, we aim to prove that the minimum value of  $|f_k(\Phi)|$  is zero. Firstly, if  $N$  is even, the minimum value 0 is obtained when

$$\theta_{2i-1} + \zeta_{2i-1}^k = (\theta_{2i} + \zeta_{2i}^k) + \pi, 1 \leq i \leq \frac{N}{2}. \quad (191)$$

Otherwise, if  $N$  is odd, the minimum value 0 is still achievable for

$$\begin{aligned} \theta_{2i-1} + \zeta_{2i-1}^k &= (\theta_{2i} + \zeta_{2i}^k) + \pi, 1 \leq i \leq \frac{N-1}{2} - 1, \\ \theta_{N-2} + \zeta_{N-2}^k &= \frac{\pi}{3}, \\ \theta_{N-1} + \zeta_{N-1}^k &= -\frac{\pi}{3}, \\ \theta_N + \zeta_N^k &= \pi. \end{aligned} \quad (192)$$

Next, we aim to prove that when the phase shifts of the RIS are designed to maximize  $|f_k(\Phi)|$ , the corresponding term  $|f_i(\Phi)|$  for the user  $i$  is bounded when  $N \rightarrow \infty$ . Note that we can prove this result rigorously under the one-dimensional uniform linear array (ULA) model. Since the USPA model is only a two-dimensional extension of the ULA model, we can deduce that the conclusion still holds.

By ignoring the elevation direction in (7) and (8) of the USPA model, we can obtain a one-dimensional ULA model for  $\bar{\mathbf{h}}_k$  and  $\mathbf{a}_N$  with AoA  $\varphi_{kr}^a$  and AoD  $\varphi_t^a$ , respectively. Then, we can rewrite  $f_k(\Phi)$  as

$$\begin{aligned} \bar{\mathbf{h}}_k &\triangleq \mathbf{a}_N(\varphi_{kr}^a) = \left[ 1, e^{j2\pi \frac{d}{\lambda} \sin \varphi_{kr}^a}, \dots, e^{j2\pi \frac{d}{\lambda} (N-1) \sin \varphi_{kr}^a} \right]^T, \\ \mathbf{a}_N &\triangleq \mathbf{a}_N(\varphi_t^a) = \left[ 1, e^{j2\pi \frac{d}{\lambda} \sin \varphi_t^a}, \dots, e^{j2\pi \frac{d}{\lambda} (N-1) \sin \varphi_t^a} \right]^T, \\ f_k(\Phi) &= \mathbf{a}_N^H \Phi \bar{\mathbf{h}}_k = \sum_{n=1}^N e^{j2\pi \frac{d}{\lambda} (n-1) (\sin \varphi_{kr}^a - \sin \varphi_t^a) + j\theta_n}. \end{aligned} \quad (193)$$



With  $\theta_n = 2\pi \frac{d}{\lambda} (n-1) (\sin \varphi_t^a - \sin \varphi_{kr}^a)$ , we have  $|f_k(\Phi)| = N$ . At the same time, for the user  $i$ , we have

$$\begin{aligned} f_i(\Phi) &= \mathbf{a}_N^H \Phi \bar{\mathbf{h}}_i = \sum_{n=1}^N e^{j2\pi \frac{d}{\lambda} (n-1) (\sin \varphi_{ir}^a - \sin \varphi_t^a) + j\theta_n} \\ &= \sum_{n=1}^N e^{j2\pi \frac{d}{\lambda} (n-1) (\sin \varphi_{ir}^a - \sin \varphi_t^a + \sin \varphi_t^a - \sin \varphi_{kr}^a)} \\ &= \sum_{n=1}^N e^{j2\pi \frac{d}{\lambda} (n-1) (\sin \varphi_{ir}^a - \sin \varphi_{kr}^a)}. \end{aligned} \quad (194)$$

Then, by using the property of geometric progression, we obtain

$$\begin{aligned} |f_i(\Phi)| &= \left| \sum_{n=1}^N \left( e^{j2\pi \frac{d}{\lambda} (\sin \varphi_{ir}^a - \sin \varphi_{kr}^a)} \right)^{(n-1)} \right| = \left| \frac{1 - e^{j2\pi \frac{d}{\lambda} N (\sin \varphi_{ir}^a - \sin \varphi_{kr}^a)}}{1 - e^{j2\pi \frac{d}{\lambda} (\sin \varphi_{ir}^a - \sin \varphi_{kr}^a)}} \right| \\ &= \left| \frac{e^{-j\pi \frac{d}{\lambda} N (\sin \varphi_{ir}^a - \sin \varphi_{kr}^a)} - e^{j\pi \frac{d}{\lambda} N (\sin \varphi_{ir}^a - \sin \varphi_{kr}^a)}}{e^{-j\pi \frac{d}{\lambda} (\sin \varphi_{ir}^a - \sin \varphi_{kr}^a)} - e^{j\pi \frac{d}{\lambda} (\sin \varphi_{ir}^a - \sin \varphi_{kr}^a)}} \times \frac{e^{j\pi \frac{d}{\lambda} N (\sin \varphi_{ir}^a - \sin \varphi_{kr}^a)}}{e^{j\pi \frac{d}{\lambda} (\sin \varphi_{ir}^a - \sin \varphi_{kr}^a)}} \right| \\ &= \frac{\sin \left( \pi \frac{d}{\lambda} N (\sin \varphi_{ir}^a - \sin \varphi_{kr}^a) \right)}{\sin \left( \pi \frac{d}{\lambda} (\sin \varphi_{ir}^a - \sin \varphi_{kr}^a) \right)}. \end{aligned} \quad (195)$$

Therefore, if the user  $i$  does not have the same AoA as user  $k$ , the term  $|f_i(\Phi)|$  is bounded when  $N \rightarrow \infty$ . Then, following a similar process, we can prove that the term  $\left| \bar{\mathbf{h}}_k^H \bar{\mathbf{h}}_i \right|^2$  is bounded when  $N \rightarrow \infty$ .

## APPENDIX G

Instantaneous CSI-based schemes need to estimate the cascaded channel and the direct channel in each coherence interval, and then optimize the phase shifts of the RIS in each coherence interval. In the following, we give a brief introduction of the instantaneous CSI-based scheme in single-user systems, including the system model, channel estimation, problem formulation, and phase shift design.

Assume that only the user  $k$  exists in the system. The specific realizations of the channel  $\mathbf{H}_2$ ,  $\mathbf{h}_k$ , and  $\mathbf{d}_k$  in the  $i$ -th coherence interval are denoted by  $\mathbf{H}_2^{(i)}$ ,  $\mathbf{h}_k^{(i)}$ , and  $\mathbf{d}_k^{(i)}$ , respectively. Besides, the phase shifts matrix  $\Phi$  in the  $i$ -th coherence interval is equal to  $\Phi^{(i)} = \text{diag} \{ \mathbf{v}^{(i)} \}$ , where  $\mathbf{v}^{(i)} = [e^{j\theta_1^{(i)}}, \dots, e^{j\theta_N^{(i)}}]^T$ . Then, the equivalent channel in the  $i$ -th coherence interval can be expressed as

$$\mathbf{q}_k^{(i)} = \mathbf{H}_2^{(i)} \Phi^{(i)} \mathbf{h}_k^{(i)} + \mathbf{d}_k^{(i)} = \mathbf{H}_2^{(i)} \text{diag} \left( \mathbf{h}_k^{(i)} \right) \mathbf{v}^{(i)} + \mathbf{d}_k^{(i)}. \quad (196)$$

Let  $\mathbf{G}_k^{(i)} \triangleq \mathbf{H}_2^{(i)} \text{diag} \left( \mathbf{h}_k^{(i)} \right)$  represent the cascaded channel in the  $i$ -th coherence interval. Next, the instantaneous CSI-based scheme needs to respectively estimate the  $M \times N$  cascaded channel matrix  $\mathbf{G}_k^{(i)}$  and the  $M \times 1$  direct channel vector  $\mathbf{d}_k^{(i)}$  in each channel coherence time.

The estimation of  $\mathbf{G}_k^{(i)}$  and  $\mathbf{d}_k^{(i)}$  can be performed by using a two-phase pilot-based scheme [36]. In the first phase, the direct link  $\mathbf{d}_k^{(i)}$  can be estimated by using the MMSE estimator, and the needed pilot length is equal to the number of users, i.e., 1. In the second phase, using the estimated direct channel, the cascaded channel  $\mathbf{G}_k^{(i)}$  can be estimated by using the LMMSE estimator, and the needed pilot length is equal to the number of RIS elements, i.e.,  $N$ . Therefore, the overall pilot needed in the considered instantaneous CSI-based scheme is  $N + 1$ . Then, we denote the estimated cascaded channel and direct channel as  $\hat{\mathbf{G}}_k^{(i)}$  and  $\hat{\mathbf{d}}_k^{(i)}$ , respectively. The detailed process of the estimation is omitted here, and interested readers can refer to [36, Section V].

Based on the estimated channels  $\hat{\mathbf{G}}_k^{(i)}$  and  $\hat{\mathbf{d}}_k^{(i)}$ , the BS can design the MRC beamforming as  $\mathbf{w}^H = \left( \hat{\mathbf{G}}_k^{(i)} \mathbf{v}^{(i)} + \hat{\mathbf{d}}_k^{(i)} \right)^H$ . Then, the received signal at the BS in the  $i$ -th coherence interval can be expressed as

$$\begin{aligned} \mathbf{y}^{(i)} &= \sqrt{p} \mathbf{w}^H \left( \mathbf{G}_k^{(i)} \mathbf{v}^{(i)} + \mathbf{d}_k^{(i)} \right) x_k^{(i)} + \mathbf{w}^H \mathbf{n}^{(i)} \\ &= \sqrt{p} \mathbf{w}^H \left( \hat{\mathbf{G}}_k^{(i)} \mathbf{v}^{(i)} + \hat{\mathbf{d}}_k^{(i)} \right) x_k^{(i)} + \sqrt{p} \mathbf{w}^H \left( \tilde{\mathbf{G}}_k^{(i)} \mathbf{v}^{(i)} + \tilde{\mathbf{d}}_k^{(i)} \right) x_k^{(i)} + \mathbf{w}^H \mathbf{n}^{(i)}, \end{aligned} \quad (197)$$

where  $\tilde{\mathbf{G}}_k^{(i)} = \mathbf{G}_k^{(i)} - \hat{\mathbf{G}}_k^{(i)}$  and  $\tilde{\mathbf{d}}_k^{(i)} = \mathbf{d}_k^{(i)} - \hat{\mathbf{d}}_k^{(i)}$  denote the channel estimation errors.

Then, we can express the effective SNR as

$$\text{SNR}_k^{(i)}(\mathbf{v}^{(i)}) = \frac{p \left| \mathbf{w}^H \left( \hat{\mathbf{G}}_k^{(i)} \mathbf{v}^{(i)} + \hat{\mathbf{d}}_k^{(i)} \right) \right|^2}{p \left| \mathbf{w}^H \left( \tilde{\mathbf{G}}_k^{(i)} \mathbf{v}^{(i)} + \tilde{\mathbf{d}}_k^{(i)} \right) \right|^2 + \sigma^2 \|\mathbf{w}^H\|^2}, \quad (198)$$

and the effective rate of user  $k$  in the  $i$ -th coherence interval is given by

$$R_k^{(i)} = \left( 1 - \frac{N+1}{\tau_c} \right) \log_2 \left( 1 + \text{SNR}_k^{(i)}(\mathbf{v}^{(i)}) \right), \quad (199)$$

where the factor  $\left( 1 - \frac{N+1}{\tau_c} \right)$  represents the rate loss due to the pilot estimation overhead.

Next, the instantaneous CSI-based schemes need to optimize the phase shifts  $\mathbf{v}^{(i)}$  in the  $i$ -th coherence interval. We note that the maximization of  $R_k^{(i)}$  is equivalent to the maximization of  $\text{SNR}_k^{(i)}$ . However, it is challenging to find an optimal solution for the maximization of the SNR when considering the channel estimation error from imperfect CSI. Therefore, we resort to a low-complexity sub-optimal solution which only uses the RIS to maximize the desired signal power. The optimization problem is formulated as follows

$$\max_{\mathbf{v}^{(i)}} \left| \mathbf{w}^H \left( \hat{\mathbf{G}}_k^{(i)} \mathbf{v}^{(i)} + \hat{\mathbf{d}}_k^{(i)} \right) \right|^2 \quad (200a)$$

$$\text{s.t.} \quad 0 \leq \theta_n^{(i)} < 2\pi, \forall n. \quad (200b)$$

A closed-form solution for the problem in (200) can be obtained by using alternating optimization [10, Section III]. First, given the phase shifts vector  $\mathbf{v}^{(i)}$ , the MRC beamforming vector is set to  $\mathbf{w}^H = \left( \hat{\mathbf{G}}_k^{(i)} \mathbf{v}^{(i)} + \hat{\mathbf{d}}_k^{(i)} \right)^H$ . Then, given the MRC beamforming vector  $\mathbf{w}^H$ , the RIS phase shifts are optimized by aligning the phase of the cascaded channel with the phase of the direct channel, i.e.,  $\arg \left( \mathbf{w}^H \hat{\mathbf{G}}_k^{(i)} \mathbf{v}^{(i)} \right) = \arg \left( \mathbf{w}^H \hat{\mathbf{d}}_k^{(i)} \right)$ . Then, the solution  $\mathbf{v}^{*(i)}$  is obtained when the alternating optimization algorithm reaches convergence. Based on the optimized solution  $\mathbf{v}^{*(i)}$ , the achievable rate in the  $i$ -th coherence interval is obtained as  $R_k^{*(i)} = \left( 1 - \frac{N+1}{\tau_c} \right) \log_2 \left( 1 + \text{SNR}_k^{(i)} \left( \mathbf{v}^{*(i)} \right) \right)$ .

Finally, by repeating the above procedure for  $T_{ci}$  coherence intervals, the average achievable rate for the instantaneous CSI-based scheme is given by

$$\bar{R}_k^* = \left( 1 - \frac{N+1}{\tau_c} \right) \frac{1}{T_{ci}} \sum_{i=1}^{T_{ci}} \log_2 \left( 1 + \text{SNR}_k^{(i)} \left( \mathbf{v}^{*(i)} \right) \right). \quad (201)$$

The rate in (201), which consists of a rate loss factor equal to  $1 - \frac{N+1}{\tau_c}$ , is plotted in Fig. 3 in Section VI. It is apparent that the rate in (201) is negatively affected by the channel estimation overhead. If  $N+1 > \tau_c$ , the rate reduces to zero, since all the symbols in the coherence interval are used for pilot transmission, and no symbol is left for data transmission. To gain more insights, we consider to replace the rate loss factor in (201) with  $1 - \frac{1}{\tau_c}$ , which is the same as that in the proposed two-timescale scheme. In this case, the rate is given by

$$\bar{R}_k^* = \left( 1 - \frac{1}{\tau_c} \right) \frac{1}{T_{ci}} \sum_{i=1}^{T_{ci}} \log_2 \left( 1 + \text{SNR}_k^{(i)} \left( \mathbf{v}^{*(i)} \right) \right). \quad (202)$$

The rate in (202), which is, however, not achievable, is plotted in Fig. 3 in Section VI. Compared with (201), the only difference in (202) is that the additional, but necessary, channel estimation overhead is ignored.

## REFERENCES

- [1] K. Zhi, C. Pan, H. Ren, K. Wang, and M. ElKashlan, "Reconfigurable intelligent surface-aided MISO systems with statistical CSI: Channel estimation, analysis and optimization," 2021. [Online]. Available: <https://arxiv.org/abs/2107.05512>
- [2] M. Di Renzo, A. Zappone, M. Debbah, M. S. Alouini, C. Yuen, J. de Rosny, and S. Tretyakov, "Smart radio environments empowered by reconfigurable intelligent surfaces: How it works, state of research, and the road ahead," *IEEE J. Sel. Areas Commun.*, vol. 38, no. 11, pp. 2450–2525, Nov. 2020.
- [3] C. Pan, H. Ren, K. Wang, J. F. Kolb, M. ElKashlan, M. Chen, M. Di Renzo, Y. Hao, J. Wang, A. L. Swindlehurst *et al.*, "Reconfigurable intelligent surfaces for 6G systems: Principles, applications, and research directions," *IEEE Commun. Mag.*, 2021.
- [4] A. Kammoun, L. Sanguinetti, M. Debbah, and M. Alouini, "Asymptotic analysis of RZF in large-scale MU-MIMO systems over rician channels," *IEEE Trans. Inf. Theory*, vol. 65, no. 11, pp. 7268–7286, Nov. 2019.

- [5] R. Couillet, M. Debbah, and J. W. Silverstein, "A deterministic equivalent for the analysis of correlated MIMO multiple access channels," *IEEE Trans. Inf. Theory*, vol. 57, no. 6, pp. 3493–3514, Jun. 2011.
- [6] Y. Wu, R. Schober, D. W. K. Ng, C. Xiao, and G. Caire, "Secure massive MIMO transmission with an active eavesdropper," *IEEE Trans. Inf. Theory*, vol. 62, no. 7, pp. 3880–3900, Jul. 2016.
- [7] S. Wagner, R. Couillet, M. Debbah, and D. T. M. Slock, "Large system analysis of linear precoding in correlated MISO broadcast channels under limited feedback," *IEEE Trans. Inf. Theory*, vol. 58, no. 7, pp. 4509–4537, Jul. 2012.
- [8] G. Caire, N. Jindal, M. Kobayashi, and N. Ravindran, "Multiuser MIMO achievable rates with downlink training and channel state feedback," *IEEE Trans. Inf. Theory*, vol. 56, no. 6, pp. 2845–2866, Jun. 2010.
- [9] A. Adhikary, J. Nam, J. Ahn, and G. Caire, "Joint spatial division and multiplexing—the large-scale array regime," *IEEE Trans. Inf. Theory*, vol. 59, no. 10, pp. 6441–6463, Oct. 2013.
- [10] Q. Wu and R. Zhang, "Intelligent reflecting surface enhanced wireless network via joint active and passive beamforming," *IEEE Trans. Wireless Commun.*, vol. 18, no. 11, pp. 5394–5409, Nov. 2019.
- [11] C. Huang, A. Zappone, G. C. Alexandropoulos, M. Debbah, and C. Yuen, "Reconfigurable intelligent surfaces for energy efficiency in wireless communication," *IEEE Trans. Wireless Commun.*, vol. 18, no. 8, pp. 4157–4170, Aug. 2019.
- [12] C. Pan *et al.*, "Multicell MIMO communications relying on intelligent reflecting surfaces," *IEEE Trans. Wireless Commun.*, vol. 19, no. 8, pp. 5218–5233, Aug. 2020.
- [13] S. Zhang and R. Zhang, "Capacity characterization for intelligent reflecting surface aided MIMO communication," *IEEE J. Sel. Areas Commun.*, vol. 38, no. 8, pp. 1823–1838, Aug. 2020.
- [14] W. Mei and R. Zhang, "Multi-beam multi-hop routing for intelligent reflecting surfaces aided massive MIMO," 2021. [Online]. Available: <https://arxiv.org/abs/2101.00217>
- [15] L. Dai, B. Wang, M. Wang, X. Yang, J. Tan, S. Bi, S. Xu, F. Yang, Z. Chen, M. D. Renzo, C. B. Chae, and L. Hanzo, "Reconfigurable intelligent surface-based wireless communications: Antenna design, prototyping, and experimental results," *IEEE Access*, vol. 8, pp. 45 913–45 923, Mar. 2020.
- [16] Q. Tao, J. Wang, and C. Zhong, "Performance analysis of intelligent reflecting surface aided communication systems," *IEEE Commun. Lett.*, vol. 24, no. 11, pp. 2464–2468, Nov. 2020.
- [17] B. Ning, Z. Chen, W. Chen, Y. Du, and J. Fang, "Terahertz multi-user massive MIMO with intelligent reflecting surface: Beam training and hybrid beamforming," *IEEE Trans. Veh. Technol.*, early access 2021.
- [18] P. Wang, J. Fang, L. Dai, and H. Li, "Joint transceiver and large intelligent surface design for massive MIMO mmwave systems," *IEEE Trans. Wireless Commun.*, vol. 20, no. 2, pp. 1052–1064, Feb. 2021.
- [19] C. Pan, H. Ren, K. Wang, M. Elkashlan, A. Nallanathan, J. Wang, and L. Hanzo, "Intelligent reflecting surface aided MIMO broadcasting for simultaneous wireless information and power transfer," *IEEE J. Sel. Areas Commun.*, vol. 38, no. 8, pp. 1719–1734, Aug. 2020.
- [20] H. Lu, Y. Zeng, S. Jin, and R. Zhang, "Aerial intelligent reflecting surface: Joint placement and passive beamforming design with 3D beam flattening," *IEEE Trans. Wireless Commun.*, early access, 2021.
- [21] Y. Zhang, B. Di, H. Zhang, J. Lin, C. Xu, D. Zhang, Y. Li, and L. Song, "Beyond cell-free MIMO: Energy efficient reconfigurable intelligent surface aided cell-free MIMO communications," *IEEE Trans. Cogn. Commun. Netw.*, early access, 2021.
- [22] S. Hong, C. Pan, H. Ren, K. Wang, and A. Nallanathan, "Artificial-noise-aided secure MIMO wireless communications via intelligent reflecting surface," *IEEE Trans. Commun.*, vol. 68, no. 12, pp. 7851–7866, Dec. 2020.
- [23] H. M. Wang, J. Bai, and L. Dong, "Intelligent reflecting surfaces assisted secure transmission without eavesdropper's CSI," *IEEE Signal Process. Lett.*, vol. 27, pp. 1300–1304, Aug. 2020.

- [24] Z. Chu, W. Hao, P. Xiao, D. Mi, Z. Liu, M. Khalily, J. R. Kelly, and A. P. Feresidis, "Secrecy rate optimization for intelligent reflecting surface assisted MIMO system," *IEEE Trans. on Information Forensics and Security*, vol. 16, pp. 1655–1669, Dec. 2020.
- [25] T. Bai, C. Pan, Y. Deng, M. El Kashlan, A. Nallanathan, and L. Hanzo, "Latency minimization for intelligent reflecting surface aided mobile edge computing," *IEEE J. Sel. Areas Commun.*, vol. 38, no. 11, pp. 2666–2682, Nov. 2020.
- [26] G. Chen, Q. Wu, W. Chen, D. W. K. Ng, and L. Hanzo, "IRS-aided wireless powered MEC systems: TDMA or NOMA for computation offloading?" 2021. [Online]. Available: <https://arxiv.org/abs/2108.06120>
- [27] Z. Chu, P. Xiao, M. Shojafar, D. Mi, J. Mao, and W. Hao, "Intelligent reflecting surface assisted mobile edge computing for internet of things," *IEEE Wireless Commun. Lett.*, vol. 10, no. 3, pp. 619–623, March 2021.
- [28] S. Jia, X. Yuan, and Y. C. Liang, "Reconfigurable intelligent surfaces for energy efficiency in D2D communication network," *IEEE Wireless Commun. Lett.*, vol. 10, no. 3, pp. 683–687, Mar. 2021.
- [29] Y. Chen, B. Ai, H. Zhang, Y. Niu, L. Song, Z. Han, and H. V. Poor, "Reconfigurable intelligent surface assisted device-to-device communications," *IEEE Trans. Wireless Commun.*, early access, 2020.
- [30] G. Zhou, C. Pan, H. Ren, K. Wang, M. D. Renzo, and A. Nallanathan, "Robust beamforming design for intelligent reflecting surface aided MISO communication systems," *IEEE Wireless Commun. Lett.*, vol. 9, no. 10, pp. 1658–1662, Oct. 2020.
- [31] G. Zhou, C. Pan, H. Ren, K. Wang, and A. Nallanathan, "A framework of robust transmission design for IRS-aided MISO communications with imperfect cascaded channels," *IEEE Trans. Signal Process.*, vol. 68, pp. 5092–5106, Sep. 2020.
- [32] X. Yu, D. Xu, Y. Sun, D. W. K. Ng, and R. Schober, "Robust and secure wireless communications via intelligent reflecting surfaces," *IEEE J. Sel. Areas Commun.*, vol. 38, no. 11, pp. 2637–2652, Nov. 2020.
- [33] H. Shen, W. Xu, S. Gong, C. Zhao, and D. W. K. Ng, "Beamforming optimization for IRS-aided communications with transceiver hardware impairments," *IEEE Trans. Commun.*, vol. 69, no. 2, pp. 1214–1227, Feb. 2021.
- [34] S. Zhou, W. Xu, K. Wang, M. Di Renzo, and M.-S. Alouini, "Spectral and energy efficiency of IRS-assisted MISO communication with hardware impairments," *IEEE Wireless Commun. Lett.*, vol. 9, no. 9, pp. 1366–1369, Sep. 2020.
- [35] W. Tang, M. Z. Chen, X. Chen, J. Y. Dai, Y. Han, M. Di Renzo, Y. Zeng, S. Jin, Q. Cheng, and T. J. Cui, "Wireless communications with reconfigurable intelligent surface: Path loss modeling and experimental measurement," *IEEE Trans. Wireless Commun.*, vol. 20, no. 1, pp. 421–439, Jan. 2021.
- [36] Z. Wang, L. Liu, and S. Cui, "Channel estimation for intelligent reflecting surface assisted multiuser communications: Framework, algorithms, and analysis," *IEEE Trans. Wireless Commun.*, vol. 19, no. 10, pp. 6607–6620, Oct. 2020.
- [37] Q. U. A. Nadeem, H. Alwazani, A. Kammoun, A. Chaaban, M. Debbah, and M. S. Alouini, "Intelligent reflecting surface-assisted multi-user MISO communication: Channel estimation and beamforming design," *IEEE Open J. Commun. Soc.*, vol. 1, pp. 661–680, Jun. 2020.
- [38] E. Björnson, Ö. Özdogan, and E. G. Larsson, "Intelligent reflecting surface versus decode-and-forward: How large surfaces are needed to beat relaying?" *IEEE Wireless Commun. Lett.*, vol. 9, no. 2, pp. 244–248, Feb. 2020.
- [39] Y. Han, W. Tang, S. Jin, C.-K. Wen, and X. Ma, "Large intelligent surface-assisted wireless communication exploiting statistical CSI," *IEEE Trans. Veh. Technol.*, vol. 68, no. 8, pp. 8238–8242, Aug. 2019.
- [40] M. M. Zhao, Q. Wu, M. J. Zhao, and R. Zhang, "Intelligent reflecting surface enhanced wireless networks: Two-timescale beamforming optimization," *IEEE Trans. Wireless Commun.*, vol. 20, no. 1, pp. 2–17, Jan. 2021.
- [41] M.-M. Zhao, A. Liu, Y. Wan, and R. Zhang, "Two-timescale beamforming optimization for intelligent reflecting surface aided multiuser communication with QoS constraints," *IEEE Trans. Wireless Commun.*, pp. 1–1, early access 2021.
- [42] H. Guo, Y. C. Liang, and S. Xiao, "Intelligent reflecting surface configuration with historical channel observations," *IEEE Wireless Commun. Lett.*, vol. 9, no. 11, pp. 1821–1824, Nov. 2020.

- [43] A. Abrardo, D. Dardari, and M. Di Renzo, "Intelligent reflecting surfaces: Sum-rate optimization based on statistical CSI," 2020. [Online]. Available: <https://arxiv.org/abs/2012.10679>
- [44] Y. Gao, J. Xu, W. Xu, D. W. K. Ng, and M. S. Alouini, "Distributed IRS with statistical passive beamforming for MISO communications," *IEEE Wireless Commun. Lett.*, vol. 10, no. 2, pp. 221–225, Feb. 2021.
- [45] Y. Chen, Y. Wang, J. Zhang, and M. Di Renzo, "QoS-driven spectrum sharing for reconfigurable intelligent surfaces (RISs) aided vehicular networks," *IEEE Trans. Wireless Commun.*, early access 2021.
- [46] Q. U. A. Nadeem, A. Kammoun, A. Chaaban, M. Debbah, and M. S. Alouini, "Asymptotic max-min SINR analysis of reconfigurable intelligent surface assisted MISO systems," *IEEE Trans. Wireless Commun.*, vol. 19, no. 12, pp. 7748–7764, Dec. 2020.
- [47] J. Wang, H. Wang, Y. Han, S. Jin, and X. Li, "Joint transmit beamforming and phase shift design for reconfigurable intelligent surface assisted MIMO systems," *IEEE Trans. Cogn. Commun. Netw.*, early access, 2021.
- [48] Y. Jia, C. Ye, and Y. Cui, "Analysis and optimization of an intelligent reflecting surface-assisted system with interference," *IEEE Trans. Wireless Commun.*, vol. 19, no. 12, pp. 8068–8082, Dec. 2020.
- [49] Z. Peng, T. Li, C. Pan, H. Ren, W. Xu, and M. D. Renzo, "Analysis and optimization for RIS-aided multi-pair communications relying on statistical CSI," *IEEE Trans. Veh. Technol.*, vol. 70, no. 4, pp. 3897–3901, Apr. 2021.
- [50] K. Zhi, C. Pan, H. Ren, and K. Wang, "Power scaling law analysis and phase shift optimization of RIS-aided massive MIMO systems with statistical CSI," 2020. [Online]. Available: <https://arxiv.org/abs/2010.13525>
- [51] —, "Statistical CSI-based design for reconfigurable intelligent surface-aided massive MIMO systems with direct links," *IEEE Wireless Commun. Lett.*, vol. 10, no. 5, pp. 1128–1132, May 2021.
- [52] T. Van Chien, H. Q. Ngo, S. Chatzinotas, M. Di Renzo, and B. Ottersten, "Reconfigurable intelligent surface-assisted cell-free massive MIMO systems over spatially-correlated channels," 2021. [Online]. Available: <https://arxiv.org/abs/2104.08648>
- [53] E. Björnson, L. Sanguinetti, H. Wymeersch, J. Hoydis, and T. L. Marzetta, "Massive MIMO is a reality—what is next?: Five promising research directions for antenna arrays," *Digital Signal Process.*, vol. 94, pp. 3–20, Nov. 2019.
- [54] E. Björnson, J. Hoydis, and L. Sanguinetti, "Massive MIMO networks: Spectral, energy, and hardware efficiency," *Found. Trends Signal Process.*, vol. 11, no. 3-4, pp. 154–655, Nov. 2017.
- [55] Q. Zhang, S. Jin, K. Wong, H. Zhu, and M. Matthaiou, "Power scaling of uplink massive MIMO systems with arbitrary-rank channel means," *IEEE J. Sel. Topics Signal Process.*, vol. 8, no. 5, pp. 966–981, Oct. 2014.
- [56] H. Q. Ngo, E. G. Larsson, and T. L. Marzetta, "Energy and spectral efficiency of very large multiuser MIMO systems," *IEEE Trans. Commun.*, vol. 61, no. 4, pp. 1436–1449, Apr. 2013.
- [57] B. Hassibi and B. M. Hochwald, "How much training is needed in multiple-antenna wireless links?" *IEEE Trans. Inf. Theory*, vol. 49, no. 4, pp. 951–963, Apr. 2003.
- [58] N. O'Donoghue and J. M. F. Moura, "On the product of independent complex gaussians," *IEEE Trans. Signal Process.*, vol. 60, no. 3, pp. 1050–1063, Mar. 2012.
- [59] Ö. Özdogan, E. Björnson, and E. G. Larsson, "Massive MIMO with spatially correlated Rician fading channels," *IEEE Trans. Commun.*, vol. 67, no. 5, pp. 3234–3250, May 2019.
- [60] E. Björnson, J. Hoydis, M. Kountouris, and M. Debbah, "Massive MIMO systems with non-ideal hardware: Energy efficiency, estimation, and capacity limits," *IEEE Trans. Inf. Theory*, vol. 60, no. 11, pp. 7112–7139, Nov. 2014.
- [61] T. L. Marzetta and H. Q. Ngo, *Fundamentals of Massive MIMO*. Cambridge University Press, 2016.
- [62] J. Nam, G. Caire, M. Debbah, and H. V. Poor, "Capacity scaling of massive MIMO in strong spatial correlation regimes," *IEEE Trans. Inf. Theory*, vol. 66, no. 5, pp. 3040–3064, May 2020.

- [63] C. You, B. Zheng, and R. Zhang, "How to deploy intelligent reflecting surfaces in wireless network: BS-side, user-side, or both sides?" 2020. [Online]. Available: <https://arxiv.org/abs/2012.03403>
- [64] 3GPP, *TR 25.996, Spatial channel model for Multiple Input Multiple Output (MIMO) simulations*, Sep. 2012.
- [65] MathWorks, "Genetic algorithm." [Online]. Available: [https://www.mathworks.com/help/gads/genetic-algorithm.html?s\\_tid=CRUX\\_lftnav](https://www.mathworks.com/help/gads/genetic-algorithm.html?s_tid=CRUX_lftnav)
- [66] M. Mitchell, *An Introduction to Genetic Algorithms*. MIT press, 1998.
- [67] J. A. Tague and C. I. Caldwell, "Expectations of useful complex wishart forms," *Multidimensional Syst. Signal Process.*, vol. 5, no. 3, pp. 263–279, Jul. 1994.
- [68] S. M. Kay, *Fundamentals of Statistical Signal Processing*. Prentice Hall PTR, 1993.
- [69] A. Winkelbauer, "Moments and absolute moments of the normal distribution," 2012. [Online]. Available: <https://arxiv.org/abs/1209.4340>